SKIZZLE: A NOVEL *STREPTOCOCCUS AGALACTIAE*-SECRETED COFACTOR OF HUMAN PLASMINOGEN ACTIVATION

By

Karen G. Wiles

Dissertation

Submitted to the Faculty of the

Graduate School of Vanderbilt University

in partial fulfillment of the requirements

for the degree of

DOCTOR OF PHILOSOPHY

in

Pathology

December, 2010

Nashville, Tennessee

Approved:

Richard L. Hoover, Ph.D.

Ingrid Verhamme, Ph.D.

David Gailani, M.D.

Andrzej Krezel, Ph.D.

Eric P. Skaar, Ph.D, M.P.H.

For the men in my life: my father, my husband and my son.

ACKNOWLEDGEMENTS

I would first and foremost like to thank my advisor Paul E. Bock, Ph.D. for his patience, perseverance and support. His wisdom and guidance helped to find and nurture the scientist in me. His support on this long and non-traditional journey will never be forgotten. I am also grateful to the members of my thesis committee, Richard L. Hoover, Ph.D., Ingrid Verhamme, Ph.D., David Gailani, M.D., Andrzej Krezel, Ph.D., and Eric P. Skaar, Ph.D, M.P.H. for their professional and personal guidance. I would like to thank past and present members of the lab—including Malabika Laha, Miranda Nolan, Heather K. Kroh, Ph.D., Jonathan Creamer, Ph.D., and Peter Panizzi, Ph.D.—for their unconditional support and assistance. While not a member of the academic community, particular thanks must be paid to Cordozar Calvin Broadus (aka. Snoop Dogg), from whose vernacular my beloved protein earned its name – fo'shizzle. Finally, I am grateful for financial support from the American Heart Association, Greater Southeast Affiliate through Predoctoral Fellowship 0715393B.

Personal thanks must go to my parents, Barbara and Larry Godfrey, for giving me their unconditional love and support—and for teaching me that no dream was out of reach. I am indebted to my husband, Paul Wiles, for his unwavering strength and love and for never letting me give up. To Patrick, whose smile is the light in my day. I am also grateful for Roger and Cathy Wiles, the parents who love me as one of their own. This journey has been far from solitary and I am forever grateful for the support and encouragement of my entire family, especially Maureen McMichael, Michael Godfrey, James and Claudia Godfrey, Jean Godfrey and Margaret Weiss.

TABLE OF CONTENTS

LIST OF TABLES

LIST OF FIGURES

CHAPTER I

INTRODUCTION

Blood coagulation helps to restore the structural integrity of the vasculature following blood vessel injury by sealing ruptures in the vessel wall. The systems of hemostasis and fibrinolysis are responsible for maintenance of the balance between vessel repair and normal blood fluidity. Upon vessel injury, a clot mainly composed of activated platelets and fibrin is formed to minimize blood loss and maintain the closed, high pressure nature of the circulatory system (Fig. 1) (1-3). The rapid process of blood coagulation can be initiated through either the extrinsic or intrinsic pathways (2,4,5). Traditionally, the initial phase of coagulation is triggered by the extrinsic pathway consisting of the membrane receptor, tissue factor (TF), and FVII/FVIIa. The amplification phase of coagulation is traditionally thought to be regulated by the intrinsic pathway consisting of several plasma proteins including FXI, FIX, and FVIII (4,5). Following clot formation, the gradual processes of wound healing and clot dissolution begin. The dissolution of the clot occurs through degradation of the fibrin network, which acts as a structural framework providing integrity to the clot. Upon fibrinolytic dissolution of the clot, the slower processes of collagen deposition, formation of fibrous tissue, and wound healing occur. The rapid process of clot formation protects against blood loss during the elaborate wound healing process (1,2).

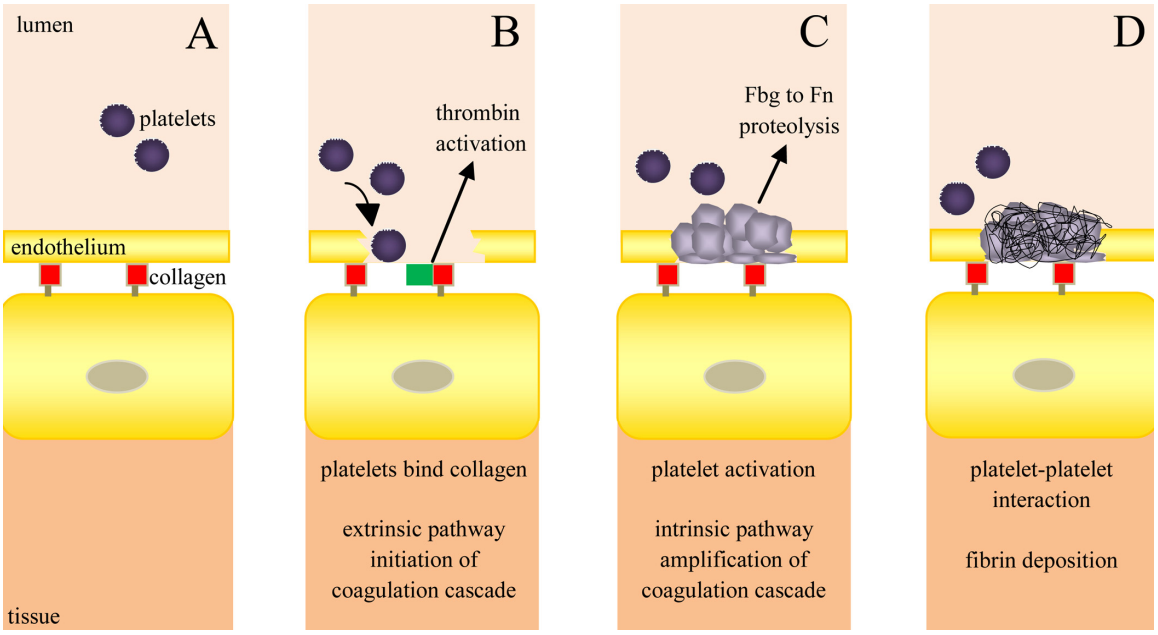

Figure 1. Schematic of hemostatic response following vessel injury adapted from Mackman et al (5). *A*. inactive platelets (*dark purple*) circulating in the lumen of a vessel. *B*. upon vessel injury platelets bind collagen exposed upon endothelial rupture, FVIIa (*green*) and TF (*red*) trigger extrinsic pathway initiation and thrombin activation. *C*. aggregation of activated platelets (*light purple*) and amplification of the coagulation cascade culminating in fibrinogen to fibrin proteolysis. *D*. platelet aggregation and fibrin deposition to restore vessel integrity.

Fibrinogen, Fibrin, and Thrombus Formation

The process of hemostasis, the normal regulation and formation of thrombi, involves a complex cascade of zymogen precursors whose proteolytic activation is required for cascade advancement, culminating in thrombus formation. This process is highly regulated by the succession of proteolytic activation reactions and by proteinase inhibitors. The cascade culminates in activation of prothrombin to thrombin by the prothrombinase complex, which includes factor Xa, factor Va, Ca^{2+}, and phospholipid membranes (6-8). Thrombin proteolytically cleaves soluble fibrinogen to insoluble fibrin. Fibrinogen is found at high concentrations (2-4 mg/ml) in plasma (9). Each half of the 340 kDa dimer is composed of three distinct polypeptide chains (Aα, Bβ and γ), which

form a 45 nm elongated coiled-coil tertiary structure with three distinct structural regions (Fig. 2) (9-11). The central E region, previously referred to as the E domain, is a dimer of the NH_2-terminal portion of all three polypeptide chains. This central domain structure contains NH_2-terminal fibrinopeptides A and B, the sequential removal of which by thrombin results in fibrin generation. The two terminal D regions include the COOH-terminal portions the Bβ and γ chains and part of the Aα chain. The αC region is comprised of the compact COOH-terminal portion of the Aα chain, connected to the linear D-E-D structure through the flexible αC-connector region (9-13).

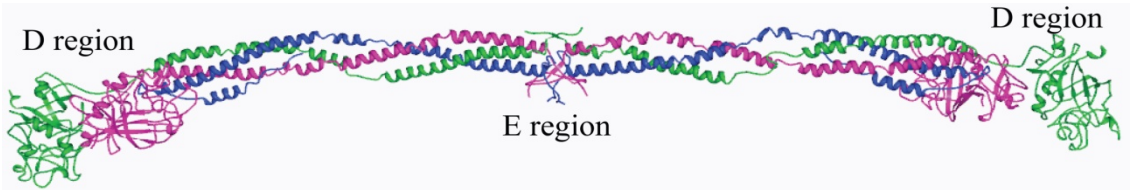

Figure 2. Human fibrinogen. Crystal structure of human fibrinogen highlighting the α chains (*blue*), β chains (*pink*), and γ chains (*green*), generated using PDB Protein Workshop 3.7 (PDB file 3GHG) (14,15).

Conversion of fibrinogen to insoluble fibrin involves proteolytic cleavage by thrombin resulting in removal of fibrinopeptides A and B from the Aα and Bβ chains. Cleavage of the fibrinopeptides exposes polymerization sites ("knobs") in the E region, which interact with complimentary sites ("holes") in the D region of adjacent fibrin molecules (Fig. 3) (14). Following removal of the fibrinopeptides, the two intramolecular αC domains disassociate and reassociate in an intermolecular arrangement to promote protofibril formation. In addition to triggering fibrinogen proteolysis, thrombin also activates factor XIII, which cross-links fibrin to reinforce its structural integrity. In addition to cross-linked connections between the polymerization sites (knobs) in the E

region and complimentary sites (holes) in the D region of adjacent fibrin molecules, cross-linking occurs between the COOH-terminal ends of the γ-chains in the D regions of neighboring molecules (γ-γ) and between intermolecular αC domain-interactions (9-14).

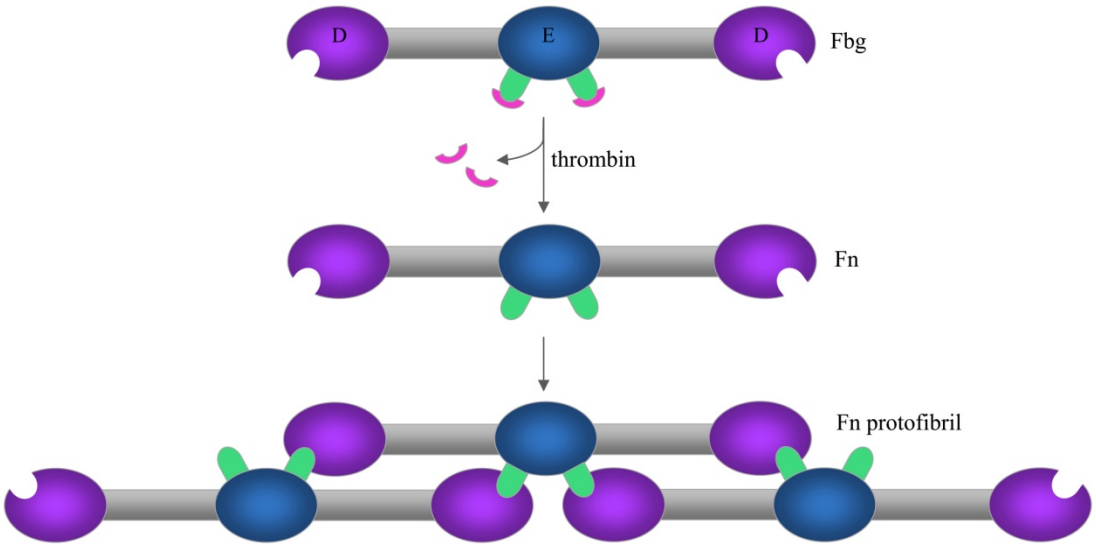

Figure 3. Cartoon of fibrin generation and fibrin protofibril formation adapted from Weisel (11). Fibrinopeptides (*pink*) are released following proteolysis by thrombin. Knobs (*green*) located on the central E region (*blue*) pair with holes (*white*) located on the terminal D region (*purple*) to promote fibrin protofibril formation.

Plasminogen and Plasmin

The human fibrinolytic system is responsible for degradation of these cross-linked fibrin networks and the resulting dissolution of thrombi in the vasculature. Plasminogen (Pg) is a 791 amino acid, 92 kDa protein synthesized in the liver and found at plasma concentrations of ~1.6-2.1 μM (1,16,17). Zymogen Pg consists of an NH_2-terminal PAN (Pg/apple/nematode) module, five homologous kringle domains, each stabilized by a series of disulfide bonds, and a COOH-terminal serine proteinase catalytic domain (18-25). Two main post-translationally modified forms of Pg are found in plasma, with a

different number of carbohydrate modifications. Pg I contains both N-linked (Asn^{288}) and O-linked (Thr^{345}) polysaccharides and Pg II contains only the O-linked (Thr^{345}) polysaccharide post-translational modification (26,27). Zymogen Pg is converted through proteolysis to the active serine proteinase, plasmin (Pm). The native form of Pg, [Glu]Pg, is characterized by its NH_2-terminal glutamic acid residue. Following cleavage by Pm, the NH_2-terminal 77-residue PAN module is removed to form [Lys]Pg (84 kDa), characterized by an NH_2-terminal lysine residue (21).

The fibrinolytic system utilizes two plasminogen activators, urokinase (uPA) and tissue-type plasminogen activator (tPA) to convert Pg to Pm. Proteolytic Pg activation by these proteinases occurs through cleavage of the Arg^{561}-Val^{562} peptide bond in the Pg catalytic domain to form Pm. This cleavage results in a conformational change in which the new Pg NH_2-terminus inserts into the NH_2-terminal binding cleft in the catalytic domain. The result is formation of an active site within the Pm catalytic domain containing the catalytic triad (Asp^{645}, His^{602}, Ser^{740}), with the NH_2-terminal heavy-chain and COOH-terminal light-chain of Pm connected through two or more disulfide bonds (24,26). As a serine proteinase, Pm degrades cross-linked fibrin networks within thrombi, resulting in blood clot dissolution, which will be discussed in more detail below. When generated in the extracellular milieu, Pm can degrade fibronectin and other extracellular matrix proteins allowing for higher permeability between cell layers (27).

Much of the functional interaction between Pg/Pm and fibrin occurs through the Pg/Pm kringle domains. The kringle domains (~10 kDa each) have highly conserved sequence homology and homology with similar domains found in prothrombin, tissue-type plasminogen activator, urokinase, and factor XII (27). Three of the Pg kringle

domains (kringles 1, 4, and 5) contain lysine binding sites (LBS) with moderate to low affinity for L-lysine and higher affinity for the lysine analogs, 6-aminohexanoic acid (6-AHA), and *trans*-4(aminomethyl)-cyclohexane carboxylic acid (19-23,26,27).

Early studies of the interaction between 6-AHA and Pg/Pm indicate that 6-AHA inhibits Pm activity with a K_I of ~0.32 M and inhibits Pg activation by streptokinase with a K_I of 0.96 mM (28,29). While there is some variation in the determined parameters among different studies, results of a representative study of 6-AHA binding to [Glu]Pg reveal one tight interaction (n = 0.93, K_D = 9 μM) and five weak interactions (n = 4.93, K_D = 5 mM) (20,27,30-32). [Glu]Pg and [Lys]Pg are held in separate structural conformations due to interaction of Lys^{50} and/or Lys^{62} in the NH_2-terminal PAN module of [Glu]Pg with the LBS of kringle 5 (33). As a result of the NH_2-terminal PAN module interaction with kringle 5, [Glu]Pg is held in a compact structural conformation. Early studies on the effect of 6-AHA binding on the physical properties of [Glu]Pg reveal a conformational change occurring as a function of 6-AHA concentration with a K_D of ~ 0.45 mM (19).

As it lacks the NH_2-terminal PAN module and resulting LBS interaction with kringle 5, [Lys]Pg adopts a partially extended conformation (16,34). A study on potential conformational changes in [Glu]Pg and [Lys]Pg suggested the existence of two conformational states. The T-state represented the compact conformation of [Glu]Pg and the R-state represented the expanded form of either [Lys]Pg or [Glu]Pg saturated with 6-AHA. Binding of 6-AHA was thought to have no effect on the conformation of [Lys]Pg (35).

A concurrent, landmark study revealed the presence of three distinct Pg conformations. This study employed three experimental methods (size exclusion high performance liquid chromatography (FPLC), small-angle x-ray scattering, and dynamic laser light scattering) to determine parameters (molecular elution time, radius of gyration, and stokes radius, respectively) for the effect of 6-AHA on [Glu]Pg and [Lys]Pg conformation (36). The authors used benzamidine, which selectively binds kringle 5, to disrupt the kringle 5-PAN interaction and isolate its effect on overall [Glu]Pg conformation (36). The results supported the presence of three distinct conformations summarized as follows: (1) the compact α-conformation is [Glu]Pg in the absence of ligand, (2) the partially extended β-conformation of [Lys]Pg/[Lys]Pm in the absence of ligand or [Glu]Pg in the presence of 50 mM benzamidine, and (3) the fully extended γ-conformation of [Lys]Pg/[Lys]Pm in the presence of 6-AHA or [Glu]Pg in the presence of 6-AHA ± benzamidine (Fig. 4) (36).

Physiological chloride ion stabilizes [Glu]Pg in the α-conformation, in which the LBS of kringle 4 is masked (34,37-40). The α-conformation of [Glu]Pg, however, is in an equilibrium with a low concentration (~25-40%) of a partially extended, β-conformation [Glu]Pg (20,32,34,41,42). Binding of a kringle 4-specific monoclonal antibody has been shown to enhance uPA activation of [Glu]Pg, indicating a shift from the kringle 4-accesible β-conformation to the γ-conformation (43,44). The extended β- and γ-conformations offer more accessibility of the LBS for protein interaction, and therefore, [Lys]Pg and ligand-bound [Glu]Pg are better substrates for activation than [Glu]Pg in the α-conformation (16,34-36,45). As chloride ion stabilizes [Glu]Pg in the α-conformation, chloride is classified as an inhibitor of [Glu]Pg activation (34,45,46).

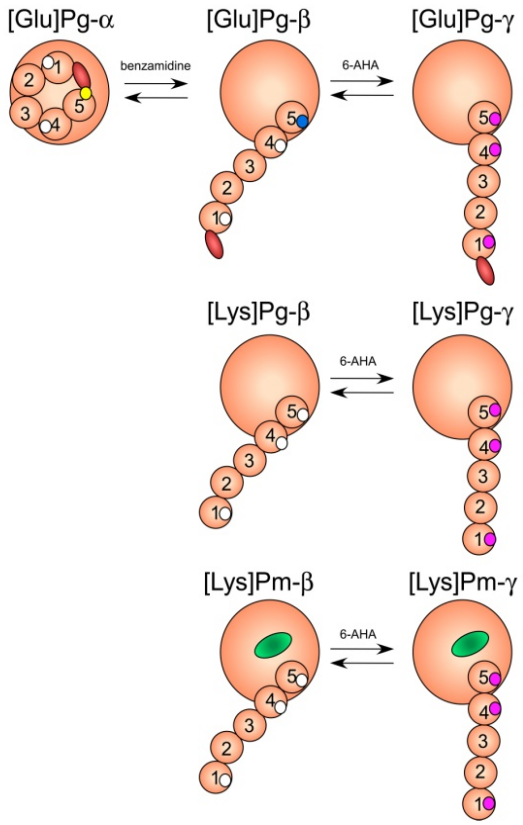

Figure 4. Schematic of Pg conformations. Native [Glu]Pg-α with the PAN-module (*red*) occupying the LBS of kringle 5 (*yellow*) and unoccupied kringle 1 and 4 LBS (*white*), with transition to [Glu]Pg-β and [Glu]Pg-γ upon LBS occupation by benzamidine (*blue*) and 6-AHA (*pink*), respectively. [Lys]Pg, and [Lys]Pm (active site in *green*) β- and γ-conformations illustrated with kringle LBS in the absence of ligand (*white*) and in the presence 6-AHA (*pink*), respectively.

Plasminogen Activation

Endogenous Pg activation occurs through proteolysis by one of two activators, urokinase and tissue-type plasminogen activator (tPA). The native form of urokinase, high molecular weight single-chain urokinase (uPA), is a 54 kDa protein which contains a serine proteinase catalytic domain (catalytic triad: Asp^{255}, His^{204}, Ser^{356}) in its COOH-terminal region, an epidermal growth factor domain, a finger-like domain, and one kringle domain in the NH_2-terminal region (Fig. 5) (47,48). The kringle domain of uPA

does not contain an LBS and therefore uPA lacks the fibrin-binding properties observed for tPA (27). The epidermal growth factor domain and kringle domain are removed following cleavage of the Glu^{143}-Leu^{144} peptide bond by metalloprotease, pump-1 to form low molecular weight urokinase (33 kDa) (47,49). Both uPA and low molecular weight urokinase are cleaved by Pm or kallikrein at the Lys^{158}-Ile^{159} peptide bond, to the more enzymatically active two-chain urokinase (47,48,50-52).

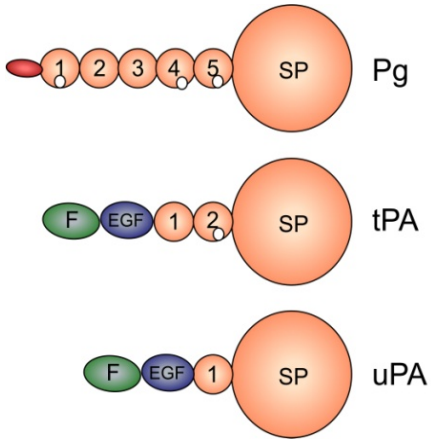

Figure 5. Cartoons of the semi-conserved domain structure of native Pg, tPA and uPA. Serine proteinase (*SP*), kringles (*1-5*), epidermal growth factor (*EGF*) and finger-like (*F*) domains with LBS illustrated as *white circles* (18,27).

Several studies have shown that activation of [Glu]Pg by uPA is enhanced by 6-AHA. This enhancement is due to the 6-AHA-induced α- to β/γ-conformational transition to a more rapidly activated [Glu]Pg molecule (34,45). The same enhancement occurs upon L-lysine binding of [Glu]Pg (53).

The low activity zymogen-like form of tPA, single-chain tPA (sctPA), is a 70 kDa protein (27). One structural difference from uPA is the presence of a second kringle domain within sctPA (tPA-kringle 2) which contains an LBS with high affinity for

lysine-sepharose, 6-AHA (K_D ~70 μM, (54)), intact fibrin (K_D ~1.4-3.3 nM (27,55)), and fibrin fragments (K_D ~1.2 nM (55)). The more active two-chain form of tPA (tctPA) is formed following cleavage of the Arg^{275}-Ile^{276} peptide bond by Pm (46). The activity of tPA toward Pg is greatly enhanced in the presence of effectors such as fibrin, cyanogen bromide fragments of fibrinogen, and 6-AHA. In steady-state kinetic studies of [Glu]Pg and [Lys]Pg activation by uPA and tPA, binding of 6-AHA results in a decrease in K_m with no appreciable effect on k_{cat} seen for uPA and varying degrees of k_{cat} enhancement seen for tPA (12,41,45,53,56-59).

Chloride is an inhibitor of uPA- and tPA-mediated [Glu]Pg activation as it stabilizes [Glu]Pg in the compact α-conformation, which is only very slowly activated by uPA and tPA. The K_I for chloride ion-mediated inhibition of [Glu]Pg activation by uPA and tPA is ~ 9 mM for each enzyme (34,46). One study of uPA-mediated [Glu]Pg activation determined the order of inhibitory level of several ions with the following ranked from highest level of inhibition to lowest: $I^->SCN^->Cl^->IO_3^->HCOO^->F^->OAc^-$ (45). As a result, acetate (OAc^-) is commonly used in place of chloride to study [Glu]Pg in the extended β/γ-conformations independent of changes in ionic strength. The effector molecules bind through the Pg LBS to extend the conformation of [Glu]Pg to the β/γ-conformations, thereby reversing the chloride-mediated inhibition and enhancing activation by uPA and tPA (34,45,46,55).

While lysine and 6-AHA serve as excellent tools for *in vitro* study of Pg kringle domain interactions, it is the study of fibrin-Pg interactions that is most physiologically relevant. Early studies suggested that Pg bound the central E region of fibrin, however it is now accepted that Pg kringle 5 binds within the D region of fibrin (Fig. 6) (12,33,60).

It is also through the D region that interaction with tPA-kringle 2, but not uPA, occurs (12,61). As an example of the highly regulated nature of thrombosis and fibrinolysis, it is the culmination of the coagulation cascade at fibrinogen to fibrin proteolysis that exposes cryptic tPA and Pg binding sites in the D region of fibrin, triggering initiation of fibrinolysis (12). Binding of fibrin to Pg kringle 5 results in the α- to β- conformational transition in [Glu]Pg which enhances binding and subsequent Pm generation. A ternary complex is formed upon binding of tPA and Pg to fibrin resulting in Pg activation. The Pm generated cleaves fibrin between the D and E regions. The limited fibrin proteolysis results in new COOH-terminal Lys residues which have been shown to bind the remaining LBS on Pg, promoting the β- to γ-conformational transition and accelerating Pm activation, fibrin proteolysis, and clot dissolution (12,33,55).

The process of Pg activation stimulation by fibrin is inhibited by the glycoprotein metallocarboxypeptidase, thrombin-activatable fibrinolysis inhibitor (TAFI). The mechanism of inhibition by TAFI will be described in more detail to follow. Briefly, TAFI hydrolyzes lysine and arginine residues, resulting in removal of the carboxy-terminal lysine residues of fibrin generated upon limited proteolysis by Pm that are responsible for enhanced Pg binding and activation to Pm. The removal of these residues impedes the cofactor function of fibrin in tPA-mediated Pg activation (62).

In contrast to easily isolated and controlled solution studies, studies of tPA-mediated activation of Pg in plasma are inherently complicated to interpret. Single-chain tPA (sctPA) is cleaved to the more enzymatically active two-chain form (tctPA) in clot lysis assays performed with ^{125}I-sctPA (63). Clot lysis assays have also shown that prior to total clot lysis, ~ 20 % of [Glu]Pg is proteolytically converted to [Lys]Pg (64). These

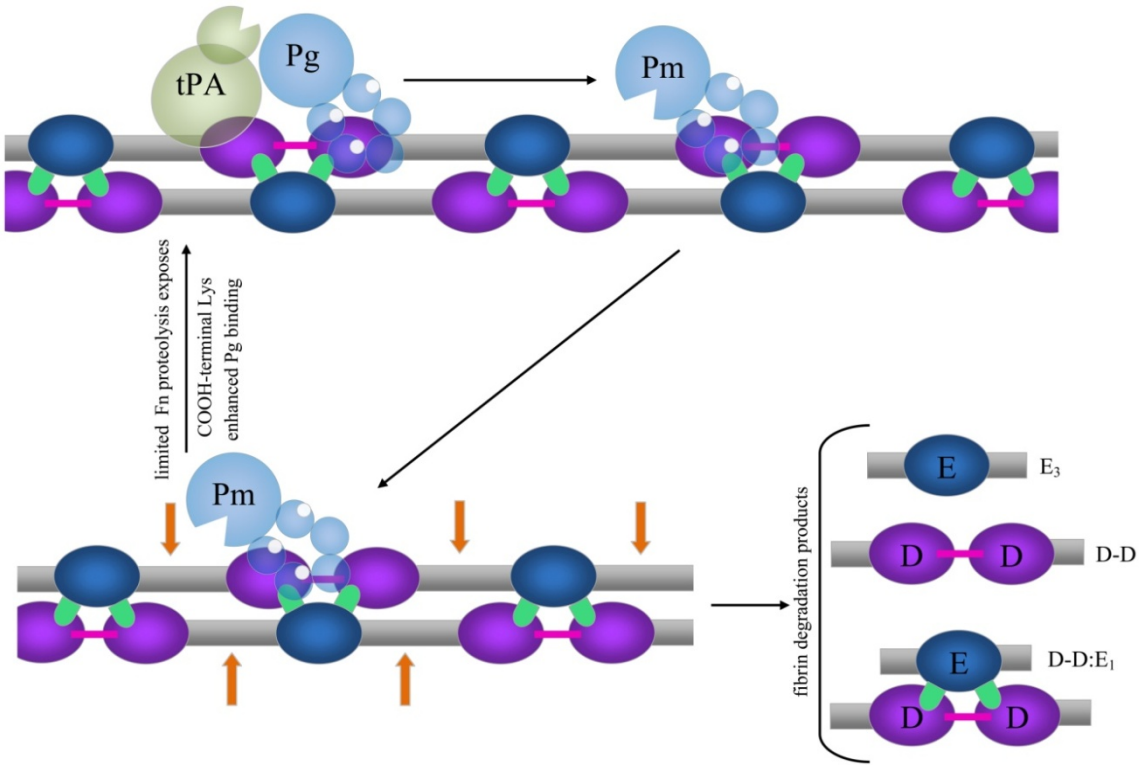

Figure 6. Illustration of fibrin-bound tPA-mediated Pg activation and fibrin degradation (12). Pg kringle 5 and tPA-kringle 2 bind fibrin in the D region (*purple*) forming a ternary complex, followed by proteolysis in the catalytic domain of Pg to Pm. Pm cleaves fibrin between the D (*purple*) and E (*blue*) regions represented by *orange arrows* resulting in FXIIIa-cross-linked (*pink*) fibrin degradation products (E_3, *D-D and* $D\text{-}D\text{:}E_1$). Limited proteolysis results in exposure of novel COOH-terminal fibrin Lys residues which bind Pg kringle 1 and kringle 4 to enhance binding and in turn enhance Pm generation and fibrin proteolysis. The fibrin degradation product *D-D:E1* is the smallest unit shown to stimulate Pg activation by tPA (12).

two proteolytic cleavage events, from less active/less activated precursors to more active/more readily activated species, cause clot lysis assays to be inherently complicated to interpret. For this reason, clot lysis assays will be used in this thesis for mainly qualitative purposes.

Administration of purified plasminogen activators is currently a main therapeutic approach to treatment of myocardial infarction. In addition to some bacterial plasminogen activators to be discussed later, several recombinant forms of uPA and tPA are currently

used as drug treatments with varying degrees of efficacy (65,66). Effective thrombolytic therapy must balance efficient reversal of vessel occlusion with the risk for intracranial hemorrhage (65,66). As the use of bacterial-derived therapeutic agents comes with the potential for immune or allergic response, genetic optimization of recombinant tPA and uPA remains the focus of the majority of research in the field (65,66).

Inhibitors of Plasmin and Plasminogen Activation

Inhibition of the fibrinolytic system is critical to maintaining the balance between proper vascular repair to prevent bleeding and aberrant thrombus formation. The balance of this system is partly regulated by inhibition of the main enzymes involved: Pm, uPA and tPA. The majority of plasma proteases are regulated by a class of inhibitors called serine protease inhibitors or serpins, which have a highly conserved fold structure consisting of a bundle of nine α-helices, and a β-sandwich of three β-sheets (67). The mechanism of serpin inhibition is well studied and complex. Briefly, serpins form an encounter complex (or Michaelis complex) with the serine protease, where the reactive center loop of the serpin is recognized by the protease as a substrate (bait). This is followed by cleavage of the reactive center loop and dragging of the acyl-enzyme to the opposite pole of the serpin by insertion of the reactive center loop into β-sheet A. The result is formation of a terminal covalent complex where the protease is trapped in an inactive state (67).

The main inhibitor of circulating Pm is the serpin α_2-antiplasmin (α_2-AP), a 63 kDa glycoprotein which circulates at ~ 70 μg/ml and has a half-life of ~ 2.6 days (12,27,67,68). Pm bound to fibrin is protected from inactivation by α_2-AP, allowing for

efficient fibrin proteolysis. The main inhibitor of uPA and tPA is the serpin, plasminogen activator inhibitor-1 (PAI-1), a 50 kDa glycoprotein that has a half-life of ~1.2 hours (67,69). This serpin is the main physiological inhibitor of plasminogen activation (67). As with α_2-AP and Pm, fibrin-bound tPA is protected from inactivation by PAI-1 (67-69). The major non-serpin inhibitor of fibrinolysis is TAFI, which circulates as a zymogen and is activated proteolytically by thrombin, trypsin, or plasmin (62,68). Activated TAFI is a metallocarboxypeptidase that cleaves the Pm-generated COOH-terminal Lys residues from fibrin, preventing further Pg/Pm binding and inhibiting further fibrin proteolysis (62,68). The presence of inhibitors in the fibrinolytic cascade ensures that thrombus formation is restricted to sites of vessel injury and ensures thrombus dissolution only following vessel repair.

Thrombosis and Fibrinolysis in Bacterial Infection

Many bacterial species target the human haemostatic and fibrinolytic systems in their mechanisms of pathogenesis. These processes are manipulated by many bacterial types; however, for these purposes only mechanisms employed by the gram-positive staphylococci and streptococci will be discussed. *Staphylococcus aureus* causes skin infections such as impetigo and serious invasive diseases like endocarditis, septic arthritis, and sepsis (70). Acute bacterial endocarditis (ABE) is a disease of high (~ 40 %) mortality with risk factors including intravenous drug use, and heart valve replacement (71). The streptococci are composed of heterogeneous groups of pathogens which differ in their disease states. Group A, C, and G streptococci cause pharyngitis (strep throat), scarlet fever, and skin infections like impetigo, as well as severe invasive infections like

toxic shock-like syndrome, endocarditis, and necrotizing fasciitis (70). Group B streptococci (GBS) cause severe diseases including sepsis, meningitis, arthritis, and endocarditis in neonates, pregnant women, and immune-compromised patients (72,73). *Streptococcus agalactiae* (GBS) serotype V is emerging as an invasive GBS pathogen with particular morbidity and mortality in neonates (74-76).

The blood coagulation system is targeted by two main proteins secreted by *S. aureus*. Staphylocoagulase (SC) and von Willebrand factor-binding protein (VWBP) are members of a recently established family of structural homologs known as zymogen activator and adhesion proteins (ZAAPs) (77). Although the specific mechanism of action differs, both SC and VWBP circumvent the blood coagulation system to cause unregulated, non-proteolytic prothrombin activation, resulting in fibrinogen to fibrin proteolysis (77-80). This mechanism is involved in the pathogenesis of ABE, which involves formation of bacteria-containing thrombotic vegetations on heart valves (81). The efficient, unregulated deposition of fibrin by these secreted *S. aureus* proteins is thought to contribute to the high mortality of this disease (77,78,80).

In addition, the initial host-defense response to bacterial infection is tissue-factor initiated blood clotting to form a protective fibrin wall of defense against invasion. Activation of the fibrinolytic system is a mechanism of bacterial pathogenesis employed by staphylococci and streptococci through expression of cell-surface Pg binding proteins and the secretion of Pg activators to escape the fibrin barriers. In this mechanism, the bacteria can hijack the host fibrinolytic system to cause increased Pm generation, which can degrade the fibrin barrier and extracellular matrix proteins to disseminate spread of the bacteria through soft tissue (27). Activation of Pg localized on the cell surface

through Pg binding proteins such as Pg-binding Group A M-like protein (PAM, Group A, C, G streptococci), glyceraldehyde-3-phosphate dehydrogenase (GAPDH, Group A, B, C streptococci), and α-enolase (Group A, B streptococci) can result in coating of the cell surface with Pg or active Pm (18,82-86). Pg activating proteins secreted by the bacteria, such as streptokinase and staphylokinase, are not enzymes themselves but form complexes with Pg or Pm to facilitate Pg activation. This proteolysis can occur localized to bacterial cell surfaces through Pg-binding proteins or systemically by secreted Pg activators in the vascular system.

Bacterial Plasminogen Activators

Streptokinase (SK), a 47 kDa protein secreted from Group A, C and G streptococci, is a well studied bacterial Pg activator (18). SK consists of three β-grasp domains (α, β, and γ) joined by flexible linker segments (Fig. 7) (87,88). It activates Pg through a non-proteolytic mechanism of conformational activation known as the molecular sexuality mechanism (89). Briefly, when SK binds Pg, an immediate conformational change occurs and SK inserts its own NH_2-terminus into the Pg NH_2-terminal binding pocket. This results in another conformational change within the catalytic domain of Pg generating the oxyanion hole and primary substrate binding site (S1site) required for proteolytic activity. This conformationally active SK•Pg* complex then binds a second Pg molecule in the substrate mode which is proteolytically converted to Pm (90-98). Binding of Pg as a substrate occurs through an LBS interaction between kringle 5 and residues Arg^{253}, Lys^{256}, and Lys^{257} in the 250-loop of SK (99). The Pm generated binds more tightly to SK than Pg, forming a SK•Pm catalytic complex that

propagates Pg activation (98). Similar to fibrin-bound Pm, Pm bound by SK is protected from inhibition by α_2-AP (100).

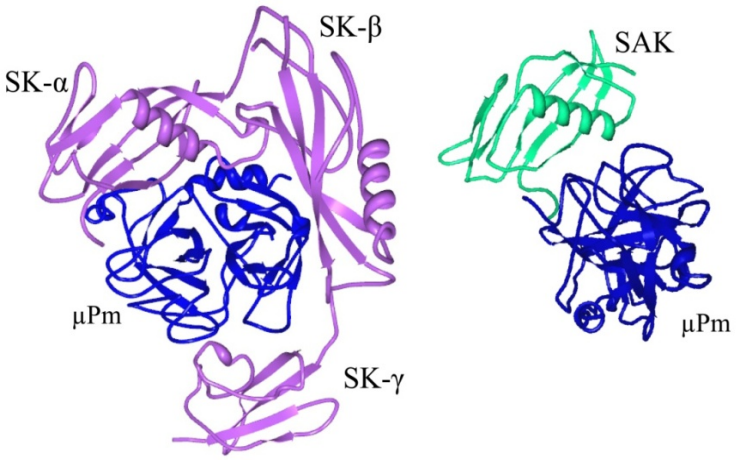

Figure 7. Crystal structure of bacterial Pg activators with human Pm catalytic domain. Complexes of SK (*purple*) and SAK (*green*) with the human Pm catalytic domain, μPm (*blue*) illustrating structural similarity between the SK-α domain and SAK, generated using PDB Protein Workshop 3.7 with PDB files 1BML (SK) and 1BUI (SAK) (15,87,101).

Staphylokinase (SAK) is a 16 kDa protein homologous to the α-domain of SK that is secreted by *Staphylococcus aureus* (Fig. 7) (101). Proteolytic Pg activation by SAK occurs in the presence of catalytic concentrations of Pm. Pg activation occurs when SAK binds Pm, altering its substrate specificity into a protease capable of activating Pg (102-104). In contrast to SK, SAK-bound Pm is susceptible to inhibition by α_2-AP and therefore requires a fibrin cofactor *in vivo* (100). PauB and its homolog from *S. uberis*, PauA appear to follow a mechanism similar to SK, including formation of a non-proteolytically activated Pg complex, followed by proteolysis of a substrate molecule of Pg, but are specific for activation of bovine Pg (105-109).

Streptococcus agalactiae Pathogenesis

Streptococcus agalactiae (Group B streptococci) interacts with the fibrinolytic system through surface expression of two known Pg binding proteins, α-enolase and GAPDH (82-84,100,110). While complete proteomic studies have not been performed, there are no known *Streptococcus agalactiae*-secreted proteins with human fibrinolytic activity. Group B streptococci is the only species of streptococci that does not express SK. Genomic sequencing of a *Streptococcus agalactiae* serotype V clinical isolate (2603 V/R) revealed 2,175 predicted genes (74-76,111,112). The gene of interest in this work, *NP_688136.1*, corresponds to a novel protein subsequently named skizzle (SkzL), with unknown function. A sequence homology search revealed that SkzL contains 22% identity to SK from *S. equisimilis* and *S. pyogenes*, 33% identity to SAK from *S. aureus*, and 24% identity to PauB from *S. uberis*. As a result, it was hypothesized that SkzL would bind Pg and activate Pg to Pm. Initial studies, however, revealed that SkzL does not directly activate Pg to Pm.

As the work in Chapters 2 and 3 of this thesis shows, SkzL binds tightly to [Lys]Pg and Pm and weakly to [Glu]Pg in an LBS-dependent manner facilitated by the SkzL COOH-terminal Lys^{415} residue. As SkzL enhances [Glu]Pg activation by uPA to levels seen with 6-AHA, it is hypothesized that SkzL-binding induces the [Glu]Pg α- to γ-conformational transition. While the exact mechanism is still unclear, SkzL enhances activation of [Glu]Pg and [Lys]Pg activation by tPA, likely through formation of a ternary complex. SkzL enhances plasma clot lysis by both tPA and uPA, providing the rationale for a physiological role for the interaction of SkzL with Pg in the context of *S. agalactiae* pathogenesis.

References

1. Colman, R. W. C., Alexander W.; Goldhaber, Samuel Z.; Marder, Victor J.; George, James N. (ed) (2006) *Hemostasis and Thrombosis: Basic Principles and Clinical Practice*, Lippincott Williams and Wilkins

2. Furie, B., and Furie, B. C. (1988) *Cell* **53**, 505-518

3. Schenone, M., Furie, B. C., and Furie, B. (2004) *Curr Opin Hematol* **11**, 272-277

4. Gailani, D., and Renne, T. (2007) *Arterioscler Thromb Vasc Biol* **27**, 2507-2513

5. Mackman, N., Tilley, R. E., and Key, N. S. (2007) *Arterioscler Thromb Vasc Biol* **27**, 1687-1693

6. Bock, P. E., Panizzi, P., and Verhamme, I. M. (2007) *J Thromb Haemost* **5 Suppl 1**, 81-94

7. Bianchini, E. P., Orcutt, S. J., Panizzi, P., Bock, P. E., and Krishnaswamy, S. (2005) *Proc. Natl. Acad. Sci. U S A* **102**, 10099-10104

8. Hacisalihoglu, A., Panizzi, P., Bock, P. E., Camire, R. M., and Krishnaswamy, S. (2007) *J. Biol. Chem.* **282**, 32974-32982

9. Wolberg, A. S. (2007) *Blood Rev* **21**, 131-142

10. Mosesson, M. W. (2005) *J Thromb Haemost* **3**, 1894-1904

11. Weisel, J. W. (2005) *Adv Protein Chem* **70**, 247-299

12. Medved, L., and Nieuwenhuizen, W. (2003) *Thromb. Haemost.* **89**, 409-419

13. Mosesson, M. W. (1998) *Semin Thromb Hemost* **24**, 169-174

14. Kollman, J. M., Pandi, L., Sawaya, M. R., Riley, M., and Doolittle, R. F. (2009) *Biochemistry* **48**, 3877-3886

15. Moreland, J. L., Gramada, A., Buzko, O. V., Zhang, Q., and Bourne, P. E. (2005) *BMC Bioinformatics* **6**, 21

16. Ponting, C. P., Marshall, J. M., and Cederholm-Williams, S. A. (1992) *Blood Coagul Fibrinolysis* **3**, 605-614

17. Sottrup-Jensen. (1978) *Progress in chemical fibrinolysis and thrombolysis*, Raven Press, New York

18. Lahteenmaki, K., Kuusela, P., and Korhonen, T. K. (2001) *FEMS Microbiol. Rev.* **25**, 531-552

19. Brockway, W. J., and Castellino, F. J. (1972) *Arch Biochem Biophys* **151**, 194-199

20. Markus, G., DePasquale, J. L., and Wissler, F. C. (1978) *J. Biol. Chem.* **253**, 727-732

21. Robbins, K. C., Boreisha, I. G., Arzadon, L., and Summaria, L. (1975) *J. Biol. Chem.* **250**, 4044-4047

22. Sjoholm, I. (1973) *Eur. J. Biochem.* **39**, 471-479

23. Violand, B. N., Byrne, R., and Castellino, F. J. (1978) *J. Biol. Chem.* **253**, 5395-5401

24. Robbins, K. C., Summaria, L., Hsieh, B., and Shah, R. J. (1967) *J. Biol. Chem.* **242**, 2333-2342

25. Summaria, L., Hsieh, B., and Robbins, K. C. (1967) *J. Biol. Chem.* **242**, 4279-4283

26. Castellino, F. J., and Powell, J. R. (1981) *Methods Enzymol.* **80 Pt C**, 365-378

27. Henkin, J., Marcotte, P., and Yang, H. C. (1991) *Prog. Cardiovasc. Dis.* **34**, 135-164

28. Abiko, Y., Iwamoto, M., and Tomikawa, M. (1969) *Biochim Biophys Acta* **185**, 424-431

29. Brockway, W. J., and Castellino, F. J. (1971) *J. Biol. Chem.* **246**, 4641-4647

30. Lerch, P. G., Rickli, E. E., Lergier, W., and Gillessen, D. (1980) *Eur. J. Biochem.* **107**, 7-13

31. Lin, L. F., Houng, A., and Reed, G. L. (2000) *Biochemistry* **39**, 4740-4745

32. Markus, G., Priore, R. L., and Wissler, F. C. (1979) *J. Biol. Chem.* **254**, 1211-1216

33. Cockell, C. S., Marshall, J. M., Dawson, K. M., Cederholm-Williams, S. A., and Ponting, C. P. (1998) *Biochem J* **333 (Pt 1)**, 99-105

34. Urano, T., Chibber, B. A., and Castellino, F. J. (1987) *Proc. Natl. Acad. Sci. U S A* **84**, 4031-4034

35. McCance, S. G., and Castellino, F. J. (1995) *Biochemistry* **34**, 9581-9586

36. Marshall, J. M., Brown, A. J., and Ponting, C. P. (1994) *Biochemistry* **33**, 3599-3606

37. Castellino, F. J., Brockway, W. J., Thomas, J. K., Liano, H. T., and Rawitch, A. B. (1973) *Biochemistry* **12**, 2787-2791

38. Hochschwender, S. M., and Laursen, R. A. (1981) *J. Biol. Chem.* **256**, 11172-11176

39. Plow, E. F., and Collen, D. (1981) *J. Biol. Chem.* **256**, 10864-10869

40. Vali, Z., and Patthy, L. (1982) *J. Biol. Chem.* **257**, 2104-2110

41. Markus, G. (1996) *Fibrinolysis* **10**, 75-85

42. Weisel J. W., N. C., Korsholm B., Petersen L. C., Suenson E. (1984) *J. Mol. Biol.* **235**, 1117-1135

43. Cummings, H. S., and Castellino, F. J. (1985) *Arch Biochem Biophys* **236**, 612-618

44. Ploplis, V. A., Cummings, H. S., and Castellino, F. J. (1982) *Biochemistry* **21**, 5891-5897

45. Urano, T., Sator de Serrano, V., Chibber, B. A., and Castellino, F. J. (1987) *J. Biol. Chem.* **262**, 15959-15964

46. Urano, T., Sator de Serrano, V., Gaffney, P. J., and Castellino, F. J. (1988) *Biochemistry* **27**, 6522-6528

47. de Munk, G. A., Groeneveld, E., and Rijken, D. C. (1993) *Thromb. Haemost.* **70**, 481-485

48. Lijnen, H. R., De Cock, F., and Collen, D. (1994) *Eur. J. Biochem.* **224**, 567-574

49. Novokhatny, V., Medved, L., Lijnen, H. R., and Ingham, K. (1995) *J. Biol. Chem.* **270**, 8680-8685

50. Lijnen, H. R., Nelles, L., Van Hoef, B., Demarsin, E., and Collen, D. (1988) *Eur. J. Biochem.* **177**, 575-582

51. Lijnen, H. R., Van Hoef, B., Nelles, L., and Collen, D. (1990) *J. Biol. Chem.* **265**, 5232-5236

52. Nelles, L., Lijnen, H. R., Collen, D., and Holmes, W. E. (1987) *J. Biol. Chem.* **262**, 5682-5689

53. Peltz, S. W., Hardt, T. A., and Mangel, W. F. (1982) *Biochemistry* **21**, 2798-2804

54. de Munk, G. A., Caspers, M. P., Chang, G. T., Pouwels, P. H., Enger-Valk, B. E., and Verheijen, J. H. (1989) *Biochemistry* **28**, 7318-7325

55. Fleury, V., Loyau, S., Lijnen, H. R., Nieuwenhuizen, W., and Angles-Cano, E. (1993) *Eur. J. Biochem.* **216**, 549-556

56. Hoylaerts, M., Rijken, D. C., Lijnen, H. R., and Collen, D. (1982) *J. Biol. Chem.* **257**, 2912-2919

57. Zamarron, C., Lijnen, H. R., and Collen, D. (1984) *J. Biol. Chem.* **259**, 2080-2083

58. Ranby, M. (1982) *Biochim Biophys Acta* **704**, 461-469

59. Silverstein, R. L., Nachman, R. L., Leung, L. L., and Harpel, P. C. (1985) *J. Biol. Chem.* **260**, 10346-10352

60. Lucas, M. A., Fretto, L. J., and McKee, P. A. (1983) *J. Biol. Chem.* **258**, 4249-4256

61. Horrevoets, A. J., Smilde, A., de Vries, C., and Pannekoek, H. (1994) *J. Biol. Chem.* **269**, 12639-12644

62. Bouma, B. N., and Mosnier, L. O. (2003) *Pathophysiol Haemost Thromb* **33**, 375-381

63. Rijken, D. C., Hoylaerts, M., and Collen, D. (1982) *J. Biol. Chem.* **257**, 2920-2925

64. Fredenburgh, J. C., and Nesheim, M. E. (1992) *J. Biol. Chem.* **267**, 26150-26156

65. Armstrong, P. W., and Collen, D. (2001) *Circulation* **103**, 2862-2866

66. Collen, D., and Lijnen, H. R. (1991) *Blood* **78**, 3114-3124

67. Rau, J. C., Beaulieu, L. M., Huntington, J. A., and Church, F. C. (2007) *J Thromb Haemost* **5 Suppl 1**, 102-115

68. Fay, W. P., Garg, N., and Sunkar, M. (2007) *Arterioscler Thromb Vasc Biol* **27**, 1231-1237

69. Kvassman, J. O., Verhamme, I., and Shore, J. D. (1998) *Biochemistry* **37**, 15491-15502

70. Nitsche-Schmitz, D. P., Rohde, M., and Chhatwal, G. S. (2007) *Thromb. Haemost.* **98**, 488-496

71. Rivera, J., Vannakambadi, G., Hook, M., and Speziale, P. (2007) *Thromb. Haemost.* **98**, 503-511

72. Schuchat, A. (1999) *Lancet* **353**, 51-56

73. Pietrocola, G., Schubert, A., Visai, L., Torti, M., Fitzgerald, J. R., Foster, T. J., Reinscheid, D. J., and Speziale, P. (2005) *Blood* **105**, 1052-1059

74. Blumberg, H. M., Stephens, D. S., Modansky, M., Erwin, M., Elliot, J., Facklam, R. R., Schuchat, A., Baughman, W., and Farley, M. M. (1996) *J. Infect. Dis.* **173**, 365-373

75. Brochet, M., Couve, E., Zouine, M., Vallaeys, T., Rusniok, C., Lamy, M. C., Buchrieser, C., Trieu-Cuot, P., Kunst, F., Poyart, C., and Glaser, P. (2006) *Microbes Infect.*

76. Fluegge, K., Schweier, O., Schiltz, E., Batsford, S., and Berner, R. (2004) *Eur. J. Clin. Microbiol. Infect. Dis.* **23**, 818-824

77. Panizzi, P., Friedrich, R., Fuentes-Prior, P., Bode, W., and Bock, P. E. (2004) *Cell Mol. Life Sci.* **61**, 2793-2798

78. Kroh, H. K., Panizzi, P., and Bock, P. E. (2009) *Proc. Natl. Acad. Sci. U S A* **106**, 7786-7791

79. Panizzi, P., Friedrich, R., Fuentes-Prior, P., Kroh, H. K., Briggs, J., Tans, G., Bode, W., and Bock, P. E. (2006) *J. Biol. Chem.* **281**, 1169-1178

80. Panizzi, P., Friedrich, R., Fuentes-Prior, P., Richter, K., Bock, P. E., and Bode, W. (2006) *J. Biol. Chem.* **281**, 1179-1187

81. Korzeniowski OM, K. D. (1992) *Infective Endocarditis*, W.B. Saunders, Philadelphia

82. Bergmann, S., Wild, D., Diekmann, O., Frank, R., Bracht, D., Chhatwal, G. S., and Hammerschmidt, S. (2003) *Mol. Microbiol.* **49**, 411-423

83. Magalhaes, V., Veiga-Malta, I., Almeida, M. R., Baptista, M., Ribeiro, A., Trieu-Cuot, P., and Ferreira, P. (2007) *Microbes Infect.* **9**, 1276-1284

84. Whiting, G. C., Evans, J. T., Patel, S., and Gillespie, S. H. (2002) *J. Med. Microbiol.* **51**, 837-843

85. Boyle, M. D., and Lottenberg, R. (1997) *Thromb. Haemost.* **77**, 1-10

86. Cork, A. J., Jergic, S., Hammerschmidt, S., Kobe, B., Pancholi, V., Benesch, J. L., Robinson, C. V., Dixon, N. E., Aquilina, J. A., and Walker, M. J. (2009) *J. Biol. Chem.* **284**, 17129-17137

87. Wang, X., Lin, X., Loy, J. A., Tang, J., and Zhang, X. C. (1998) *Science* **281**, 1662-1665

88. Wang, X., Tang, J., Hunter, B., and Zhang, X. C. (1999) *FEBS Lett.* **459**, 85-89

89. Bode, W., and Huber, R. (1976) *FEBS Lett.* **68**, 231-236

90. Boxrud, P. D., and Bock, P. E. (2000) *Biochemistry* **39**, 13974-13981

91. Boxrud, P. D., and Bock, P. E. (2004) *J. Biol. Chem.* **279**, 36642-36649

92. Boxrud, P. D., Verhamme, I. M., and Bock, P. E. (2004) *J. Biol. Chem.* **279**, 36633-36641

93. Boxrud, P. D., Verhamme, I. M., Fay, W. P., and Bock, P. E. (2001) *J. Biol. Chem.* **276**, 26084-26089

94. Gladysheva, I. P., Sazonova, I. Y., Houng, A., Hedstrom, L., and Reed, G. L. (2007) *Biochemistry* **46**, 8879-8887

95. Wang, S., Reed, G. L., and Hedstrom, L. (1999) *Biochemistry* **38**, 5232-5240

96. Wang, S., Reed, G. L., and Hedstrom, L. (2000) *Eur. J. Biochem.* **267**, 3994-4001

97. Bean, R. R., Verhamme, I. M., and Bock, P. E. (2005) *J. Biol. Chem.* **280**, 7504-7510

98. Boxrud, P. D., Fay, W. P., and Bock, P. E. (2000) *J. Biol. Chem.* **275**, 14579-14589

99. Tharp, A. C., Laha, M., Panizzi, P., Thompson, M. W., Fuentes-Prior, P., and Bock, P. E. (2009) *J. Biol. Chem.* **284**, 19511-19521

100. Bergmann, S., and Hammerschmidt, S. (2007) *Thromb. Haemost.* **98**, 512-520

101. Parry, M. A., Fernandez-Catalan, C., Bergner, A., Huber, R., Hopfner, K. P., Schlott, B., Guhrs, K. H., and Bode, W. (1998) *Nat. Struct. Biol.* **5**, 917-923

102. Esmon, C. T., and Mather, T. (1998) *Nat. Struct. Biol.* **5**, 933-937

103. Grella, D. K., and Castellino, F. J. (1997) *Blood* **89**, 1585-1589

104. Jespers, L., Vanwetswinkel, S., Lijnen, H. R., Van Herzeele, N., Van Hoef, B., Demarsin, E., Collen, D., and De Maeyer, M. (1999) *Thromb. Haemost.* **81**, 479-485

105. Ward, P. N., Field, T. R., Rosey, E. L., Abu-Median, A. B., Lincoln, R. A., and Leigh, J. A. (2004) *J. Mol. Biol.* **342**, 1101-1114

106. Johnsen, L. B., Rasmussen, L. K., Petersen, T. E., Etzerodt, M., and Fedosov, S. N. (2000) *Biochemistry* **39**, 6440-6448

107. Sazonova, I. Y., Houng, A. K., Chowdhry, S. A., Robinson, B. R., Hedstrom, L., and Reed, G. L. (2001) *J. Biol. Chem.* **276**, 12609-12613

108. Ward, P. N., and Leigh, J. A. (2002) *J Bacteriol* **184**, 119-125

109. Ward, P. N., and Leigh, J. A. (2004) *Indian J. Med. Res.* **119 Suppl**, 136-140

110. Hughes, M. J., Moore, J. C., Lane, J. D., Wilson, R., Pribul, P. K., Younes, Z. N., Dobson, R. J., Everest, P., Reason, A. J., Redfern, J. M., Greer, F. M., Paxton, T., Panico, M., Morris, H. R., Feldman, R. G., and Santangelo, J. D. (2002) *Infect. Immun.* **70**, 1254-1259

111. Fluegge, K., Supper, S., Siedler, A., and Berner, R. (2004) *Antimicrob Agents Chemother* **48**, 4444-4446

112. Tettelin, H., Masignani, V., Cieslewicz, M. J., Eisen, J. A., Peterson, S., Wessels, M. R., Paulsen, I. T., Nelson, K. E., Margarit, I., Read, T. D., Madoff, L. C., Wolf, A. M., Beanan, M. J., Brinkac, L. M., Daugherty, S. C., DeBoy, R. T., Durkin, A. S., Kolonay, J. F., Madupu, R., Lewis, M. R., Radune, D., Fedorova, N. B., Scanlan, D., Khouri, H., Mulligan, S., Carty, H. A., Cline, R. T., Van Aken, S. E., Gill, J., Scarselli, M., Mora, M., Iacobini, E. T., Brettoni, C., Galli, G., Mariani, M., Vegni, F., Maione, D., Rinaudo, D., Rappuoli, R., Telford, J. L., Kasper, D. L., Grandi, G., and Fraser, C. M. (2002) *Proc. Natl. Acad. Sci. U S A* **99**, 12391-12396

CHAPTER II

SKIZZLE IS A NOVEL PLASMINOGEN- AND PLASMIN-BINDING PROTEIN FROM *STREPTOCOCCUS AGALACTIAE* THAT TARGETS PROTEINS OF HUMAN FIBRINOLYSIS TO PROMOTE PLASMIN GENERATION

Karen G. Wiles*, Peter Panizzi[§], Heather K. Kroh*, and Paul E. Bock*

*Department of Pathology, Vanderbilt University, Nashville, TN 37232

[§]Center for Systems Biology, Massachusetts General Hospital, Boston, MA 02114

(This research was originally published in the Journal of Biological Chemistry. Karen G. Wiles, Peter Panizzi, Heather K. Kroh, and Paul E. Bock. Skizzle is a novel plasminogen- and plasmin-binding protein from *Streptococcus agalactiae* that targets proteins of human fibrinolysis to promote plasmin generation. 2010; 285(27): 21153-21164.

Abstract

Skizzle (SkzL), secreted by *Streptococcus agalactiae*, has moderate sequence identity to streptokinase and staphylokinase, bacterial activators of human plasminogen (Pg). SkzL binds [Glu]Pg with low affinity (K_D 3-16 μM), and [Lys]Pg and plasmin (Pm) with indistinguishable high affinity (K_D 80 nM and 50 nM, respectively). Binding of SkzL to Pg and Pm is completely lysine-binding site-dependent, as shown by the effect of the lysine analog, 6-aminohexanoic acid. Deletion of the COOH-terminal SkzL Lys^{415} residue reduces affinity for [Lys]Pg and active site-blocked Pm 30-fold, implicating Lys^{415} in a lysine-binding site interaction with a Pg/Pm kringle. SkzL binding to active site fluorescein-labeled Pg/Pm analogs demonstrates distinct high and low affinity interactions. High affinity binding is mediated by Lys^{415}, whereas the source of low affinity binding is unknown. SkzL enhances the activation of [Glu]Pg by urokinase (uPA) ~20-fold, to a maximum rate indistinguishable from that for [Lys]Pg and [Glu]Pg activation in the presence of 6-aminohexanoic acid. SkzL binds preferentially to the partially extended, β-conformation of [Glu]Pg, which is in unfavorable equilibrium with the compact, α-conformation, thereby converting [Glu]Pg to the fully extended, γ-conformation and accelerating the rate of its activation by uPA. SkzL enhances [Lys]Pg and [Glu]Pg activation by single-chain tissue-type Pg activator, ~42-fold and ~650-fold, respectively. SkzL increases the rate of plasma clot lysis by uPA and single-chain tissue-type Pg activator ~2-fold, confirming its cofactor activity in a physiological model system. The results suggest a role for SkzL in *S. agalactiae* pathogenesis through fibrinolytic enhancement.

Introduction

Group B streptococci (GBS)[1] cause severe diseases including sepsis, meningitis, arthritis, and endocarditis in neonates and immune-compromised patients (1,2). *Streptococcus agalactiae* serotype V is emerging as an invasive GBS pathogen with particular morbidity and mortality in neonates (3-5), but the mechanism of GBS pathogenesis is not fully understood. Unlike group A, C, and G streptococci, GBS does not express streptokinase (SK), a pathogenicity factor in group A streptococcal infection (6). Activation of the fibrinolytic system is a mechanism of bacterial pathogenesis employed by many bacteria through expression of cell-surface plasminogen (Pg)-binding proteins and the secretion of Pg activators. In this mechanism, aberrant upregulation of the fibrinolytic system increases plasmin (Pm) generation, which degrades fibrin and extracellular matrix to disseminate the bacteria through soft tissue (7). Activation of Pg on the cell-surface through Pg-binding proteins, such as Pg-binding group A streptococcal M-like protein (PAM; group A, C, and G streptococci), glyceraldehyde-3-phosphate dehydrogenase (GAPDH; group A, B, and C streptococci), and α-enolase (group A and B streptococci) results in coating of the cell surface with Pg or active Pm (8-12). A recent study indicated that Pg activation on the surface of *S. agalactiae* occurs through the GAPDH-bound Pg complex, facilitating GBS virulence and promoting bacterial dissemination in a murine model (10). Secreted Pg-activating proteins, such as SK and staphylokinase (SAK), are not enzymes themselves but form complexes with Pg or Pm to enable proteolytic Pm generation. This proteolysis can occur locally on bacterial cell surfaces through Pg-binding proteins or systemically by the free, secreted Pg-activators in the vascular system. Although complete proteomic functional studies

have not been performed, to date there are no known *S. agalactiae* secreted proteins with established human fibrinolytic activity.

Genomic sequencing of an *S. agalactiae* serotype V clinical isolate (2603 V/R) revealed 2,175 predicted genes (13), including *NP_688136.1*, which corresponds to a novel protein of unknown function, subsequently named skizzle (SkzL). SkzL has 22% sequence identity to SK from *Streptococcus equisimilis and pyogenes*, 33% to SAK from *Staphylococcus aureus* and 24% to PauB, a bovine Pg activator from *Streptococcus uberis* (14). In studies of genomic sequence diversity, SkzL (protein unnamed, gene name *sk1A2*) had weak similarity to SAK and SK (4). SAK, SK, and PauB facilitate the conversion of Pg into Pm, albeit through different mechanisms.

Native [Glu]Pg, the form circulating in blood, consists of an NH_2-terminal PAN (Pg/apple/nematode) module, 5 kringle domains, and a serine proteinase catalytic domain. Kringles 1, 4, and 5 contain lysine-binding sites (LBS) with moderate to low affinity for L-lysine and higher affinity for the lysine analog, 6-aminohexanoic acid (6-AHA) (15-20). Following cleavage by Pm, the NH_2-terminal 77-residue PAN module of [Glu]Pg is released to yield [Lys]Pg (18). As a result of the NH_2-terminal PAN module interaction with kringle 5, [Glu]Pg is stabilized in the compact α-conformation by physiological concentrations of chloride ion (21,22). The α-conformation of [Glu]Pg, however, is in equilibrium with a low concentration of a partially extended, β-conformation governed by the chloride ion concentration (17,22-25). Lacking the PAN module, [Lys]Pg adopts the β-conformation in the absence or presence of chloride ion (22,26). Upon low affinity binding of lysine analogs, such as 6-AHA to kringles 4 and 5, both [Glu]Pg and [Lys]Pg assume the fully extended γ-conformation (22,23,26-32).

Proteolytic Pg activation occurs through cleavage of the Arg^{561}-Val^{562} peptide bond in the catalytic domain to form Pm. SK activates Pg through a conformational, nonproteolytic molecular sexuality mechanism (33-38). The SK NH_2-terminus inserts into the NH_2-terminal binding cleft in the Pg catalytic domain, inducing a conformational change to form a functional active site capable of proteolytically activating substrate Pg molecules (34-41). Binding of Pg as a substrate occurs through LBS interaction between kringle 5 and residues Arg^{253}, Lys^{256}, and Lys^{257} in the 250-loop of SK (42). SAK facilitates activation of Pg in the presence of catalytic concentrations of Pm. Binding of SAK to Pm changes the substrate specificity of Pm, allowing activation of Pg (43-45). PauB and its homolog, PauA appear to follow a mechanism similar to SK, including formation of a nonproteolytically activated Pg complex, followed by proteolysis of substrate molecules of Pg, but are specific for activation of bovine Pg (46-50).

Human Pg is proteolytically activated endogenously by either of two activators, urokinase and tissue-type plasminogen activator (tPA). High molecular weight single-chain urokinase (uPA) contains a catalytic domain in the COOH-terminal region and an epidermal growth factor domain and one kringle domain in the NH_2-terminal region (51,52). The epidermal growth factor and kringle domains are liberated by cleavage at Glu^{143}-Leu^{144} by the metalloproteinase, pump-1 to form low molecular weight urokinase (52). Single-chain urokinase is converted to the more enzymatically active form, two-chain urokinase, through cleavage of Lys^{158}-Ile^{159} in the catalytic domain by Pm or kallikrein (51-55). The low activity zymogen-like form of tPA, single-chain tPA (sctPA), is a 70-kDa protein that is cleaved by Pm at Arg^{275}-Ile^{276} to form the more active two-chain tPA (56). One structural difference between tPA and uPA is the presence of a

second kringle domain in tPA containing an LBS with high affinity for lysine, 6-AHA, and fibrin fragments (57,58).

The modest sequence identity between SkzL and SK includes conservation of the NH_2-terminal (Ile^1-Ala^2-Gly^3) residues and the COOH-terminal Lys^{415} residue (Lys^{414} for SK) required for SK-induced Pg activation (36-39,59). Despite the presence of these residues and predicted secondary structure similarity to SK, SkzL could not be shown to activate Pg to Pm, conformationally or proteolytically, in the absence or presence of catalytic concentrations of Pm. The conservation of the COOH-terminal Lys residue suggested a potential binding interaction of SkzL with the LBS of a Pg and Pm kringle. The present studies were undertaken to characterize the binding interactions of SkzL with Pg and Pm and to elucidate its function as a potential fibrinolytic cofactor of uPA- and sctPA-catalyzed Pg activation. The studies show that SkzL is secreted from *S. agalactiae* serotype V and binds both Pg and Pm in a LBS-dependent manner, primarily through Lys^{415}. SkzL enhances uPA-catalyzed activation of [Glu]Pg by facilitating its conversion from the compact α-conformation to the fully extended γ-conformation, and enhances uPA-mediated plasma clot lysis. SkzL also enhances [Glu]Pg and [Lys]Pg activation by sctPA and plasma clot lysis by sctPA. To our knowledge, SkzL is the first secreted protein from *S. agalactiae* to be identified that usurps the human fibrinolytic system, presumably to enable dissemination of infection.

Experimental Procedures

Protein Purification and Characterization

[Glu]Pg, [Lys]Pg, and Pm (all carbohydrate form 2) were prepared as previously described (41,60,61). [5F]FFR-[Lys]Pg, [5F]FFR-[Glu]Pg, and [5F]FFR-Pm were generated by a thiol-specific reaction with 5-(iodoacetamido)fluorescein following inactivation of the SK-induced active site in [Lys]Pg and [Glu]Pg with N^{α}-[(acetylthio)acetyl]-D-Phe-Phe-Arg-CH_2Cl essentially as previously described (39-41,62). Native Pm activity was calculated based on known parameters for D-Val-Leu-Lys-*p*-nitroanalide (VLK-*p*NA) hydrolysis (41). Human high molecular weight uPA (Calbiochem) was reconstituted in ultra-pure water (yielding a solution containing 150 mM Cl^- contributed by NaCl and Tris-Cl). Protein concentration of uPA and sctPA were determined by bicinchoninic acid protein assay (Pierce). sctPA (Molecular Innovations) was stored in 0.5 M HEPES, 0.5 M NaCl, pH 7.4 buffer to ensure solubility and was limited to one freeze-thaw cycle to maintain stable activity.

The gene for SkzL (*NP_688136.1*) was cloned from *S. agalactiae* 2603 V/R genomic DNA (ATCC) into a modified Pet30b vector (59) containing a tobacco etch virus (TEV) protease-cleavable NH_2-terminal His_6 tag. SkzL was expressed by Rosetta2(DE3)plysS *Escherichia coli* (Novagen) in 0.1 mg/ml kanamycin following 0.5 mM isopropyl β-D-thiogalactopyranoside induction for 4 h at 30 °C. Following bacterial lysis by sonication, protein in the clarified supernatant was purified by Ni^{2+}-iminodiacetic acid-Sepharose (5 ml) chromatography in 50 mM HEPES, 325 mM NaCl, 20 mM imidazole, pH 7.4, eluted with a 50 ml gradient of 20-500 mM imidizole in the

equilibration buffer. Trace protein contaminants, including dimeric SkzL, were removed by anion exchange chromatography on Q-Sepharose (Amersham Biosciences) equilibrated with 50 mM HEPES, 50 mM NaCl, 1 mM EDTA, pH 7.4, eluted with a gradient of 50-500 mM NaCl over 30 column volumes. A 1:10 molar equivalent of recombinant tobacco etch virus protease was added to SkzL and the mixture was incubated for 12 h to liberate the His_6 tag, followed by repeated Ni^{2+}-iminodiacetic acid-Sepharose chromatography to separate noncleaved protein and free His_6 tag from cleaved protein (59). To preserve disulfide bond integrity, cleavage was performed in the absence of dithiothreitol. Tobacco etch virus protease cleavage resulted in the proper SkzL NH_2-terminal sequence as confirmed by NH_2-terminal sequencing (Ile^1-Ala^2-Gly^3-Pro^4-Ser^5). Cysteine-to-serine substitution mutants and the COOH-terminal lysine deletion mutant (SkzLΔK415) were generated by Quikchange site-directed mutagenesis (Stratagene) and purified as described. [5F]-SkzL was generated by reaction of free thiol groups with 5-(iodoacetamido)fluorescein followed by chromatography on Sephadex G-25 and dialysis to remove excess probe. Probe incorporation was determined to be 1.0 mol probe/mol SkzL by absorbance measurements at 280 and 498 nm with an absorption coefficient of 84,000 M^{-1} cm^{-1} for fluorescein and an $A_{280}/A_{498\ nm}$ ratio of 0.19 in 6 M guanidine, 100 mM Tris-HCl, 1 mM EDTA, pH 8.5 buffer (63).

All proteins were snap-frozen and stored in 50 mM HEPES, 125 mM NaCl, pH 7.4 at -80 °C. Protein concentrations were determined from the 280 nm-absorbance using the following absorption coefficients ($(mg/ml)^{-1}cm^{-1}$) and molecular masses (Da): [Glu]Pg, 1.69 and 92,000; [Lys]Pg and Pm, 1.69 and 84,000 (60,64). The SkzL absorption coefficient at 280 nm of 1.23 was calculated from the amino acid sequence

and confirmed by absorbance measurements (65). The molecular mass of 47,400 Da for SkzL was determined in excellent agreement with that calculated from the amino acid sequence by mass spectrometry using a Waters Acquity Ultraperformance LC/Thermo Finnigan LTQ with a lysozyme standard for optimization and calibration.

S. agalactiae Protein Expression

S. agalactiae serotype V was cultured in Todd-Hewitt yeast broth at 37 °C. Bacterial supernatant was obtained at various time points by centrifugation at 39,000 x g for 15 min. Secreted proteins were obtained by precipitation with trichloroacetic acid (7.5%) and washed with acetone for use in western blotting. A polyclonal rabbit anti-SkzL antibody was generated and purified by affinity chromatography on SkzL-coupled CNBr-activated Sepharose 4B (ProSci Inc.). Proteins were subjected to SDS-PAGE on 4-15% gradient gels, transferred onto polyvinylidine fluoride membranes, and developed with a BM Chemiluminescence Western Blotting Kit (Roche).

Fluorescence Equilibrium Binding

Titrations of 50 nM [5F]FFR-[Lys]Pg, [5F]FFR-[Glu]Pg, and [5F]FFR-Pm with wtSkzL and SkzLΔK415 were performed in 50 mM HEPES, 125 mM NaCl, 1 mM EDTA, 1 mg/ml PEG 8,000, 10 μM FFR-CH_2Cl, and 1 mg/ml bovine serum albumin, pH 7.4 at 25 °C using PEG 20,000-coated acyclic cuvettes. Titrations of active site-blocked fluorescent Pg/Pm analogs with wtSkzL and SkzLΔK415 performed without the use of polarizers revealed a high affinity decrease in fluorescence intensity, and a low affinity decrease in fluorescence anisotropy. Consequently, identical titrations were performed

with vertical excitation and emission at the magic angle to eliminate anisotropy effects. Excitation was at 500 nm and emission was measured at 516 nm with 4-nm band-passes.

Fluorescence titrations of native [Glu]Pg, [Lys]Pg, and FFR-Pm binding to 100 nM and 500 nM [5F]-SkzL were performed using identical buffer conditions. Fluorescence was measured with excitation at 492 nm and emission at 510 nm with 8-nm band-passes without the use of fluorescence polarization. Competitive binding experiments with 100 nM [5F]-SkzL in the absence and presence of fixed concentrations of wtSkzL or SkzLΔK415 to [Lys]Pg and FFR-Pm were performed under identical conditions. In these titrations, mixtures of [5F]-SkzL and either wtSkzL or SkzLΔK415 were pre-incubated for 10 min at 25 °C prior to titration with [Lys]Pg or FFR-Pm. Following correction for buffer blank and probe dilution (≤ 10%), data were expressed as the fractional change in the initial fluorescence, $(F_{obs}-F_o)/F_o = \Delta F/F_o$. Titrations were analyzed by nonlinear least-squares fitting of the quadratic binding Equation 1,

$$\frac{\Delta F}{F_o} = \left(\frac{\Delta F_{max}}{F_o}\right)\left[\frac{\left(n[P]_o + [L]_o + K_D\right) - \sqrt{\left(n[P]_o + [L]_o + K_D\right)^2 - 4n[P]_o[L]_o}}{2n[P]_o}\right] \qquad \textbf{Eqn. 1}$$

where $\Delta F_{max}/F_o$ is the maximum fluorescence change; K_D is the dissociation constant; n is the stoichiometric factor; $[P]_o$ is the total concentration of probe-labeled protein, and $[L]_o$ is the total ligand concentration (39-41,62). Competitive titrations were analyzed by nonlinear least-squares fitting of the cubic competitive binding equation for tight binding interactions to give dissociation constants for both ligand and competitor, with the stoichiometry fixed at 1 for the competitors (66).

Direct titrations of wtSkzL binding to [5F]FFR-[Lys]Pg and [5F]FFR-Pm performed without polarizers revealed an apparent anisotropy decrease, representing a second distinct binding interaction. These data were analyzed by nonlinear least-squares fitting of the sum of the solution to the quadratic equation (Equation 1) as $\Delta F_1/F_o$, with n=1 for the high affinity interaction, and a hyperbola for the weak interaction with the assumption that $[L]_{free} \approx [L]_o$ for this interaction,

$$\frac{\Delta F}{F_o} = \frac{\Delta F_1}{F_o} + \left(\frac{(\Delta F_{max\ 2} / F_o)[L]_o}{K_{D2} + [L]_o} \right) \qquad \textbf{Eqn. 2}$$

where K_{D1} obtained from the quadratic equation and K_{D2} are the dissociation constants for the high and low affinity interactions, respectively, $\Delta F_{max\ 1}/F_o$ from the quadratic equation and $\Delta F_{max\ 2}/F_o$ are the corresponding maximum fluorescence changes, and $[L]_o$ is the total ligand concentration. Experimental error in the fitted parameters represents ± 2 S.D.

Chromogenic Substrate Hydrolysis

The initial rates of hydrolysis of 200 µM pyro-Glu-Pro-Arg-*p*NA (pyro-EPR-*p*NA) by 10 nM Pm in PEG 20,000-coated microtiter plates was measured continuously at 405 nm as a function of SkzL concentration. k_{cat} and K_m were determined by fitting of the substrate dependence in the absence and presence of SkzL by the Michaelis-Menten equation. Rates of substrate hydrolysis were normalized to a 1-cm path length by a correction factor of 1.66 for reaction volumes of 300 µl. Titrations as a function of SkzL were normalized to the rate of pyro-EPR-*p*NA hydrolysis in the absence of SkzL and

analyzed by Equation 2 (wtSkzL) or Equation 1 (SkzLΔK415) to determine dissociation constants.

Plasminogen Activation Kinetics

The kinetics of activation of 100 nM [Glu]Pg or 100 nM [Lys]Pg by uPA (0.32 or 0.11 nM, respectively) or sctPA (3 nM) as a function of SkzL concentration were performed by continuous measurement of hydrolysis of 200 μM VLK-*p*NA at 405 nm and 25 °C, as previously described (35,42). Assays were performed in chloride containing buffer (100 mM HEPES, 100 mM NaCl, 1 mM EDTA, 1 mg/ml PEG 8,000, pH 7.4) or no chloride buffer (100 mM HEPES, 100 mM sodium acetate, 1 mM EDTA, 1 mg/ml PEG 8,000, pH 7.4) using PEG 20,000-coated polystyrene cuvettes. In assays containing SkzL, uPA or sctPA and SkzL diluted in buffer were preincubated in the cuvette at 25 °C for 10 min prior to addition of Pg and substrate. Progress curves at varying SkzL concentrations were fit by the parabolic rate equation and truncated to include only data linear when plotted as absorbance against time^2 and less than 10% substrate consumption.

Plasma Clot Lysis

Plasma clot lysis was measured by incubation of 160 μL normal human plasma at 37 °C with final concentrations of 6 nM thrombin, 10 mM $CaCl_2$, and 7 nM uPA or 1.5 nM sctPA, in a final volume of 200 μL. All proteins were diluted in 50 mM HEPES, 125 mM NaCl, pH 7.4 prior to addition. Increasing concentrations of SkzL were preincubated for 10 min at 37 °C with 10 mM $CaCl_2$ and either uPA or sctPA in the

above buffer prior to addition of thrombin and plasma to initiate the assay. Turbidity was measured at 650 nm in a microtiter plate reader. Results are reported as time to half-clot lysis as a function of SkzL concentration, and analyzed by Equation 1, where $[P]_o$ was 1.6 μM, representing the dilution-corrected plasma Pg concentration of 2.0 μM (67).

Results

Structural Characterization of SkzL

SkzL was cloned, expressed, and purified as a 47,400-Da monomer. The molecular mass was determined by mass spectrometry in excellent agreement with the molecular mass calculated from the amino acid sequence. SkzL exhibits 22% sequence identity to SK including conservation of the NH_2-terminal and COOH-terminal residues of SK required for Pg activation. Primary sequence alignment and secondary structure prediction shows the relatively weak structural similarity of SkzL to SK (Fig. 1) (68-70).

One distinguishing primary structural feature of SkzL that is absent in SK is the presence of three Cys residues: Cys^{120}, Cys^{393}, and Cys^{401}. During the expression and purification of monomeric SkzL, trace amounts of a disulfide-bonded dimeric form was generated. Dimeric and monomeric SkzL were separated by anion exchange chromatography as described in "Experimental Procedures" to yield pure monomeric SkzL and a 1:1 mixture of monomeric and dimeric SkzL (Fig. 2*A*, *lanes 2, 3, 6,* and *7*). Results of cysteine-to-serine mutagenesis studies indicated that Cys^{120} was buried within the protein and that Cys^{393} and Cys^{401} occurred partially as free thiols and partially as an internal disulfide bond (Appendix Table A1). The results also indicated that trace levels

of disulfide-mediated dimeric SkzL may occur through Cys^{393} or Cys^{401}. These results were confirmed by mass spectrometry analysis of a thiol-specific 5-fluorescein-labeled analog of SkzL monomer (Fig. 2*A*, *lanes 1* and *5*).). Labeled and unmodified SkzL were subjected to chymotrypsin cleavage followed by liquid chromatography-tandem mass spectrometry. A mass shift of 387 Da, corresponding to the probe modification, was found in peptides containing either Cys^{393} or Cys^{401} (^{389}PQAACYP^{395} and ^{399}FACENTDSKYN^{409}), indicating modification of both Cys residues under non-denaturing conditions. Peptides with unmodified Cys^{393} and Cys^{401} residues were also found. No modification was seen for Cys^{120} (^{117}PVTCT^{121}), supporting the results of the thiol quantification assays.

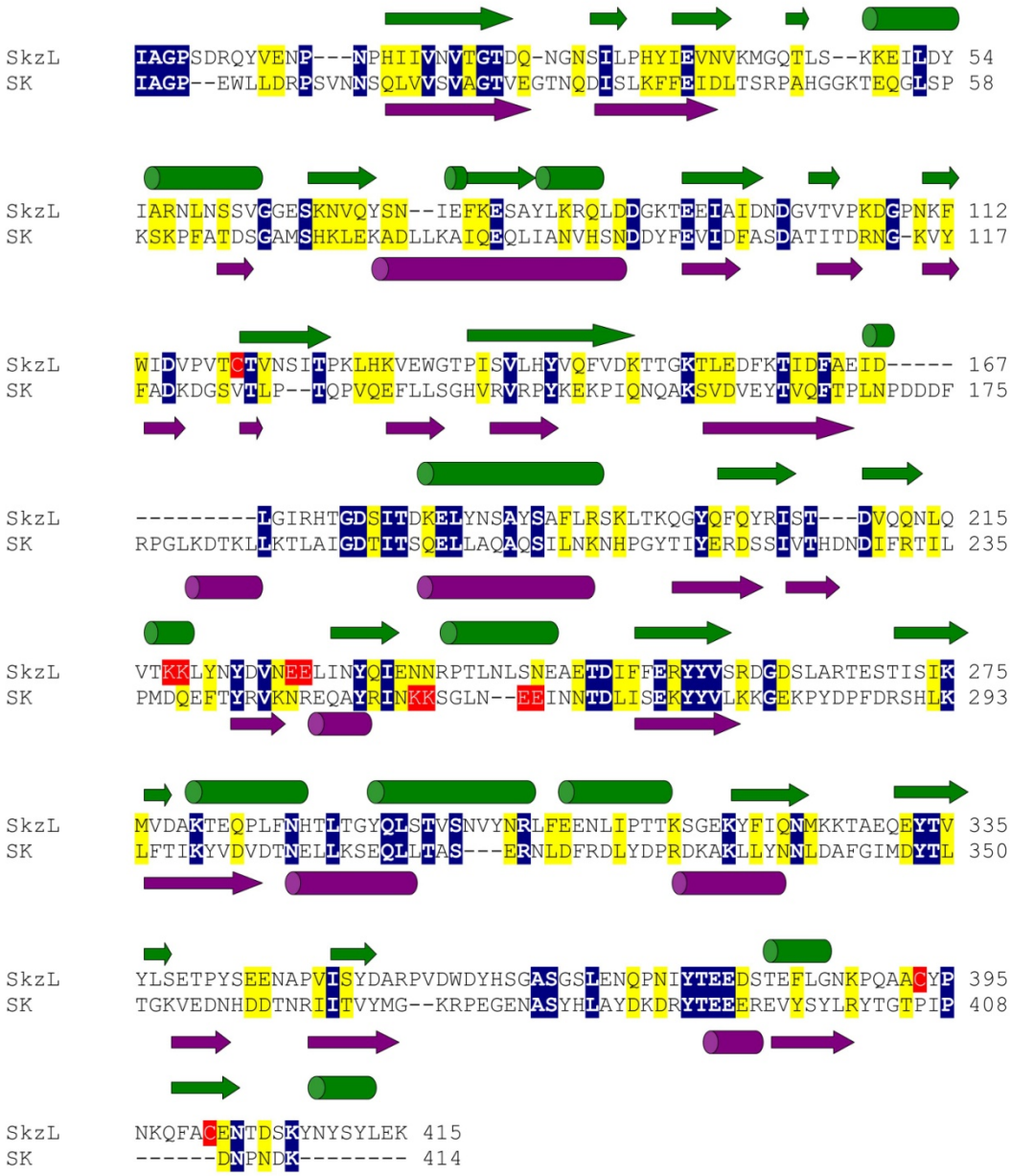

Figure 1. Sequence alignment and secondary structure prediction for SkzL and SK. Sequence alignment of SkzL and SK from *S. equisimilis* was performed using the Clustal 2.0.10 multiple sequence alignment algorithm (69). Identical residue pairs are highlighted in *blue* with conserved residues in *yellow*. Secondary structure prediction was performed by PSIPRED for SkzL in *green* and SK in *violet* (68). SkzL Cys^{120}, Cys ^{393}, and Cys^{401} are highlighted in *red*. The pairs of Lys and Glu residues representing part (Lys^{256} and Lys ^{257}) of the SK motif involved in kringle 5-mediated Pg substrate recognition, and the pairs of Lys and Glu residues in SkzL that may be involved in the low affinity LBS-dependent interaction of SkzL with Pg are also highlighted in *red* (70).

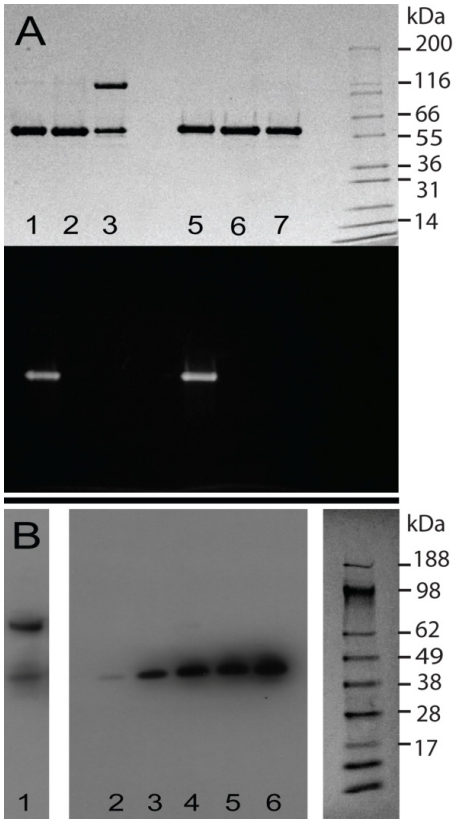

Figure 2. Secretion of SkzL by *Streptococcus agalactiae*. *A,* Protein-stained (*top*) and fluorescence (*bottom*) SDS-PAGE of non-reduced (*lanes 1-3*) and reduced (*lanes 5-7*) recombinant SkzL. [5F]-SkzL monomer (*lanes 1, 5*), purified SkzL monomer (*lanes 2, 6*), a 1:1 mixture of SkzL monomer and SkzL dimer (*lanes 3, 7*), with the migration positions of molecular mass markers indicated (kDa). *B,* Western blotting of a mixture of recombinant SkzL monomer and dimer (*lane 1*) and proteins secreted from the lag, mid-logarithmic, late-logarithmic, early stationary, and late stationary growth phases (*lanes 2-6*), with molecular mass markers (kDa) from the corresponding Ponceau S-stained membrane. SDS-PAGE and blotting were performed, and membranes were probed with a polyclonal anti-SkzL antibody as described under "Experimental Procedures".

Secretion of SkzL by *S. agalactiae*

As shown by western blotting with a polyclonal anti-SkzL antibody, SkzL was secreted in monomeric form by *S. agalactiae* serotype V in all growth phases (Fig. 2*B*). The subsequent studies were restricted to monomeric SkzL as this was the secreted and putative physiological form of the protein. Mass spectrometry of triplicate bacterial

supernatant samples confirmed that SkzL was present in both the mid-logarithmic and stationary phases of *S. agalactiae* growth (Appendix Table A2). Nineteen proteins were consistently observed in the *S. agalactiae* secretome during at least one growth phase, including the Pg-binding proteins, α-enolase and GAPDH. All peptides identified distinct proteins with no cross-identifications. NP_687847.1, a putative staphylocoagulase homolog, was also identified in the proteomic analysis (71).

Binding of Pg and FFR-Pm to [5F]-SkzL

Fluorescence equilibrium binding studies were performed to quantitate binding of native [Glu]Pg, [Lys]Pg, and active site-blocked, FFR-Pm to SkzL labeled at Cys^{393} and Cys^{401} with 5-(iodoacetamido)fluorescein ([5F]-SkzL). Titrations were performed in the absence and presence of 6-AHA to disrupt potential LBS interactions mediated by the kringle domains of Pg/Pm (Fig. 3). Binding of [Glu]Pg to [5F]-SkzL was weak, with a dissociation constant of ~3 μM (Fig. 3*A*; Table 1). Titrations of [Lys]Pg and FFR-Pm were performed at two [5F]-SkzL concentrations to determine stoichiometry (Fig. 3*B* and *C*). Binding of [Lys]Pg and FFR-Pm to [5F]-SkzL was characterized by similar dissociation constants of 15 ± 2 nM and 23 ± 8 nM, respectively, and unit stoichiometries (Table 1). Binding of all three proteins was eliminated by 10 mM 6-AHA, indicating completely LBS-dependent interactions.

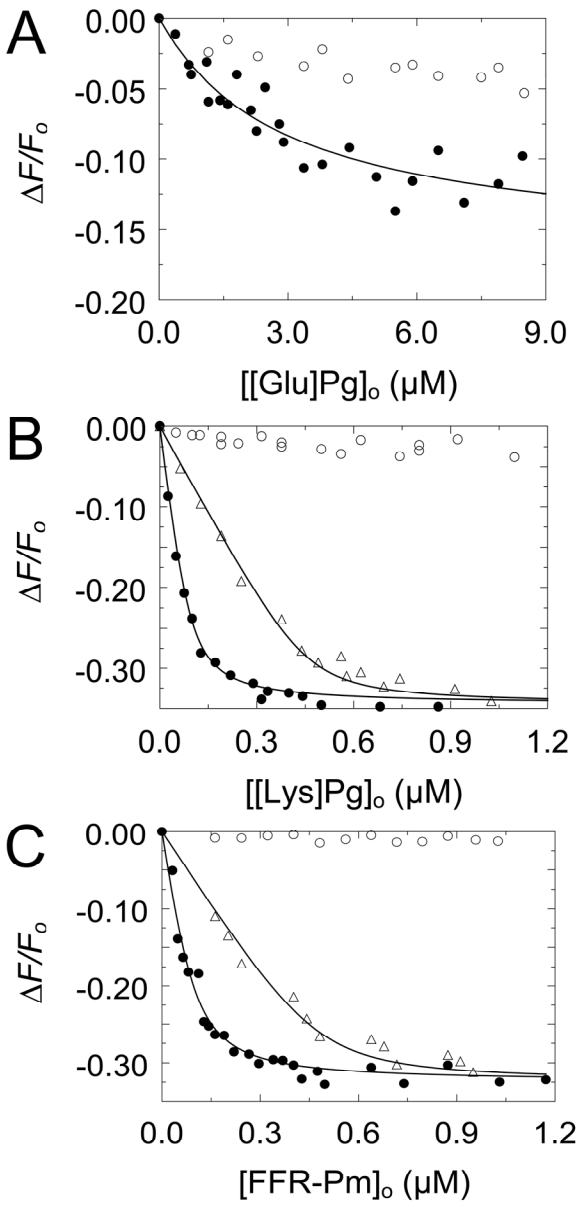

Figure 3. Fluorescence titrations of [5F]-SkzL with [Glu]Pg, [Lys]Pg, and FFR-Pm. *A,* Titrations of the fractional change in fluorescence ($\Delta F/F_o$) of 100 nM [5F]-SkzL as a function of total [Glu]Pg concentration ($[[Glu]Pg]_o$) in the absence (●) and presence (○) of 10 mM 6-AHA. *B*, titrations of 100 nM (●) and 500 nM (Δ) [5F]-SkzL as a function of total [Lys]Pg ($[[Lys]Pg]_o$) concentration in the absence of 6-AHA, and titration of 100 nM [5F]-SkzL with [Lys]Pg in the presence (○) of 10 mM 6-AHA. *C*, titrations as in *B* of 100 nM (●) and 500 nM (Δ) [5F]-SkzL, as a function of total FFR-Pm concentration ($[FFR\text{-}Pm]_o$) in the absence of 6-AHA, and titration as in *B* of 100 nM [5F]-SkzL with FFR-Pm in the presence (○) of 10 mM 6-AHA. *Solid lines* represent the least-squares fits of the data by the quadratic binding equation (Equation 1) with the parameters listed in Table 1. Experiments were performed and the data analyzed as described under "Experimental Procedures".

To determine the affinity of wtSkzL for native [Lys]Pg and Pm, competitive binding studies were performed by titration of [5F]-SkzL with [Lys]Pg and FFR-Pm in the absence and presence of two fixed concentrations of unlabeled wtSkzL (Fig. 4*A* and *C*). Analysis of the competitive titrations for wtSkzL binding to [Lys]Pg and FFR-Pm gave K_D values of 82 ± 13 nM and 49 ± 23 nM, respectively, 2-5 fold weaker than binding to [5F]-SkzL (Table 1). These K_D values, unlike those for [5F]-SkzL, are independent of perturbations of the affinity due to the presence of the fluorescence probe, which accounts for the higher affinity of labeled SkzL for all of the proteins. It was not possible to carry out competitive binding experiments for [Glu]Pg because of the prohibitively high concentrations that would be required.

Table 1. Parameters for binding of [Glu]Pg, [Lys]Pg, and FFR-Pm to [5F]-SkzL and competitive binding of wtSkzL or SkzLΔK415. Dissociation constants (K_D ligand), maximum fluorescence changes ($\Delta F_{max}/F_o$), and stoichiometric factors (n) are listed from direct titrations of [5F]-SkzL with the indicated Pg/Pm ligands. Results of competitive binding studies for the indicated ligand and competitor were analyzed by simultaneous fitting of the titration in the absence and presence of one or two fixed concentrations of competitor to obtain the dissociation constant for the ligand (K_D ligand) and competitor (K_D competitor), with the stoichiometric factor for the ligand interaction fixed at its determined value, and fixed at 1 for the competitors. For analysis of the [Glu]Pg titrations, n was fixed at 1. ND represents not determined. Experimental error in parameters represents ± 2 S.D. Binding studies were performed and the data analyzed as described under "Experimental Procedures".

Probe	Ligand	Competitor	K_D ligand	n	K_D competitor	$\Delta F_{max}/F_o$
			(*nM*)	(*mol/mol*)	(*nM*)	*(%)*
[5F]-	[Glu]Pg	wtSkzL	3000 ±		ND	- 20 ± 3
[5F]-	[Lys]Pg	wtSkzL	15 ± 2	0.92 ± 0.03	82 ± 13	- 35 ± 1
[5F]-	[Lys]Pg	SkzLΔK415	14 ± 7		2500 ± 1200	- 34 ± 1
[5F]-	FFR-Pm	wtSkzL	23 ± 8	0.97 ± 0.05	49 ± 23	- 30 ± 1
[5F]-	FFR-Pm	SkzLΔK415	9 ± 3		1500 ± 600	- 34 ± 1

To elucidate the potential role of the COOH-terminal Lys^{415} residue in mediating LBS interactions, experiments were also performed with a SkzL mutant lacking this residue (SkzLΔK415). Competitive binding studies in the absence and presence of SkzLΔK415 (Fig. 4, *B* and *D*) gave probe-independent K_D values for SkzLΔK415 binding to native [Lys]Pg and FFR-Pm of 2.5 ± 1.2 μM and 1.5 ± 0.6 μM, respectively (Table 1). Deletion of Lys^{415} resulted in a 30-fold decreased affinity for native [Lys]Pg and FFR-Pm compared to wtSkzL, indicating a major role of Lys^{415} in mediating the interactions.

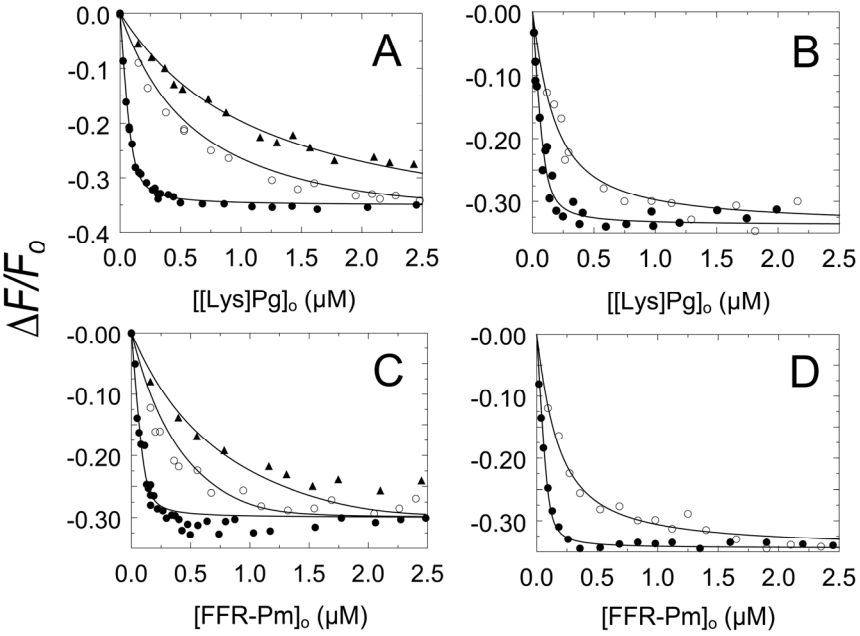

Figure 4. Competitive binding of wtSkzL and SkzLΔK415 to Pg/Pm. *A*, Titrations of the fractional change in fluorescence ($\Delta F/F_o$) of 100 nM [5F]-SkzL as a function of total [Lys]Pg concentration ($[[Lys]Pg]_o$) in the absence (●) and presence of 2000 (○) and 5000 nM (▲) wtSkzL. *B*, Titrations as in *A* of 100 nM [5F]-SkzL with [Lys]Pg in the absence (●) and presence of 20 μM (○) SkzLΔK415. *C*, Titrations as in *A* of 100 nM [5F]-SkzL as a function of total FFR-Pm concentration ($[FFR\text{-}Pm]_o$) in the absence (●) and presence of 760 (○) and 2000 nM (▲) of wtSkzL. *D*, Titrations as in *A* of 100 nM [5F]-SkzL with FFR-Pm in the absence (●) and presence of 20 μM (○) SkzLΔK415. *Solid lines* represent least-squares fits of the data by the cubic competitive binding equation with the parameters listed in Table 1. Experiments were performed and the data analyzed as described under "Experimental Procedures".

LBS-mediated Binding of SkzL to Active Site-labeled Fluorescent Pg/Pm Analogs

To examine the interactions from a different perspective, equilibrium binding studies were performed using active site fluorescein-labeled analogs of [Glu]Pg, [Lys]Pg, and FFR-Pm in the absence and presence of 6-AHA (Fig. 5). Binding to [5F]FFR-[Glu]Pg was very weak (K_D ~10 μM), 3-fold weaker than observed with [5F]-SkzL, and was abolished by 10 mM 6-AHA (Fig. 5,*A* and *B*; Table 2). The source of the weaker K_D values obtained for [5F]FFR-[Glu]Pg, -[Lys]Pg, and -Pm is explained by 2-3-fold decreases in affinity due to active-site labeling of the proteins. Titrations of [5F]FFR-[Glu]Pg with SkzLΔK415 demonstrated no apparent fluorescence change, suggesting the absence of binding or an interaction occurring more weakly than could be detected under the experimental conditions used. Titrations of [5F]FFR-[Lys]Pg and [5F]FFR-Pm with wtSkzL revealed bimodal behavior, suggestive of two binding interactions. The high affinity interactions occurred with equivalent dissociation constants of 160-170 nM (Fig. 5,*C* and *E*; Table 2). The low affinity interactions were not well determined, with dissociation constants of ~18 and ~20 μM, respectively, and appeared to be due to a decrease in anisotropy. When vertically polarized light was used for excitation and emission polarizers were set to the magic angle to eliminate anisotropy, only the high affinity SkzL interaction was observed, with K_D values for labeled [Glu]Pg, [Lys]Pg and Pm indistinguishable from those obtained for the bimodal titrations (Fig. 5, *D* and *F*; Table 2). The values for the high affinity interactions were 2-3-fold weaker than the K_D values from the competitive binding experiments (Table 1), due to fluorescence probe labeling of the active site.

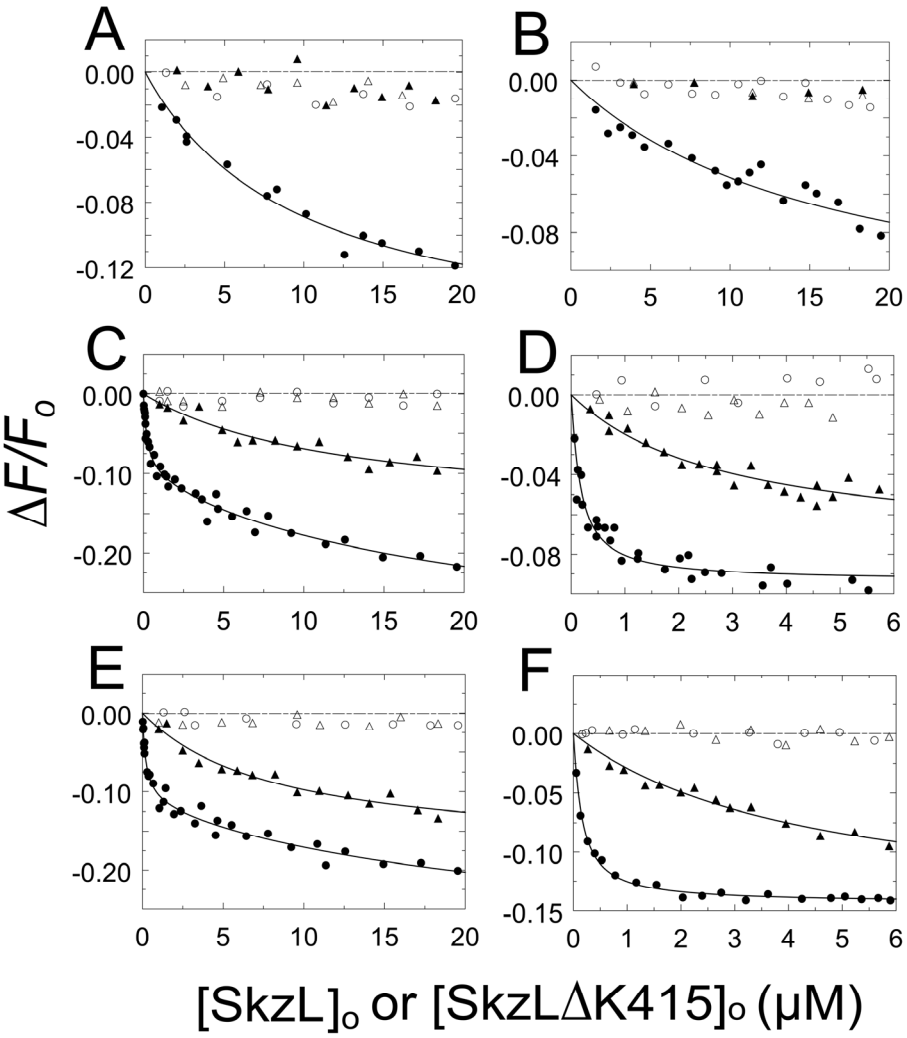

Figure 5. Binding of wtSkzL and SkzLΔK415 to [5F]FFR-[Glu]Pg, [5F]FFR-[Lys]Pg, and [5F]FFR-Pm. *A* and *B*, Titrations of the fractional change in fluorescence ($\Delta F/F_o$) of 50 nM [5F]FFR-[Glu]Pg as a function of total wtSkzL concentration ($[SkzL]_o$) in the absence (●) and presence (○) of 10 mM 6-AHA, and as a function of total SkzLΔK415 concentration ($[SkzL\Delta K415]_o$) in the absence (▲) and presence (Δ) of 10 mM 6-AHA. *C and D*, Titrations as in *A* and *B* of 50 nM [5F]FFR-[Lys]Pg as a function of total wtSkzL concentration in the absence (●) and presence (○) of 10 mM 6-AHA, and as a function of total SkzLΔK415 concentration in the absence (▲) and presence (Δ) of 10 mM 6-AHA. *E* and *F*, Titrations as in *A* and *B* of 50 nM [5F]FFR-Pm as a function of total wtSkzL concentration in the absence (●) and presence (○) of 10 mM 6-AHA, and as a function of total SkzLΔK415 concentration in the absence (▲) and presence (Δ) of 10 mM 6-AHA. *Solid lines* represent the least-squares fits of the data by Equation 1 (*A, B, D,* and *F*) or Equation 2 *(C,* and *E*) with the parameters listed in Table 2. The *dashed line* represents zero. Titrations were performed without polarizers (*A, C, E*), or with vertically polarized excitation and emission at the magic angle (*B, D, F*). Titrations were performed and analyzed as described under "Experimental Procedures".

Titrations of [5F]FFR-[Lys]Pg, and [5F]FFR-Pm with SkzLΔK415 under non-magic angle (Fig. 5, *C* and *E*) and magic angle (Fig. 5, *D* and *F*) conditions gave weak K_D values of 3-12 μM (Table 2). The low affinity binding of SkzLΔK415 was eliminated in the presence of 6-AHA, consistent with more than one LBS-dependent interaction between SkzL and Pg/Pm.

Table 2. Parameters for wtSkzL and SkzLΔK415 binding to active site fluorescein-labeled Pg/Pm analogs. Dissociation constants for the high affinity (K_{D1}) and low affinity (K_{D2}) interactions and corresponding maximum fluorescence changes ($\Delta F_{max\ 1}/F_o$) and ($\Delta F_{max\ 2}/F_o$) from titrations of [5F]FFR-[Glu]Pg, [5F]FFR-[Lys]Pg, and [5F]FFR-Pm (*Probe-labeled protein*) with wtSkzL or SkzLΔK415 (*Ligand*) as indicated. Titrations were performed without polarizers or with vertically polarized excitation and emission at the magic angle (*magic angle*) to eliminate anisotropy. Experimental error in the parameters represents ± 2 S.D. Experiments were performed and the results analyzed as described under "Experimental Procedures".

Probe-labeled protein	Ligand	magic angle	K_{D1}	K_{D2}	$\Delta F_{max\ 1}/F_o$	$\Delta F_{max\ 2}/F_o$
			(*nM*)	(*nM*)	(*%*)	(*%*)
[5F]FFR-[Glu]Pg	wtSkzL	no	10000 ± 3200		- 18 ± 2	
[5F]FFR-[Glu]Pg	wtSkzL	yes	16000 ± 9000		- 14 ± 4	
[5F]FFR-[Glu]Pg	SkzLΔK415	no	no binding		no binding	
[5F]FFR-[Glu]Pg	SkzLΔK415	yes	no binding		no binding	
[5F]FFR-[Lys]Pg	wtSkzL	no	170 ± 90	~18000	- 10 ± 2	- 22 ± 10
[5F]FFR-[Lys]Pg	wtSkzL	yes	150 ± 40		- 9 ± 1	
[5F]FFR-[Lys]Pg	SkzLΔK415	no	12000 ± 8000		- 15 ± 5	
[5F]FFR-[Lys]Pg	SkzLΔK415	yes	2800 ± 1300		- 8 ± 1	
[5F]FFR-Pm	wtSkzL	no	160 ± 80	~20000	- 11 ± 2	-18 ± 12
[5F]FFR-Pm	wtSkzL	yes	140 ± 14		- 14 ± 2	
[5F]FFR-Pm	SkzLΔK415	no	8000 ± 3000		- 18 ± 3	
[5F]FFR-Pm	SkzLΔK415	yes	4400 ± 1600		- 16 ± 3	

LBS-mediated Binding of SkzL to Active Pm

To detect any changes in Pm chromogenic substrate kinetics on binding to SkzL, assays were performed by continuous measurement of the initial rates of pyro-EPR-*p*NA hydrolysis by Pm as a function of SkzL concentration. Comparison of the Michaelis-Menten kinetic parameters in the absence and presence of 1 or 5 μM SkzL, showed a 1.7-fold decrease in k_{cat} compared to free Pm, no significant change in K_m, and a 2-fold decrease in k_{cat}/K_m (Table 3).

Table 3. Parameters for the effect of SkzL on pyro-EPR-*p*NA hydrolysis by Pm. Kinetic parameters (k_{cat}, K_m, k_{cat}/K_m) obtained from Michaelis-Menten analysis of the substrate dependence. Experiments were performed in the absence and presence of 1 μM and 5 μM total SkzL concentration ($[SkzL]_o$). Experimental error in the parameters represents ± 2 S.D. Experiments were performed and the results analyzed as described under "Experimental Procedures".

$[SkzL]_o$	k_{cat}	K_m	k_{cat}/K_m
(μM)	*(s^{-1})*	*(μM)*	*($s^{-1}\mu M^{-1}$)*
0	78 ± 2	130 ± 2	0.60
1	46 ± 1	140 ± 11	0.33
5	47 ± 1	160 ± 22	0.30

SkzL had no effect on the rate of hydrolysis of chromogenic substrates with Lys at the P1[2] position (D-VLK-*p*NA, pyro-Glu-Phe-Lys-*p*NA, and D-Val-Phe-Lys-*p*NA). However, similar effects on k_{cat} were seen with other substrates with Arg at the P1 position (D-Ile-Pro-Arg-*p*NA and D-Val-Leu-Arg-*p*NA) (results not shown). Titration with SkzL at 200 μM pyro-EPR-*p*NA showed two distinct LBS-dependent binding interactions between SkzL and native Pm, with apparent dissociation constants of 170 ±

140 nM and ~9 μM, where the latter value was poorly determined (Fig. 6). Titration with SkzLΔK415 demonstrated a loss of the high affinity interaction and an LBS-dependent low affinity interaction with a K_D of 3.8 ± 1.2 μM (Fig. 6).

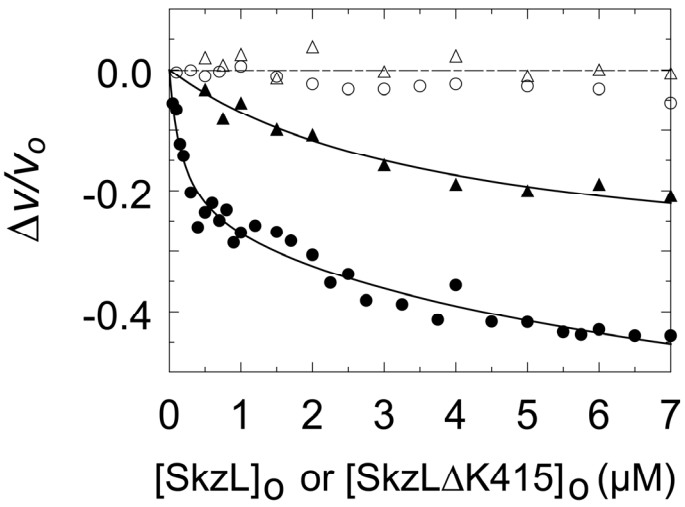

Figure 6. Effect of SkzL on pyro-EPR-*p*NA hydrolysis by Pm. Titrations of the fractional change in initial velocity ($\Delta v/v_o$) of 10 nM Pm as a function of total wtSkzL concentration ($[SkzL]_o$) in the absence (●) and presence (○) of 10 mM 6-AHA, and as a function of total SkzLΔK415 concentration ($[SkzL\Delta K415]_o$) in the absence (▲) and presence (Δ) of 10 mM 6-AHA. S*olid lines* represent the least-squares fits of the data by Equation 1 (▲) or Equation 2 (●), with the parameters given under "Results". The *dashed line* represents zero. Titrations were performed and analyzed as described under "Experimental Procedures".

Effect of SkzL on Plasminogen Activation by uPA

Chromogenic substrate kinetic assays of Pm formation were performed to determine the effect of SkzL on activation of [Glu]Pg and [Lys]Pg by uPA. To investigate the possible effects of SkzL on Pg conformation, assays were done in the absence and presence of 10 mM 6-AHA and in low chloride ion buffer, with the uPA preparation as the only source of Cl^- (0.45 mM in the reactions) and in buffer containing

100 mM Cl^-. In the presence of 100 mM Cl^-, saturating SkzL concentrations resulted in a ~2-fold decreased rate of [Lys]Pg activation with minimum rates of Pm generation equivalent to those in the presence of 10 mM 6-AHA (Fig. 7*A*).

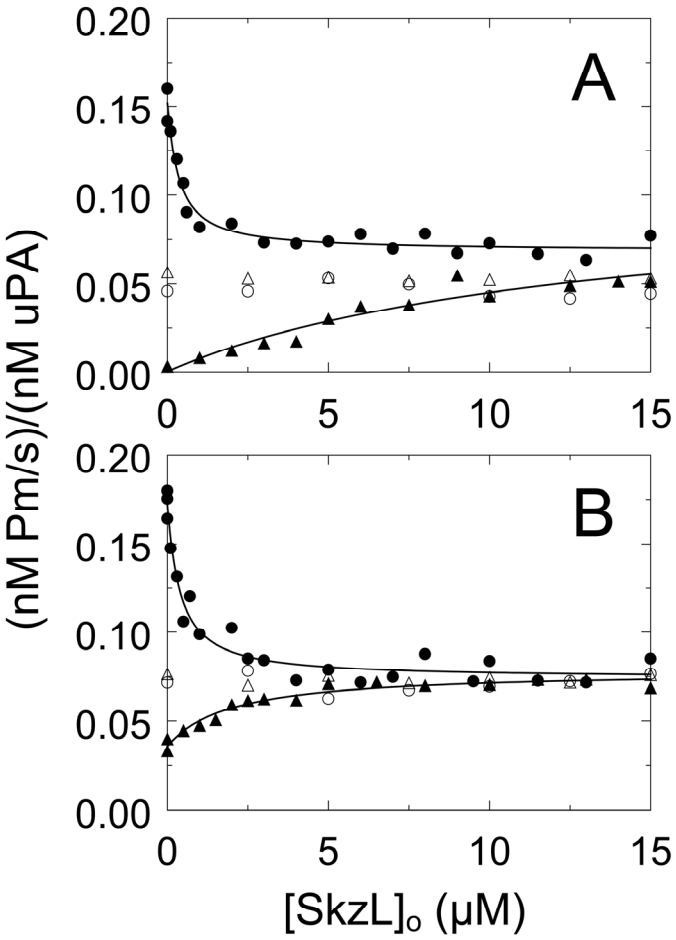

Figure 7. Effect of SkzL on Pg activation by uPA. Assays were performed in buffer containing 100 mM chloride (*A*) or 0.45 mM chloride (*B*). Initial rates of Pm generation (*(nM Pm/s)/(nM uPA)*) for activation of 100 nM [Lys]Pg by 0.11 nM uPA in the absence (●) and presence (○) of 10 mM 6-AHA as a function of total SkzL concentration ($[SkzL]_o$). Initial rates of Pm generation (*(nM Pm/s)/(nM uPA)*) for activation of 100 nM [Glu]Pg by 0.32 nM uPA in the absence (▲) and presence (Δ) of 10 mM 6-AHA as a function of total SkzL concentration ($[SkzL]_o$). S*olid lines* represent the least-squares fits of the data by the quadratic binding equation with the parameters listed in Table 4. Experiments were performed and the data analyzed as described under "Experimental Procedures".

Fitting of the SkzL-dependence in the absence of 6-AHA yielded an apparent K_D value for SkzL-[Lys]Pg binding of 300 ± 120 nM (Fig. 7*A*; Table 4), which was ~4-fold weaker than the K_D value of 80 nM obtained for SkzL binding to [Lys]Pg in competitive binding studies. An identical phenomenon was seen at low Cl^- concentration, with an indistinguishable apparent K_D of 340 ± 150 nM (Fig. 7*B*; Table 4), consistent with the lack of effect of Cl^- on the [Lys]Pg β- to γ- conformational change.

Table 4. Parameters for the effect of SkzL on Pg activation by uPA. Dissociation constants (K_D) for the SkzL-dependent change in the rate of Pm generation for activation of 100 nM [Glu]Pg or [Lys]Pg by 0.11 nM uPA. Experiments were performed in the presence of low and high total chloride ion concentration (*[chloride ion]$_o$*). Experimental error in the parameters represents ± 2 S.D. Experiments were performed and the results analyzed as described under "Experimental Procedures".

Substrate	[chloride ion]$_o$	K_D
	(mM)	*(nM)*
[Lys]Pg	100	300 ± 120
[Lys]Pg	0.45	340 ± 150
[Glu]Pg	100	13000 ± 12000
[Glu]Pg	0.45	1900 ± 900

The rate of Pm generation from [Glu]Pg by uPA in the presence of chloride ion was greatly enhanced, ~20-fold to a rate indistinguishable from that for [Lys]Pg at saturating concentrations of SkzL or 6-AHA (Fig. 7*A*; Table 4). Fitting of the SkzL dependence gave an apparent K_D value for SkzL-[Glu]Pg binding of 13 ± 12 μM, in good agreement with the estimates of 10-16 μM for SkzL binding to [5F]FFR-[Glu]Pg (Table 2). The rate of [Glu]Pg activation by uPA in the presence of 10 mM 6-AHA was essentially the same as the rate in the presence of saturating concentrations of SkzL. This

indicated that, similar to the effect of 6-AHA, the α-conformation of [Glu]Pg was being extended by SkzL to resemble the γ-conformation of [Lys]Pg. The basal rate of [Glu]Pg activation by uPA was enhanced ~11-fold at low Cl^- concentration compared with high Cl^- concentration (Fig. 7*B*; Table 4). Saturating SkzL concentrations resulted in a slight, ~2-fold further enhancement of [Glu]Pg activation. This small enhancement resulted in rates of Pm generation equivalent to those in the presence of 10 mM 6-AHA (Fig. 7*B*; Table 4).

Effect of SkzL on Plasminogen Activation by sctPA

Chromogenic substrate kinetic assays of Pm formation were performed to determine the effect of SkzL on activation of [Lys]Pg and [Glu]Pg by sctPA. The rate of Pm generation from [Lys]Pg and [Glu]Pg by sctPA was greatly enhanced ~42-fold and ~650-fold, respectively, in a totally LBS-dependent manner (Fig. 8), although the maximum rate at saturating SkzL was 3.4-fold higher for [Lys]Pg compared to [Glu]Pg. Fitting of the SkzL dependence gave K_D values for [Lys]Pg and [Glu]Pg of 12 ± 7 μM and 14 ± 13 μM, respectively. While the apparent K_D of SkzL for [Glu]Pg was consistent with those obtained in the binding studies, the K_D value for [Lys]Pg was ~60-140-fold weaker than the affinity determined in the binding studies for the high affinity interaction (Table 2). This very large difference suggested that a different mechanism was involved for sctPA.

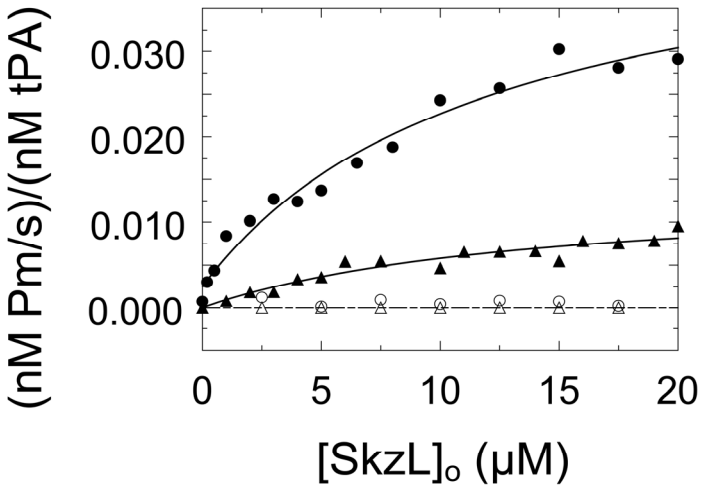

Figure 8. Effect of SkzL on Pg activation by sctPA. Initial rates of Pm generation (*(nM Pm/s)/(nM sctPA)*) for activation of 100 nM [Lys]Pg by 3 nM sctPA in the absence (●) and presence (○) of 10 mM 6-AHA as a function of total SkzL concentration ($[SkzL]_o$). Initial rates of Pm generation (*(nM Pm/s)/(nM sctPA)*) for activation of 100 nM [Glu]Pg by 3 nM sctPA in the absence (▲) and presence (Δ) of 10 mM 6-AHA as a function of total SkzL concentration ($[SkzL]_o$). *Solid lines* represent the least-squares fits by the quadratic binding equation with parameters given under "Results", and the *dashed line* represents zero. Experiments were performed and data analyzed as described under "Experimental Procedures".

SkzL Enhances uPA- and sctPA-mediated Plasma Clot Lysis

Plasma clot lysis experiments were performed to assess the role of SkzL as an effector of uPA- and sctPA-mediated Pg activation in a physiological model system of fibrinolysis. Human plasma and 6 nM human thrombin were reacted with a preincubated mixture of either 7 nM uPA or 1.5 nM sctPA and increasing concentrations of SkzL. The results were expressed as time to half-clot lysis as a function of SkzL concentration (72). SkzL enhanced clot lysis by uPA and sctPA, decreasing the time to half-clot lysis by ~2-fold (Fig. 9). No clot lysis was observed in the absence of uPA or sctPA.

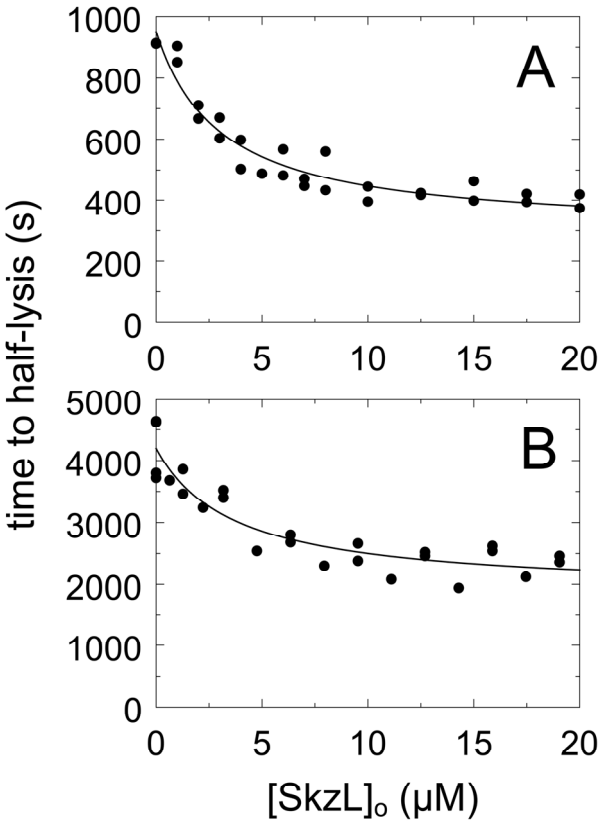

Figure 9. Effect of SkzL on uPA- and sctPA-mediated plasma clot lysis. Clot lysis represented by the time to half-lysis (*time to half-lysis*) (●) as a function of total SkzL concentration ($[SkzL]_o$) for reactions containing uPA (*A*) or sctPA (*B*). Following dilution of all proteins in 50 mM HEPES, 125 mM NaCl, pH 7.4, SkzL was preincubated with 10 mM $CaCl_2$, 7 nM uPA or 1.5 nM sctPA for 10 min at 37 °C prior to addition of 6 nM thrombin and 160 μL of plasma (200 μL assay volume). Clot lysis was measured by turbidity as described under "Experimental Procedures". Analysis of clot lysis by uPA and sctPA gave apparent K_D values of 1.9 ± 0.9 μM and 2.5 ± 2.5 μM, respectively.

Discussion

SkzL from *S. agalactiae* has modest homology to the bacterial Pg activators, SAK, SK, and PauB, and is secreted as the monomeric, 47,400-Da form by *S. agalactiae* throughout its growth cycle. Nineteen proteins were identified in the *S. agalactiae* secretome, including α-enolase and GAPDH, which are known to bind Pg. In contrast to SK, SAK, and PauB, SkzL does not conformationally or proteolytically activate Pg to Pm

(results not shown). SkzL, however, binds Pg and Pm in a LBS-dependent manner, resulting in enhanced [Glu]Pg activation by the endogenous human Pg activators, uPA and sctPA. To our knowledge, SkzL is the first *S. agalactiae*-secreted protein that targets uPA, sctPA, and Pg to facilitate activation of the human fibrinolytic system.

Equilibrium binding studies show that SkzL binds to [Glu]Pg with low affinity, likely due to low accessibility of the LBS in the kringle domains of the compact [Glu]Pg α-conformation. Nevertheless, the low affinity interaction of SkzL with [Glu]Pg is eliminated by 6-AHA, indicating that LBS interactions are involved. Competitive binding studies indicate that wtSkzL binds to unlabeled, native [Lys]Pg and FFR-Pm with near-equivalent K_D values of 80 and 50 nM, respectively. The large increase in affinity compared to [Glu]Pg is likely due to the increased LBS accessibility in the partially extended [Lys]Pg/Pm β-conformation. Binding of SkzL to [Lys]Pg and FFR-Pm is blocked by 6-AHA, indicating that binding is entirely mediated by LBS interactions.

Due to the use of multiple experimental approaches to quantitate SkzL binding to different forms of Pg and Pm, it is important to address some apparent discrepancies among the dissociation constants obtained. [5F]-SkzL binds with 5- and 2-fold enhanced affinity for native [Lys]Pg and FFR-Pm, respectively, compared to the affinity of unlabeled wtSkzL determined by competitive binding. The dissociation constants determined by competitive binding are independent of effects that fluorescence probe-labeling may have on binding affinity. The enhanced binding of [5F]-SkzL may be a result of the location of probe incorporation. [5F]-labeled SkzL has a stoichiometry of labeling of 1.0 mol of [5F]/mol of SkzL, which reflects probe incorporation on Cys^{393} and Cys^{401}, only 14 residues from Lys^{415} (see Fig. 1). On this basis, higher affinity binding to

[5F]-SkzL may reflect a favorable direct interaction of Pg with the probes. Conversely, wtSkzL binds with 2- and 3-fold reduced affinity to active site-labeled [5F]FFR-[Lys]Pg and [5F]FFR-Pm, respectively. The small decrease in affinity associated with Pg/Pm active site-labeling may result from distortion of the conformation of the catalytic domain of Pg/Pm due to the presence of the probe and linking tripeptide inhibitor. These opposing effects of probe labeling on [Glu]Pg binding are compounded in comparison of [Glu]Pg binding to [5F]-SkzL and SkzL binding to [5F]FFR-[Glu]Pg, which differ by 3-5-fold.

SkzL binding to active site-labeled, [5F]FFR-[Lys]Pg and [5F]FFR-Pm revealed a high affinity interaction (K_D ~140-170 nM) represented by a decrease in fluorescence intensity and a low affinity interaction (K_D ~20 μM) represented by a decrease in anisotropy. The latter values were not well determined because little saturation was obtained at the highest SkzL concentrations achievable (20 μM). Titrations performed with vertically polarized excitation and emission at the magic angle resulted in near-elimination of the anisotropy change and observation of the high affinity interaction (K_D 140-150 nM) only, indicating that the low affinity interaction is associated with a decrease in anisotropy. Considering the 2-3-fold weakening of SkzL binding due to probe labeling, these values of 140-150 nM for the labeled proteins are close enough (≤ 3-fold) to the values of 50 and 80 nM for high affinity SkzL binding to unlabeled FFR-Pm and native [Lys]Pg to support the conclusion that they represent the same interaction. It should be noted that 2-fold differences in dissociation constants are generally not considered significant.

Because the low affinity interactions had some of the hallmarks of nonspecific binding, the presence of two distinct interactions between SkzL and Pm was confirmed through analysis of the effect of SkzL on the rates of pyro-EPR-*p*NA hydrolysis by Pm. These studies demonstrated mediation of the high affinity LBS-dependent interaction by Lys^{415} and the presence of a second LBS-dependent ~9 μM K_D interaction, which was poorly determined.

Deletion of SkzL Lys^{415} results in undetectable binding of [Glu]Pg, suggesting that binding is mediated by Lys^{415} exclusively. Binding of both native [Lys]Pg and FFR-Pm to wtSkzL is weakened 30-fold by Lys^{415} deletion. The results indicate that Lys^{415} plays a major role in the LBS-dependent binding of all forms of Pg and Pm. Loss of Lys^{415} decreases the affinity of SkzL for native [Lys]Pg and FFR-Pm to K_D values of 2.5 and 1.5 μM, respectively (Table 1), demonstrating that Lys^{415} is responsible for the high affinity interaction. The remaining interaction is also eliminated by 6-AHA, indicating that there are two sites on SkzL that mediate LBS-dependent binding to labeled [Lys]Pg/Pm. A sequence containing pairs of Lys and nearby Glu residues in SkzL (Fig. 1; Lys^{218}, Lys^{219}, Glu^{227}, Glu^{228}) is similar to that of the 250-loop of SK, with the exception of Arg^{253} (Lys^{256}, Lys^{257}, Glu^{262}, Glu^{263}) and a motif in SAK (Lys^{97}-Lys-Glu-Glu^{100}), certain residues of which are implicated in mediating LBS-dependent Pg substrate interactions with SK•Pg* and SAK•Pm catalytic complexes (42,73). The similar motif in SkzL may be responsible for the low affinity interaction. Future mutagenesis studies may be used to establish the SkzL residues involved in mediating this weak interaction.

Pg can adopt three distinct conformations that affect its potential for activation by tPA and uPA. The compact nature of the α-conformation of [Glu]Pg, stabilized by physiological chloride concentrations, makes it a poor substrate for uPA, tPA, and SK, compared with the partially extended, chloride-independent β-conformation of [Lys]Pg (17,22-25,49,66). Upon occupation of [Glu]Pg and [Lys]Pg kringles 1, 4 and 5 by 6-AHA, the transition to the fully extended γ-conformation also results in enhanced activation by uPA (21,23-25).

Because of the highly LBS-dependent nature of SkzL binding to Pg, it was hypothesized that SkzL-Pg binding could mimic the conformational change induced by 6-AHA binding, resulting in the extension of [Glu]Pg and [Lys]Pg from the α- and β-conformations, respectively, to the γ-conformation. Activation of [Lys]Pg by uPA, however, was inhibited by SkzL to a rate equivalent to that in the presence of either 10 mM 6-AHA or saturating SkzL. In these experiments, the apparent dissociation constants for SkzL-[Lys]Pg binding were ~4-fold weaker than the native affinity determined by competitive binding. This discrepancy may be due to the inability to discern both the high and low affinity interactions between SkzL and [Lys]Pg, resulting in a weaker apparent affinity representative of a mixture of binding interactions between SkzL and [Lys]Pg. Activation of [Lys]Pg by uPA is inhibited by SkzL, suggesting that while SkzL binding may alter the conformation of [Lys]Pg from the β- to the γ-conformation, similar to 6-AHA, it does not enhance [Lys]Pg activation by uPA.

In the presence of 100 mM chloride ion, activation of [Glu]Pg by uPA is very slow; however, binding of SkzL enhances the rate of Pm generation ~20-fold to the same level as [Lys]Pg in the presence of saturating SkzL or 6-AHA. Rates of Pm generation in

the presence of 6-AHA are identical to those in the presence of saturating SkzL, suggesting that occupation of the [Glu]Pg LBS and stabilization of the γ-conformation by SkzL is responsible for the observed SkzL-enhanced rate of [Glu]Pg activation. Together, the results show that SkzL is a specific effector of [Glu]Pg activation by uPA. Moreover, the mechanism of SkzL-enhanced [Glu]Pg activation by uPA is shown for the first time to be caused by SkzL-mediated transformation of [Glu]Pg from the activation-resistant, α-conformation to the more rapidly activated, γ-conformation.

This mechanism and a hypothetical interpretation of the results of the binding studies for [Lys]Pg and Pm are presented in Fig. 10. In this scheme, [Glu]Pg in the α-conformation is in unfavorable equilibrium (Reaction 1) with the β-conformation, which is governed by the Cl^- concentration (17,23-25). SkzL binds preferentially to the β-conformation, mediated by Lys^{415} binding to kringle 4, and accompanied by transition of [Glu]Pg to the γ-conformation (Reactions 1 and 2), which is more susceptible to activation by uPA (Reaction 3). The proposal of kringle 4 as the Lys^{415}-binding site is based on the preference of kringle 4 for COOH-terminal Lys residues (26,31,74), and preferential binding of SkzL to the [Glu]Pg β-conformation is supported by evidence that kringle 4 is masked in the α-conformation (26,75-77). LBS-dependent monoclonal antibody binding specific for kringle 4 has been hypothesized to induce an activation-enhancing conformational change (23,26,30) distinct from the α- to β-conformational change caused by disruption of the PAN module-kringle 5 interaction (27,78), suggesting a role for kringle 4 in modulating the β- to γ-conformational change (23,30,32). Reactions 4 and 5 illustrate that binding of SkzL to [Lys]Pg (or Pm) can occur through two distinct interactions as follows: high affinity Lys^{415}-kringle 4 binding and a weak

interaction between the internal SkzL motif and kringle 5, supported by the demonstrated specificity of kringle 5 for alkylamines and internal Lys residues (79,80). All of the putative [Lys]Pg/Pm complexes are consistent with the present results, but the Pg kringles to which the two sites on SkzL bind and the compositions of the complexes have not been substantiated experimentally and therefore remain hypothetical.

The enhanced rate of [Glu]Pg activation caused by SkzL is not specific to uPA, as kinetic studies demonstrate that SkzL also enhances Pg activation by sctPA. In contrast to the results with uPA, however, increased rates of Pm generation are seen for sctPA activation of both [Glu]Pg and [Lys]Pg. The effect of SkzL on [Glu]Pg activation by sctPA may be due to SkzL-mediated conformational changes in [Glu]Pg similar to those seen with uPA. However, the apparent dissociation constant for SkzL-enhanced [Lys]Pg activation by sctPA appears to be ~12 μM, ~60-140-fold weaker than the K_D value for SkzL-[Lys]Pg binding determined by fluorescence. This suggests that the mechanism of enhanced [Lys]Pg activation by sctPA is different, and cannot be explained by SkzL-[Lys]Pg binding interactions alone. While further studies are needed to evaluate this hypothesis, preliminary results suggest that SkzL interacts with sctPA though the LBS on kringle 2 of sctPA, which is not present in uPA. Binding of wtSkzL and SkzLΔK415 to a fluorescent sctPA analog was characterized by K_D values of 14 and 15 μM, respectively, in an LBS-dependent manner (unpublished results). This result suggests that weak SkzL binding to sctPA is due to an interaction of kringle 2 of sctPA with a site distinct from Lys^{415} on SkzL. As SkzL binding to [Lys]Pg is largely mediated by Lys^{415}, such an interaction with sctPA may result in higher order complex formation, which will require further experimentation to evaluate.

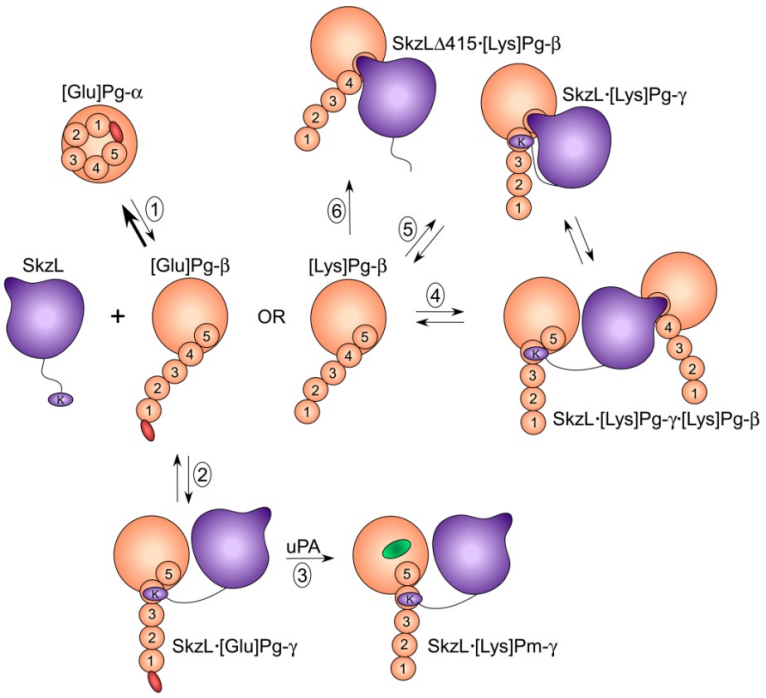

Figure 10. Diagram of the proposed mechanism of SkzL-mediated [Glu]Pg activation by uPA, and postulated LBS-dependent complexes formed with [Lys]Pg and Pm mediated by two sites on SkzL. SkzL is shown in *purple* with Lys^{415} (*K*) on a flexible segment, and the postulated SkzL internal motif that mediates kringle binding is represented by the "*nose*". [Glu]Pg in *light orange* is shown with the NH_2-terminal PAN module in *red*, 5 numbered kringle domains, and the COOH-terminal catalytic domain. [Glu]Pg in the compact, α-conformation (*[Glu]Pg-α*) is shown as a spiral structure that is maintained by the PAN domain interacting with kringle 5. [Glu]Pg is in equilibrium (Reaction 1) with a low concentration of the partially extended, β-conformation (*[Glu]Pg-β*), in which the PAN module has been released by kringle 5. The proposed mechanism of SkzL-enhanced [Glu]Pg activation by uPA is shown in Reactions 1, 2, and 3. SkzL binds preferentially to the β-conformation of [Glu]Pg, mediated by Lys^{415} binding to the LBS of kringle 4, which converts the SkzL•[Glu]Pg complex to the γ-conformation (*SkzL•[Glu]Pg-γ*), thereby accelerating the rate of [Glu]Pg activation to [Lys]Pm (active site in *green*) by uPA (Reaction 3). Conversion of the initial product, [Glu]Pm into [Lys]Pm by the Pm generated is not shown. [Lys]Pg, lacking the PAN module, is represented in the partially extended, β-conformation (*[Lys]Pg-β*). Hypothetical complexes formed by wtSkzL and [Lys]Pg or Pm mediated by its two binding sites are; Reaction 4, formation of a ternary, SkzL• $[Lys]Pg_2$ complex in which one Pg molecule is bound through the Lys^{415}-kringle 4 interaction in the γ-conformation and binding of the other Pg molecule mediated by the SkzL internal motif-kringle 5 interaction, with Pg in the β-conformation (*SkzL•[Lys]Pg-γ•[Lys]Pg-β*); and Reaction 5, formation of an SkzL•[Lys]Pg complex in the γ-conformation with both the internal motif and Lys^{415} engaged with their respective kringles. Reaction 6 illustrates the complex formed between SkzLΔK415 and [Lys]Pg or Pm mediated by the internal motif in SkzL.

The present studies show that SkzL is a novel protein that is modestly homologous to SK, secreted from *S. agalactiae*, and acts as a cofactor of sctPA and uPA in accelerating Pg activation. Recent studies have established that an interaction of cell surface-bound GAPDH with Pg contributes to the virulence of GBS invasive infection in an *in vivo* murine model (10). The present studies reveal SkzL as an additional component in the interactions between GBS and the proteins of the human fibrinolytic system. As a secreted protein, SkzL may play a role as a Pg-binding protein different from the cell surface-bound Pg-binding proteins, α-enolase and GAPDH, in the context of GBS infection, or it could act in cooperation with these proteins through as yet, unknown interactions. SkzL has high affinity for Pg and Pm relative to the plasma Pg concentration of 2 μM (67), and binds through a strictly LBS-dependent mechanism involving the kringle domains of Pg and Pm. SkzL is a novel effector of uPA-mediated [Glu]Pg activation through a LBS-dependent mechanism similar to 6-AHA (22,29). The studies suggest that the role of SkzL as an effector of Pg activation by uPA is specific for the circulating form of Pg in blood, [Glu]Pg. SkzL also enhances sctPA-mediated [Glu]Pg and [Lys]Pg activation through a different mechanism that will be examined in further studies. The finding that SkzL enhances clot lysis by both physiological Pg activators in plasma provides strong support for a role of SkzL in the interaction of GBS with the human fibrinolytic system. SkzL has the potential to be a new virulence factor in life-threatening *S. agalactiae* infections of neonates and immune-compromised individuals.

Acknowledgements

We thank Dr. Lisa Zimmerman of the Vanderbilt University Mass Spectrometry Research Center Proteomics Core for her work on the *Streptococcus agalactiae* secreted protein profile. The authors also thank Drs. Jonathan Creamer and Anthony Tharp for assistance in protein purification and data analysis respectively.

Footnotes

*This work was supported in whole or in part by National Institutes of Health Grant RO1 HL056181 from the National Heart, Lung, and Blood Institute to P. E. B. The content is solely the responsibility of the authors and does not necessarily represent the official views of the National Heart, Lung, and Blood Institute or the National Institutes of Health. K. G. W was supported in part by Predoctoral Fellowship 0715393B from the American Heart Association, Greater Southeast Affiliate.

[1]The abbreviations used are: GBS, Group B streptococci; GAPDH, glyceraldehyde-3-phosphate dehydrogenase; SkzL, skizzle; wtSkzL, recombinant wild-type SkzL; SK, streptokinase; SAK, staphylokinase; Pg, plasminogen; [Glu]Pg, native plasminogen; [Lys]Pg, plasminogen lacking the amino-terminal 77-residue PAN module; Pm, [Lys]plasmin; uPA, high molecular weight urokinase; sctPA, single-chain tissue-type plasminogen activator; FFR-CH_2Cl, D-Phe-Phe-Arg-CH_2Cl; [5F]FFR-[Glu]Pg, [5F]FFR-[Lys]Pg, and [5F]FFR-Pm, [Glu]Pg, [Lys]Pg, or Pm labeled at the active site with 5-(iodoacetamido)fluorescein attached to the thiol generated on N^{α}-[(acetylthio)acetyl]-D-Phe-Phe-Arg-CH_2Cl; DTNB, 5, 5'–dithiobis-(2-nitrobenzoic acid); DTT, dithiothreitol; 6-AHA, 6-aminohexanoic acid; *p*NA, *para*-nitroaniline; VLK-*p*NA, D-Val-Leu-Lys-*p*-

nitroanalide; pyro-EPR-*p*NA, pyro-Glu-Pro-Arg-*p*NA; LBS, lysine-binding sites; [5F]-SkzL, SkzL labeled at Cys^{393} and Cys^{401} with 5-(iodoacetamido)fluorescein; SkzLΔK415, skizzle lacking the COOH-terminal Lys^{415} residue; SDS-PAGE, sodium dodecyl sulfate-polyacrylamide gel electrophoresis.

[2]Schechter-Berger (81) notation referring to the residues of a substrate (from the NH_2-terminal end) as …P4-P3-P2-P1-P1'-P2'… with the scissile bond at P1-P1'.

References

1. Schuchat, A. (1999) *Lancet* **353**, 51-56

2. Pietrocola, G., Schubert, A., Visai, L., Torti, M., Fitzgerald, J. R., Foster, T. J., Reinscheid, D. J., and Speziale, P. (2005) *Blood* **105**, 1052-1059

3. Blumberg, H. M., Stephens, D. S., Modansky, M., Erwin, M., Elliot, J., Facklam, R. R., Schuchat, A., Baughman, W., and Farley, M. M. (1996) *J. Infect. Dis.* **173**, 365-373

4. Brochet, M., Couve, E., Zouine, M., Vallaeys, T., Rusniok, C., Lamy, M. C., Buchrieser, C., Trieu-Cuot, P., Kunst, F., Poyart, C., and Glaser, P. (2006) *Microbes Infect.*

5. Fluegge, K., Schweier, O., Schiltz, E., Batsford, S., and Berner, R. (2004) *Eur. J. Clin. Microbiol. Infect. Dis.* **23**, 818-824

6. Sun, H., Ringdahl, U., Homeister, J. W., Fay, W. P., Engleberg, N. C., Yang, A. Y., Rozek, L. S., Wang, X., Sjobring, U., and Ginsburg, D. (2004) *Science* **305**, 1283-1286

7. Henkin, J., Marcotte, P., and Yang, H. C. (1991) *Prog. Cardiovasc. Dis.* **34**, 135-164

8. Bergmann, S., Wild, D., Diekmann, O., Frank, R., Bracht, D., Chhatwal, G. S., and Hammerschmidt, S. (2003) *Mol. Microbiol.* **49**, 411-423

9. Lahteenmaki, K., Kuusela, P., and Korhonen, T. K. (2001) *FEMS Microbiol. Rev.* **25**, 531-552

10. Magalhaes, V., Veiga-Malta, I., Almeida, M. R., Baptista, M., Ribeiro, A., Trieu-Cuot, P., and Ferreira, P. (2007) *Microbes Infect.* **9**, 1276-1284

11. Whiting, G. C., Evans, J. T., Patel, S., and Gillespie, S. H. (2002) *J. Med. Microbiol.* **51**, 837-843

12. Cork, A. J., Jergic, S., Hammerschmidt, S., Kobe, B., Pancholi, V., Benesch, J. L., Robinson, C. V., Dixon, N. E., Aquilina, J. A., and Walker, M. J. (2009) *J. Biol. Chem.* **284**, 17129-17137

13. Tettelin, H., Masignani, V., Cieslewicz, M. J., Eisen, J. A., Peterson, S., Wessels, M. R., Paulsen, I. T., Nelson, K. E., Margarit, I., Read, T. D., Madoff, L. C., Wolf, A. M., Beanan, M. J., Brinkac, L. M., Daugherty, S. C., DeBoy, R. T., Durkin, A. S., Kolonay, J. F., Madupu, R., Lewis, M. R., Radune, D., Fedorova, N. B., Scanlan, D., Khouri, H., Mulligan, S., Carty, H. A., Cline, R. T., Van Aken, S. E., Gill, J., Scarselli, M., Mora, M., Iacobini, E. T., Brettoni, C., Galli, G., Mariani, M., Vegni, F., Maione, D., Rinaudo, D., Rappuoli, R., Telford, J. L., Kasper, D. L., Grandi, G., and Fraser, C. M. (2002) *Proc. Natl. Acad. Sci. U S A* **99**, 12391-12396

14. Altschul, S. F., Gish, W., Miller, W., Myers, E. W., and Lipman, D. J. (1990) *J. Mol. Biol.* **215**, 403-410

15. Brockway, W. J., and Castellino, F. J. (1972) *Arch Biochem Biophys* **151**, 194-199

16. Tordai, H., Banyai, L., and Patthy, L. (1999) *FEBS Lett.* **461**, 63-67

17. Markus, G., DePasquale, J. L., and Wissler, F. C. (1978) *J. Biol. Chem.* **253**, 727-732

18. Robbins, K. C., Boreisha, I. G., Arzadon, L., and Summaria, L. (1975) *J. Biol. Chem.* **250**, 4044-4047

19. Sjoholm, I. (1973) *Eur. J. Biochem.* **39**, 471-479

20. Violand, B. N., Byrne, R., and Castellino, F. J. (1978) *J. Biol. Chem.* **253**, 5395-5401

21. Castellino, F. J., Brockway, W. J., Thomas, J. K., Liano, H. T., and Rawitch, A. B. (1973) *Biochemistry* **12**, 2787-2791

22. Urano, T., Chibber, B. A., and Castellino, F. J. (1987) *Proc. Natl. Acad. Sci. U S A* **84**, 4031-4034

23. Markus, G. (1996) *Fibrinolysis* **10**, 75-85

24. Markus, G., Priore, R. L., and Wissler, F. C. (1979) *J. Biol. Chem.* **254**, 1211-1216

25. Weisel J. W., N. C., Korsholm B., Petersen L. C., Suenson E. (1984) *J. Mol. Biol.* **235**, 1117-1135

26. Ponting, C. P., Marshall, J. M., and Cederholm-Williams, S. A. (1992) *Blood Coagul Fibrinolysis* **3**, 605-614

27. Marshall, J. M., Brown, A. J., and Ponting, C. P. (1994) *Biochemistry* **33**, 3599-3606

28. McCance, S. G., and Castellino, F. J. (1995) *Biochemistry* **34**, 9581-9586

29. Urano, T., Sator de Serrano, V., Chibber, B. A., and Castellino, F. J. (1987) *J. Biol. Chem.* **262**, 15959-15964

30. Cummings, H. S., and Castellino, F. J. (1985) *Arch Biochem Biophys* **236**, 612-618

31. Lerch, P. G., Rickli, E. E., Lergier, W., and Gillessen, D. (1980) *Eur. J. Biochem.* **107**, 7-13

32. Ploplis, V. A., Cummings, H. S., and Castellino, F. J. (1982) *Biochemistry* **21**, 5891-5897

33. Bode, W., and Huber, R. (1976) *FEBS Lett.* **68**, 231-236

34. Boxrud, P. D., and Bock, P. E. (2004) *J. Biol. Chem.* **279**, 36642-36649

35. Boxrud, P. D., Verhamme, I. M., and Bock, P. E. (2004) *J. Biol. Chem.* **279**, 36633-36641

36. Boxrud, P. D., Verhamme, I. M., Fay, W. P., and Bock, P. E. (2001) *J. Biol. Chem.* **276**, 26084-26089

37. Wang, S., Reed, G. L., and Hedstrom, L. (1999) *Biochemistry* **38**, 5232-5240

38. Wang, S., Reed, G. L., and Hedstrom, L. (2000) *Eur. J. Biochem.* **267**, 3994-4001

39. Bean, R. R., Verhamme, I. M., and Bock, P. E. (2005) *J. Biol. Chem.* **280**, 7504-7510

40. Boxrud, P. D., and Bock, P. E. (2000) *Biochemistry* **39**, 13974-13981

41. Boxrud, P. D., Fay, W. P., and Bock, P. E. (2000) *J. Biol. Chem.* **275**, 14579-14589

42. Tharp, A. C., Laha, M., Panizzi, P., Thompson, M. W., Fuentes-Prior, P., and Bock, P. E. (2009) *J. Biol. Chem.* **284**, 19511-19521

43. Esmon, C. T., and Mather, T. (1998) *Nat. Struct. Biol.* **5**, 933-937

44. Grella, D. K., and Castellino, F. J. (1997) *Blood* **89**, 1585-1589

45. Jespers, L., Vanwetswinkel, S., Lijnen, H. R., Van Herzeele, N., Van Hoef, B., Demarsin, E., Collen, D., and De Maeyer, M. (1999) *Thromb. Haemost.* **81**, 479-485

46. Ward, P. N., Field, T. R., Rosey, E. L., Abu-Median, A. B., Lincoln, R. A., and Leigh, J. A. (2004) *J. Mol. Biol.* **342**, 1101-1114

47. Johnsen, L. B., Rasmussen, L. K., Petersen, T. E., Etzerodt, M., and Fedosov, S. N. (2000) *Biochemistry* **39**, 6440-6448

48. Sazonova, I. Y., Houng, A. K., Chowdhry, S. A., Robinson, B. R., Hedstrom, L., and Reed, G. L. (2001) *J. Biol. Chem.* **276**, 12609-12613

49. Ward, P. N., and Leigh, J. A. (2002) *J Bacteriol* **184**, 119-125

50. Ward, P. N., and Leigh, J. A. (2004) *Indian J. Med. Res.* **119 Suppl**, 136-140

51. Lijnen, H. R., De Cock, F., and Collen, D. (1994) *Eur. J. Biochem.* **224**, 567-574

52. de Munk, G. A., Groeneveld, E., and Rijken, D. C. (1993) *Thromb. Haemost.* **70**, 481-485

53. Lijnen, H. R., Nelles, L., Van Hoef, B., Demarsin, E., and Collen, D. (1988) *Eur. J. Biochem.* **177**, 575-582

54. Lijnen, H. R., Van Hoef, B., Nelles, L., and Collen, D. (1990) *J. Biol. Chem.* **265**, 5232-5236

55. Nelles, L., Lijnen, H. R., Collen, D., and Holmes, W. E. (1987) *J. Biol. Chem.* **262**, 5682-5689

56. Urano, T., Sator de Serrano, V., Gaffney, P. J., and Castellino, F. J. (1988) *Biochemistry* **27**, 6522-6528

57. Novokhatny, V., Medved, L., Lijnen, H. R., and Ingham, K. (1995) *J. Biol. Chem.* **270**, 8680-8685

58. de Munk, G. A., Caspers, M. P., Chang, G. T., Pouwels, P. H., Enger-Valk, B. E., and Verheijen, J. H. (1989) *Biochemistry* **28**, 7318-7325

59. Panizzi, P., Boxrud, P. D., Verhamme, I. M., and Bock, P. E. (2006) *J. Biol. Chem.* **281**, 26774-26778

60. Castellino, F. J., and Powell, J. R. (1981) *Methods Enzymol.* **80 Pt C**, 365-378

61. Deutsch, D. G., and Mertz, E. T. (1970) *Science* **170**, 1095-1096

62. Bock, P. E., Day, D. E., Verhamme, I. M., Bernardo, M. M., Olson, S. T., and Shore, J. D. (1996) *J. Biol. Chem.* **271**, 1072-1080

63. Bock, P. E. (1992) *J. Biol. Chem.* **267**, 14963-14973

64. Violand, B. N., and Castellino, F. J. (1976) *J. Biol. Chem.* **251**, 3906-3912

65. Pace, C. N., Vajdos, F., Fee, L., Grimsley, G., and Gray, T. (1995) *Protein Sci.* **4**, 2411-2423

66. Bock, P. E., Olson, S. T., and Bjork, I. (1997) *J. Biol. Chem.* **272**, 19837-19845

67. Bachmann, F. (1994) The Plasminogen-Plasmin Enzyme System. in *Hemosasis and Thrombosis: Basic Principles and Clinical Practice* (Colman, R. W., hirsh, J., Marder, V. J., and Salzman, E. W. ed.), Third Edition Ed., J. B. Lippincott Company, Philadelphiia. pp 1592-1622

68. Jones, D. T. (1999) *J. Mol. Biol.* **292**, 195-202

69. Larkin, M. A., Blackshields, G., Brown, N. P., Chenna, R., McGettigan, P. A., McWilliam, H., Valentin, F., Wallace, I. M., Wilm, A., Lopez, R., Thompson, J. D., Gibson, T. J., and Higgins, D. G. (2007) *Bioinformatics* **23**, 2947-2948

70. Tharp, A. C., Laha, M., Panizzi, P., Thompson, M. W., Fuentes-Prior, P., and Bock, P. E. (2009) *J. Biol. Chem.*

71. Panizzi, P., Friedrich, R., Fuentes-Prior, P., Bode, W., and Bock, P. E. (2004) *Cell Mol. Life Sci.* **61**, 2793-2798

72. Fredenburgh, J. C., and Nesheim, M. E. (1992) *J. Biol. Chem.* **267**, 26150-26156

73. Rajamohan, G., Dahiya, M., Mande, S. C., and Dikshit, K. L. (2002) *Biochem. J.* **365**, 379-389

74. Petros, A. M., Ramesh, V., and Llinas, M. (1989) *Biochemistry* **28**, 1368-1376

75. Hochschwender, S. M., and Laursen, R. A. (1981) *J. Biol. Chem.* **256**, 11172-11176

76. Plow, E. F., and Collen, D. (1981) *J. Biol. Chem.* **256**, 10864-10869

77. Vali, Z., and Patthy, L. (1982) *J. Biol. Chem.* **257**, 2104-2110

78. Cockell, C. S., Marshall, J. M., Dawson, K. M., Cederholm-Williams, S. A., and Ponting, C. P. (1998) *Biochem J* **333 (Pt 1)**, 99-105

79. Chang, Y., Mochalkin, I., McCance, S. G., Cheng, B., Tulinsky, A., and Castellino, F. J. (1998) *Biochemistry* **37**, 3258-3271

80. Novokhatny, V. V., Matsuka Yu, V., and Kudinov, S. A. (1989) *Thromb Res* **53**, 243-252

81. Schechter, I., and Berger, A. (1967) *Biochem Biophys Res Commun* **27**, 157-162

APPENDIX A

STUDIES REPORTED IN CHAPTER 2 AS SUPPLEMENTAL DATA

Analysis of the three Cys residues of SkzL

Experimental Procedures

One difference between SK and SkzL is the presence of three Cys residues, Cys^{120}, Cys^{393}, and Cys^{401}. Site-directed mutagenesis (Stratagene QuikChange) was used to create single (C120S, C393S, C401S), double (C120S/C393S, C120S/C401S, C393S/C401S), and triple (C120S/C393S/C401S) Cys-to-Ser substitution mutants that were purified as described for wild type. Thiols were quantitated by reaction of SkzL (3-5 μM) with 450 μM 5, 5' –dithiobis-(2-nitrobenzoic acid) (DTNB) monitored at 412 nm. Thiol concentrations were determined under non-denaturing (100 mM HEPES, 0.3 M NaCl, 1 mM EDTA, pH 7.0) and denaturing conditions (6 M guanidine, 100 mM HEPES, 0.3 M NaCl, 1 mM EDTA, pH 7.0) using absorption coefficients 14150 $M^{-1}cm^{-1}$ and 16434 $M^{-1}cm^{-1}$, respectively. For determination of intra-molecular disulfide bonds, 50-100 μM wild-type SkzL and Cys-to-Ser substitution mutants were reacted with a 5-fold molar excess of DTT for 10 min at 25 °C followed by chromatography on ~1 ml freshly poured Sephadex G-25 spin columns (Bio-Rad), and the concentration of thiols was determined as described.

Results and Discussion

Analysis of wild-type SkzL showed one thiol under native conditions and two thiols under denaturing conditions (Appendix Table A1), indicating that one Cys is buried within the protein and one Cys residue was unaccounted for. Reduction of SkzL revealed the observation of two free thiols under non-denaturing conditions and a total of 2.6 thiols under denaturing conditions. This result suggests the presence of a partially reduced internal disulfide bond. Single Ser substitution mutants of Cys^{393} or Cys^{401} contained one thiol under native conditions and 2 thiols under denaturing conditions with no effect of DTT, indicating the loss of an internal disulfide bond. The single Ser mutant lacking Cys^{120} contained one thiol under native and denaturing conditions with the observation of a second thiol upon reaction with DTT, indicating that the mutant retained the internal disulfide bond.

Appendix Table A1. Quantification of SkzL Cys Residues. Cys-to-Ser substitution mutants were generated and thiols expressed as *mol thiol/mol SkzL* were quantitated as described above in "Experimental Procedures". The number of thiols are listed for those measured under non-denaturing buffer conditions (*native*), the number of thiols measured under denaturing buffer conditions (*denatured*), and the number of thiols measured under the corresponding buffer condition following reaction with a 5-fold molar excess of dithiothreitol (*+DTT*) to reduce disulfide bonds. Results represent averaged values for at least two independent preparations of each mutant.

SkzL mutation	native	native + DTT	denatured	denatured + DTT
	(*mol thiol/ mol SkzL*)	(*mol thiol/ mol SkzL*)	(*mol thiol/ mol SkzL*)	(*mol thiol/ mol SkzL*)
wild type	1.08	1.95	1.70	2.61
C120S	0.83	1.44	0.69	1.25
C393S	0.91	0.82	1.63	1.38
C401S	0.99	0.96	1.74	1.57
C120S/C393S	1.04		0.86	
C120S/C401S	0.95		0.97	
C393S/C401S	0.07		0.797	
C120S/C393S/C401S	0.01		0.01	

The results indicate that Cys^{120} is buried within the protein and that Cys^{393} and Cys^{401} each occur partially as free thiols and partially as an intramolecular disulfide bond. The results also indicate that non-physiological disulfide-mediated dimerization can occur through Cys^{393} or Cys^{401}. It is unclear what role the Cys residues and intramolecular disulfide bond play in SkzL function, although there is no evidence for the formation of covalent Pg/Pm-SkzL complexes through disulfide exchange (results not shown).

Secreted Protein Profile Analysis

Experimental Procedures

To determine the secreted protein profile of *S. agalactiae*, bacterial supernatant samples in the mid-logarithmic and stationary growth phases from three separate bacterial growths were normalized to identical optical densities and subjected to trichloroacetic acid precipitation. Samples were separated by SDS-PAGE, subjected to in-gel tryptic digestion, and analyzed by LC-MS-MS. Samples were analyzed using a Thermo Finnigan LTQ ion trap instrument following separation on a packed capillary tip with Jupiter C18 resin using an in-line solid phase C18 extraction column. Tandem MS-MS spectra were compared to the *S. agalactiae* genome using the SEAQUEST algorithm. Data were filtered using the following criteria: cross-correlation value of ≥ 1.0 for singly charge ions, ≥ 1.8 for doubly charged ions, and ≥ 2.5 for triply charged ions. A primary score of ≤ 5 and a preliminary score of ≥ 350 were required for positive peptide identification. All proteins identified by less than 2 peptides were eliminated. False positive results were filtered and proteins were reassembled using a parsimony method (1). Protein identities are reported as mean peptide count ($\pm$ 1 SD). Only proteins identified in all three bacterial growths are reported.

Appendix Table A2. Secreted protein profile for *Streptococcus agalactiae*. Mass spectrometry analysis of secreted proteins from three distinct bacterial samples obtained at the mid-logarithmic and stationary growth phases as described above in "Experimental Procedures". Only proteins identified in all three samples are represented.

		logarithmic phase		stationary phase	
accession number	protein name	mean peptide count	standard deviation	mean peptide count	standard deviation
22536202	pcsB protein (46.5 kDa)	26.0	13.1	27.3	11.8
22536217	GBS surface immunogenic	10.0	4.6	17.7	3.2
22536801	enolase	5.0	5.3	1.3	0.6
22536926	elongation factor Tu	4.7	3.1	1.3	2.3
22536996	NP_687847.1 (Zymogen Activator and Adhesion Protein (ZAAP))	32.3	14.2	22.3	16.3
22536997	NP_687848.1	17.3	2.9	12.0	1.0
22537285	**SkzL (NP_688136.1)**	**1.0**	**0.0**	**3.0**	**1.7**
22537355	hyaluronidase	5.7	2.1	6.3	2.1
22537497	surface antigen-related protein	13.7	6.5	18.0	5.6
22537823	immunogenic secreted protein (N-acetylmuramoyl-L-alanine amidase, family 4)	84.0	21.0	85.3	10.6
22537907	glycerladehyde-3-phosphate dehydrogenase	2.3	2.5	1.7	1.5
22538178	cAMP factor	9.0	1.7	21.0	11.5
22538282	LysM domain protein	3.3	1.2	3.0	1.0
22536474	ABC transporter	1.0	1.0	2.0	1.0
22536566	unknown, lipoprotein putative	1.0	1.0	1.0	1.0
22536616	surface protein Rib	1.7	0.6	3.3	1.2
22537364	NP_688215.1	1.0	0.0	2.3	2.3
22537480	5'-nucleotidase family protein	2.0	3.5	14.3	2.1
22536554	sag0371	1.7	0.6	1.0	1.0

References

1. Zhang, B., Chambers, M. C., and Tabb, D. L. (2007) *J. Proteome Res.* **6**, 3549-3557

APPENDIX B

STUDIES REPORTED IN CHAPTER 2 AS UNPUBLISHED RESULTS

Introduction

The work in Chapter 2 (published in the *Journal of Biological Chemistry* 2010; 285(27): 21153-21164) focuses on the cloning, expression, and purification of SkzL as a monomer. In addition, it addresses the characterization of the Cys residues, protein secretion from *Streptococcus agalactiae*, SkzL binding to Pg and Pm, and function of SkzL as an effector of uPA- and tPA-mediated Pg activation. Chapter 2: Appendix B will focus on results presented as either data not shown or those not included in Chapter 2.

Experimental Procedures

Conformational Activation of Pg by SkzL Assessed by SDS-PAGE

To prevent fluorescent labeling of SkzL, free thiol groups were covalently blocked by incubation of SkzL with a 5-fold molar excess of iodoacetamide for 2 h at room temperature, followed by extensive dialysis to remove excess iodoacetamide. To determine if SkzL was capable of conformational activation of Pg, 10 μM [Lys]Pg was incubated with 80 μM ATA-FFR-CH_2Cl and 16 μM iodoacetamide-blocked SkzL (or 16 μM native SK as a positive control) for 2 h at 25 °C. Excess ATA-FFR-CH_2Cl was removed by Sephadex G-25 spin column-chromatography. The ATA-FFR-CH_2Cl-blocked induced active site was reacted with 0.1 M hydroxylamine, to deacetylate the ATA-FFR-CH_2Cl inhibitor and 40 μM 5-(iodoacetamido)fluorescein (5-IAF). Excess

probe was removed by Sephadex G-25 spin-column chromatography. One reaction contained all reaction components and 4 control reactions each lacked one of the components (5-IAF, SkzL, hydroxylamine, ATA-FFR-CH_2Cl). To visualize the reaction products SDS-PAGE was performed under reducing conditions to ensure separation of the Pg and SkzL bands (1).

Analytical Ultracentrifugation

Sedimentation velocity experiments were performed on a Beckman-Coulter XLE-1 Analytical Ultracentrifuge at the University of Tennessee, Knoxville with the help of Dr. Cynthia Peterson. Interference scans were performed at 50,000 RPM at 25 °C with the vacuum set at 0 microns. The partial specific volume of SkzL was determined to be 0.7277 using the Sednterp program. Data were analyzed using the SedFit program to determine sedimentation coefficients, molecular weights, and percent abundances of species (2-4).

Chromogenic Substrate Kinetics

The potential activation of 100 nM [Lys]Pg by SkzL was measured in the absence and presence of 0.5 nM [Lys]Pm. In these assays, hydrolysis of 200 μM D-Val-Leu-Lys-*p*-nitroanalide (VLK-*p*NA) was measured at 405 nm as a function of time. Assays were performed in 50 mM HEPES, 125 mM NaCl, 1 mM EDTA, 1 mg/ml PEG 8,000, pH 7.4 using PEG 20,000 coated polystyrene cuvettes (5-8). Raw data were reported as absorbance at 405 nm ($A_{405\ nm}$) as a function of time.

Results and Discussion

Due to sequence homology to SK and conservation of key residues involved in Pg activation, it was hypothesized that SkzL would activate Pg through the molecular sexuality mechanism of NH_2-terminal insertion (9). To evaluate this hypothesis, an SDS-PAGE experiment was performed to investigate potential conformational activation of Pg through incorporation of a fluorescence probe at the induced active site. In this reaction, SkzL or SK was reacted with Pg in the presence of ATA-FFR-CH_2Cl to covalently inhibit the induced active site. Deacetylation of the thiol followed by reaction with a fluorophore-iodoacetamide would result in incorporation of a fluorescent probe in the inhibited, induced active site. As a positive control, SK resulted in efficient conformational activation of Pg and probe incorporation in the induced active. Binding of SkzL to Pg did not facilitate probe incorporation, indicating failure of SkzL to generate an induced active site upon Pg binding (Appendix Fig. B1) (1).

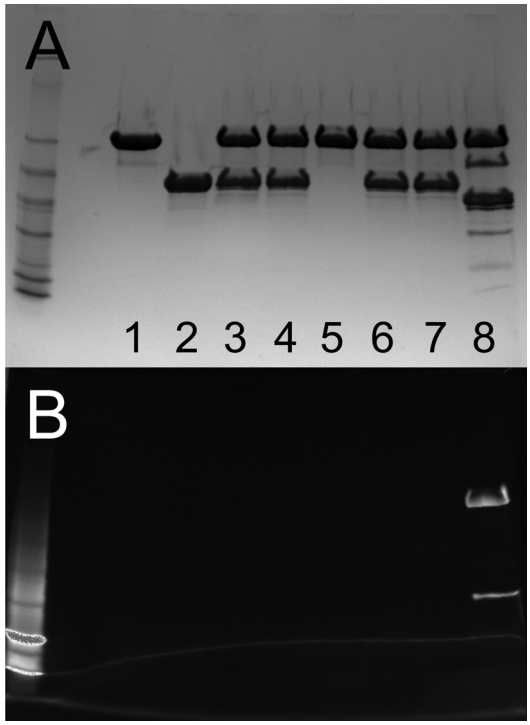

Appendix Figure B1. Fluorescence labeling following conformational activation of Pg. SDS-PAGE of fluorescence labeling reactions containing [Lys]Pg (*Lane 1*) and SkzL (*Lane 2*), to determine the potential for conformational activation. Lanes 3-6 correspond to labeling reactions in which one reaction component was omitted (*Lane 3*, hydroxylamine omitted; *Lane 4*, FFR-CH_2Cl added for 20 min to block the active site prior to incubation with ATA-FFR-CH_2Cl; *Lane 5*, SkzL omitted; *Lane 6*, ATA-FFR-CH_2Cl omitted). The complete reaction for SkzL (*Lane 7*) and SK as a positive control (*Lane 8*) contain all reaction components as described in "Experimental Procedures".

This result was confirmed using chromogenic substrate kinetic assays to evaluate the potential for Pg activation in the absence and presence of catalytic Pm concentrations. Pm generated by Pg activation results in measurable hydrolysis of the chromogenic substrate (VLK-*p*NA) as a function of time. No hydrolysis of VLK-*p*NA was seen following reaction of 100 nM [Lys]Pg with μM SkzL concentrations indicating that SkzL does not conformationally or proteolytically activate Pg. As SkzL shares sequence homology to SAK, which requires catalytic concentrations of Pm for Pg activation, assays were also performed in the presence of 0.5 nM Pm. No increase in the rate of

substrate hydrolysis above the Pm baseline was seen, indicating that SkzL does not activate Pg in the absence or presence of catalytic Pm (Appendix Fig. B2).

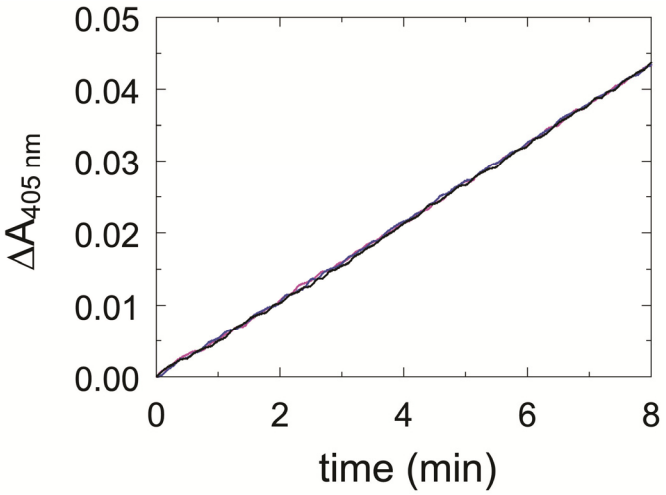

Appendix Figure B2. Measurement of VLK-*p*NA hydrolysis to detect Pg activation by SkzL. Rates of hydrolysis of VLK-*p*NA by 0.5 nM Pm incubated with 100 nM [Lys]Pg in the absence (*black line*) and presence of 1 μM (*pink line*) and 5 μM (*blue line*) SkzL. Hydrolysis of VLK-*p*NA was measured at 405 nm ($\Delta A_{405\ nm}$) as a function of time as described in "Experimental Procedures".

Results of the cysteine-to-serine mutagenesis studies in Chapter 2: Appendix A indicated that Cys^{120} is buried within the protein and that Cys^{393} and Cys^{401} each occur partially as free thiols and partially as an internal disulfide bond. The results also indicated that trace disulfide-mediated dimerization may occur through Cys^{393} or Cys^{401}. As a result of the formation of trace levels of SkzL dimer removed during purification, it was hypothesized that SkzL may form a non-covalent dimer in solution. To address this hypothesis, analytical ultracentrifugation was performed in collaboration with Dr. Cynthia Peterson at the University of Tennessee, Knoxville. Sedimentation velocity interference scans were performed with varying SkzL concentrations. A 48 kDa

monomer was the predominant species accounting for 85% of the protein with a 15% contribution from a 84 kDa species (Appendix Fig. B2). The molecular weights are in good agreement with those calculated by mass spectrometry for SkzL monomer and dimer (47 kDa and 94 kDa, respectively). Densitometry of SDS-PAGE for this protein sample at varying protein concentrations confirmed the presence of 13-17% covalent SkzL dimer. This indicates that non-covalent dimerization of SkzL in solution does not occur (2-4).

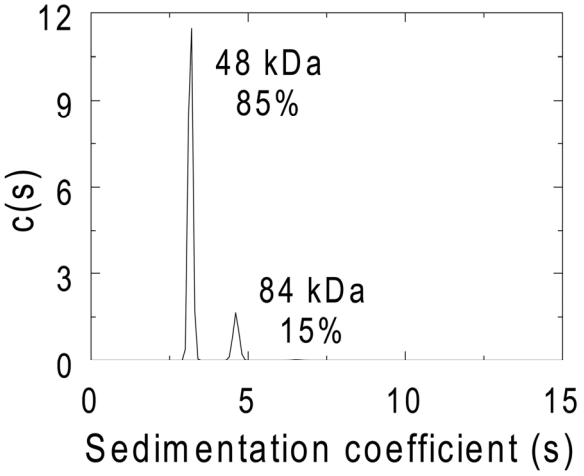

Appendix Figure B3. Analytical Ultracentrifugation of purified recombinant SkzL. Sedimentation coefficients obtained from sedimentation velocity interference scans of 1 mg/ml SkzL revealed a 48 kDa species accounting for 85% of the protein and an 84 kDa species accounting for 15%. Studies were performed and analyzed as described in "Experimental Procedures".

Both Pg and Pm contain several Cys residues which stabilize the tertiary protein structure through disulfide bonds. To determine the potential covalent complex formation between Pg/Pm and SkzL through SkzL free thiol groups, SDS-PAGE experiments were performed and no evidence of covalent complex formation was seen (data not shown).

However, proteolytic degradation of SkzL was observed at high Pm concentrations. As SkzL is hypothesized to be involved in Pm generation, it was vital to characterize the stability of SkzL in the presence of Pm. To that end, SDS-PAGE experiments were performed to evaluate SkzL stability as a function of Pm concentration. In these studies, 10 μM [5F]-SkzL was incubated with increasing Pm concentrations (0.5 nM – 2000 nM) for one hour at 25 °C in the dark to preserve fluorescence intensity. Pm proteolytic activity was quenched with 70 μM FFR-CH_2Cl and protein interactions were disrupted by addition of hot SDS buffer. Samples were subjected to SDS-PAGE on a 4-15% gradient gel followed by Coomassie blue staining. Images of fluorescent and stained gels show dramatic proteolytic degradation of SkzL as a function of Pm concentration (Appendix Fig. B3).

Through 1 h, 10 μM SkzL was determined to be stable at 0.5-10 nM Pm. Similar results were seen at 2 hours (data not shown). For studies in this thesis, concentrations of Pm generated were limited to those less than 10 nM to ensure SkzL stability.

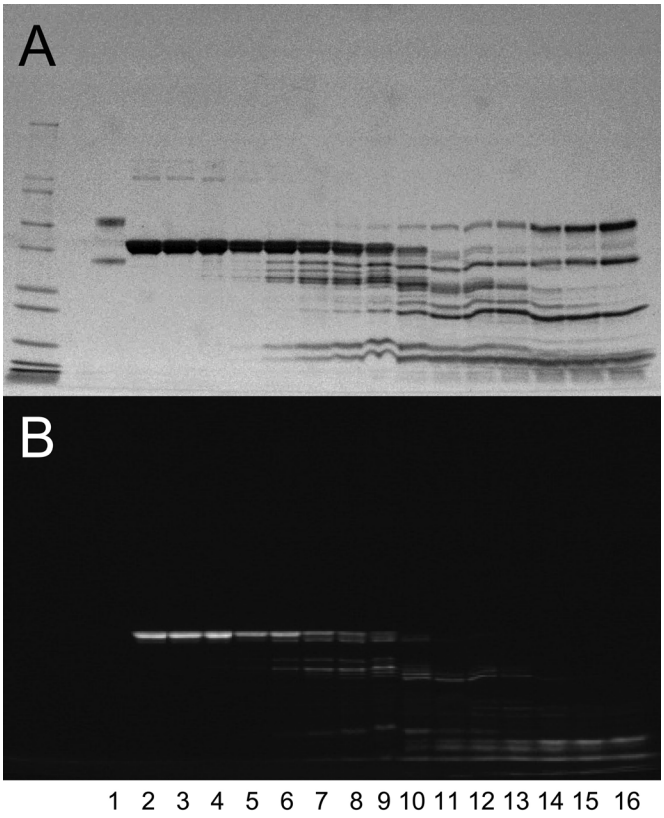

Appendix Figure B4. SkzL stability as a function of Pm concentration. SDS-PAGE of 10 μM [5F]-SkzL reacted for 1 h with increasing Pm concentrations with a Pm standard (*lane 1*). *Lanes 2-16* correspond to 0.5, 10, 25, 50, 75, 100, 200, 300, 400, 500, 1000, 1500, and 2000 nM Pm. Reactions were quenched by addition of 70 μM FFR-CH_2Cl and hot SDS buffer as described in "Experimental Procedures".

References

1. Bock, P. E., Day, D. E., Verhamme, I. M., Bernardo, M. M., Olson, S. T., and Shore, J. D. (1996) *J. Biol. Chem.* **271**, 1072-1080

2. Balbo, A., Minor, K. H., Velikovsky, C. A., Mariuzza, R. A., Peterson, C. B., and Schuck, P. (2005) *Proc. Natl. Acad. Sci. U S A* **102**, 81-86

3. Laue, T. M., and Stafford, W. F., 3rd. (1999) *Annu Rev Biophys Biomol Struct* **28**, 75-100

4. Schuck, P. (2004) *Biophys Chem* **108**, 187-200

5. Boxrud, P. D., and Bock, P. E. (2004) *J. Biol. Chem.* **279**, 36642-36649

6. Boxrud, P. D., Fay, W. P., and Bock, P. E. (2000) *J. Biol. Chem.* **275**, 14579-14589

7. Boxrud, P. D., Verhamme, I. M., and Bock, P. E. (2004) *J. Biol. Chem.* **279**, 36633-36641

8. Boxrud, P. D., Verhamme, I. M., Fay, W. P., and Bock, P. E. (2001) *J. Biol. Chem.* **276**, 26084-26089

9. Bode, W., and Huber, R. (1976) *FEBS Lett.* **68**, 231-236

CHAPTER III

SKIZZLE IS AN EFFECTOR OF TISSUE-TYPE PLASMINOGEN ACTIVATOR-MEDIATED PLASMINOGEN ACTIVATION

Abstract

Skizzle (SkzL), secreted by *Streptococcus agalactiae*, binds active site fluorescently labeled-single-chain tPA (sctPA) with low affinity (K_D ~14 μM) through Lys^{415}-independent, lysine-binding site (LBS)-dependent interaction of the putative SkzL internal motif with tPA kringle 2. SkzL enhances [Glu]Pg activation by non-cleavable sctPA (nctPA) and two-chain tPA (tctPA) ~490-fold and ~400-fold, respectively and enhances [Lys]Pg activation by nctPA and tctPA ~48-fold and ~7-fold, respectively. The apparent affinities of 6-13 μM determined for the SkzL-dependences on enhanced [Glu]Pg and [Lys]Pg activation, appear to represent SkzL-tPA binding. Deletion of the COOH-terminal SkzL Lys^{415} residue results in a ~2.5-4-fold reduction in the enhancement of [Lys]Pg activation by nctPA and tctPA, compared with wtSkzL, suggesting that Lys^{415}-dependent SkzL-Pg interactions affect the enhancement amplitude. Analyses of the Pg-dependence kinetics suggests a mechanism of SkzL•tPA•Pg•SkzL quaternary complex formation, although further work is needed to clarify this mechanism. As a result, SkzL is identified as a novel cofactor of Pg activation by tPA. Combined with enhanced rates of plasma clot lysis by tPA reported in Chapter 2, these results support a Pg activation-specific role for SkzL in the pathogenesis of *Streptococcus agalactiae* infection.

Introduction

Activation of human plasminogen (Pg) occurs endogenously through proteolysis by two activators, urokinase (uPA) and tissue-type plasminogen activator (tPA). Proteolytic Pg activation occurs by cleavage of the Arg^{561}-Val^{562} peptide bond in the Pg catalytic domain to form the active serine proteinase plasmin (Pm). Following cleavage of Pg by Pm, the NH_2-terminal 77-residue PAN (Pg/apple/nematode) module of zymogen [Glu]Pg is released to yield [Lys]Pg (1). Three of the five Pg kringle domains (kringles 1, 4, and 5) contain lysine binding sites (LBS) that exhibit moderate affinity for L-lysine and higher affinity for the lysine analog 6-aminohexanoic acid (6-AHA) (1-7).

[Glu]Pg is maintained in the compact α-conformation by interaction of the PAN module with kringle 5 (8-12). The α-conformation of [Glu]Pg, however, is in equilibrium with a low concentration of a partially extended β-conformation [Glu]Pg, governed by chloride ion concentration (3,9,13-15). Upon binding of benzamidine to kringle 5, [Glu]Pg assumes the partially extended β-conformation (9,16-19). Lacking the PAN module, [Lys]Pg is in the partially extended β-conformation (9,19). Upon occupation of the LBS, particularly that of kringle 4, by ligands such as 6-AHA, both [Glu]Pg and [Lys]Pg assume the fully extended γ-conformation (9,16-21). Because the extended β- and γ-conformations offer better binding accessibility, [Lys]Pg and ligand-bound [Glu]Pg are better substrates for activation by uPA and tPA than [Glu]Pg in the α-conformation (9,16-19). As a result, LBS ligands such as L-lysine, 6-AHA, and fibrin are considered effectors of uPA- and tPA-mediated Pg activation (9,18).

Studies reported in Chapter 2 revealed the complex binding interactions between skizzle (SkzL) and Pg/Pm. The compact zymogen, [Glu]Pg bound SkzL with weak

affinity of ~3-16 μM, mediated by LBS-dependent interaction with the SkzL COOH-terminal Lys^{415} residue. Binding of SkzL to [Lys]Pg and Pm occurred with near-equal affinity through two distinct binding interactions: a high affinity interaction with K_D's of 50-80 nM and a low affinity interaction with K_D's of 9-20 μM. The LBS-dependent high affinity interaction between SkzL and [Lys]Pg/Pm, mediated by SkzL Lys^{415}, occurs through a putative interaction with kringle 4 (19,22,23). The LBS-dependent low affinity interaction is proposed to occur through interaction of a SkzL internal motif, analogous to the motif in the SK 250-loop, with Pg kringle 5 (24,25).

Studies of the effect of SkzL on activation of [Glu]Pg and [Lys]Pg by uPA were performed to examine the effect of SkzL binding on Pg conformation (Chapter 2). It was concluded that SkzL binding induced the [Glu]Pg α/β- to γ-conformational transition, reflected by the enhanced rate of [Glu]Pg activation by uPA to rates equivalent to [Glu]Pg or [Lys]Pg activation in the presence of 6-AHA (13,20,21). Together, these results identified SkzL as a novel effector of uPA-mediated [Glu]Pg activation, with a mechanism of action analogous to 6-AHA.

One structural difference between uPA and tPA is the presence of a second kringle domain in tPA (kringle 2) containing an LBS with high affinity for effector molecules such as lysine, 6-AHA, and fibrin fragments (26,27). In studies of activation of [Glu]Pg by tPA, enhanced activation is seen in the presence of these effectors. The kinetics of enhanced activation involves a decrease in K_m with varied degrees of k_{cat} increases reported (13,28-32). Intact fibrin enhances tPA-mediated Pg activation through formation of a ternary complex in which fibrin acts as a template to enhance tPA-Pg binding and Pg activation (7,33,34). Ternary complex formation occurs through

interaction of Pg kringle 5 and tPA-kringle 2 within the fibrin D region resulting in enhanced plasma Pg to Pm proteolysis (7,33).

The results in Chapter 2 indicated that SkzL enhanced the time to half-clot lysis by single-chain tPA (sctPA) ~2-fold. Kinetics assays also demonstrated that, unlike uPA, activation of both [Glu]Pg and [Lys]Pg by sctPA were enhanced by SkzL, in an LBS-dependent manner. The work in this chapter elaborates on these findings in an effort to determine the mechanism of SkzL-mediated enhancement of Pg activation by tPA.

Zymogen-like sctPA is proteolytically cleaved by Pm in plasma, to form the more active two-chain form (tctPA). sctPA is converted into tctPA in clot lysis assays performed with ^{125}I-sctPA (35). The studies in this chapter employed a non-cleavable sctPA mutant (nctPA) containing an Arg^{257}Glu substitution mutation rendering it resistant to Pm cleavage (36). The present studies reveal that SkzL binds tPA with low affinity, in an LBS-dependent manner mediated by a site distinct from SkzL Lys^{415}. Kinetic studies with nctPA and tctPA confirm the results of studies with sctPA reported in Chapter 2, identifying SkzL as an effector of tPA-mediated Pg activation. While the exact mechanism remains unclear, SkzL-mediated enhancement is proposed to occur by formation of a $SkzL_2$•tPA•Pg quaternary complex unlike the template mechanism for fibrin-bound tPA-mediated Pg activation.

Experimental Procedures

Protein Purification and Characterization

[Glu]Pg, [Lys]Pg, and Pm (all carbohydrate form 2) were prepared as previously described (6,37,38). Human sctPA, tctPA and nctPA (the non-cleavable $Arg^{257}Glu$ sctPA mutant, Molecular Innovations) were stored in 0.5 M HEPES, 0.5 M NaCl, pH 7.4 buffer to ensure solubility and were limited to one freeze-thaw cycle to maintain stable activity. [Glu]Pg, [Lys]Pg and SkzL were purified as described in Chapter 2 and stored in 50 mM HEPES, 125 mM NaCl, pH 7.4 at -80 °C following snap-freezing (6,39).

Active Site Labeling of sctPA

Inactivation of the human sctPA (54 μM) active site was achieved by reaction with 500 μM N^{α}-[(acetylthio)acetyl]-D-Phe-Phe-Arg-CH_2Cl (ATA-FFR-CH_2Cl) for 3 h at 25 °C followed by chromatography on Sephadex G-25 to remove excess inhibitor. Deacetylation with 0.1 M NH_2OH and thiol-specific reaction with a 4-fold molar excess of tetramethylrhodamine-5-iodoacetamide dihydroiodide (TMR, Invitrogen) for 1 h at 25 °C were followed by chromatography on Sephadex G-25 and dialysis to remove excess probe (38,40-42). [TMR]FFR-sctPA was stored in 0.5 M HEPES, 0.5 M NaCl, pH 7.4 buffer at -80 °C following snap-freezing. Protein concentration was determined by bicinchoninic acid protein assay (Pierce). Probe incorporation was determined to be 1.05 mol probe/mol tPA by absorbance measurements at 280 nm and 557 nm with an absorption coefficient of 90,527 M^{-1} cm^{-1} for TMR and an $A_{280\ nm}/A_{557\ nm}$ ratio of 0.215 in 6 M guanidine, 100 mM Tris-HCl, 1 mM EDTA, pH 8.5 buffer (43).

Fluorescence Equilibrium Binding

Fluorescence titrations 100 nM [TMR]FFR-sctPA with wtSkzL or SkzLΔK415 were performed at 25 °C in 100 mM HEPES, 100 mM NaCl, 1 mM EDTA, 1 mg/ml PEG 8,000, 0.02% Tween 80, pH 7.4 buffer containing 10 μM FFR-CH_2Cl using 1% Tween 80-coated acyclic cuvettes. Fluorescence was measured with an SLM 8100 fluorometer, with excitation at 550 nm and emission at 566 nm with 8 nm band-passes. Following correction for buffer blank and probe dilution (≤ 10%), data were expressed as the fractional change in the initial fluorescence, $(F_{obs}-F_o)/F_o = \Delta F/F_o$. Titrations were analyzed by nonlinear least-squares fitting of the quadratic binding equation:

$$\frac{\Delta F}{F_o} = \left(\frac{\Delta F_{max}}{F_o}\right)\left[\frac{\left(n[\mathrm{P}]_o + [\mathrm{L}]_o + K_D\right) - \sqrt{\left(n[\mathrm{P}]_o + [\mathrm{L}]_o + K_D\right)^2 - 4n[\mathrm{nP}]_o[\mathrm{L}]_o}}{2n[\mathrm{P}]_o}\right] \quad \textbf{Eqn. 1,}$$

where $\Delta F_{max}/F_o$ is the maximum fluorescence change, K_D is the dissociation constant, n is the stoichiometric factor, which was fixed at 1, $[P]_o$ is the total concentration of probe-labeled protein, and $[L]_o$ is the total ligand concentration (38,40-42).

Plasminogen Activation Kinetics

The kinetics of activation of 100 nM [Glu]Pg or [Lys]Pg by 3 nM nctPA or 0.5 nM tctPA was measured as a function of wtSkzL or SkzLΔK415 concentration (0-20 μM). Studies of [Lys]Pg and [Glu]Pg activation as a function of wtSkzL concentration were performed in chloride containing buffer (100 mM HEPES, 100 mM NaCl, 1 mM EDTA, 1 mg/ml PEG 8,000, pH 7.4) or no chloride buffer (100 mM HEPES, 100 mM

sodium acetate, 1 mM EDTA, 1 mg/ml PEG 8,000, pH 7.4). The only contribution of chloride in experiments performed with buffer lacking chloride ion was from the initial tPA storage buffer, which after dilution was ≤ 0.1 μM chloride in the assays. Hydrolysis of 200 μM *D*-Val-Leu-Lys-nitroanalide (VLK-*p*NA) was measured at 405 nm as a function of time. Unless stated otherwise, assays were performed in the above buffer containing 100 mM NaCl using PEG 20,000-coated polystyrene cuvettes. In assays containing SkzL, tPA and SkzL were preincubated at 25 °C for 10 min prior to addition of Pg and VLK-*p*NA. Progress curves at varying SkzL or Pg concentrations were fit by the parabolic rate equation:

$$\Delta A_{405\text{ nm}} = at^2 + bt + c \qquad \textbf{Eqn. 2,}$$

where t is time, and the *a* term represents the rate of acceleration of chromogenic substrate hydrolysis by Pm formation, the *b* term is any linear rate of substrate hydrolysis, and *c* is the intercept at t = 0. Raw data were truncated to less than 10% chromogenic substrate consumption. To ensure no significant substrate depletion, raw data were truncated to include only data linear when plotted as absorbance against time^2.

The effect of fixed SkzL concentrations (0, 4, 10, and 15 μM) on [Lys]Pg activation by 3 nM nctPA (6 nM nctPA at 0 μM SkzL) or 0.2 nM tctPA were measured as a function of [Lys]Pg concentration (2 nM-2.6 μM). Data were obtained and truncated as described above and analyzed initially by global nonlinear least-squares fitting of the following rapid equilibrium equation for ternary complex formation for the template model for effect of fibrin on Pg activation by tPA (34):

$$\frac{v_o}{[\mathrm{tPA}]_o} = \frac{\left(k_{\mathrm{cat}}\left(\frac{[\mathrm{L}]_o}{K+[\mathrm{L}]_o}\right)\right)[\mathrm{Pg}]_{\mathrm{free}}}{K_B\left(\frac{K_A+[\mathrm{L}]_o}{K+[\mathrm{L}]_o}\right)+[\mathrm{Pg}]_{\mathrm{free}}} \qquad \textbf{Eqn. 3}$$

with,

$$[\mathrm{Pg}]_{\mathrm{free}} = [\mathrm{Pg}]_o - \left[\frac{\left(n[\mathrm{P}]_o+[\mathrm{L}]_o+K_C\right)-\sqrt{\left(n[\mathrm{Pg}]_o+[\mathrm{L}]_o+K_C\right)^2-4n[\mathrm{Pg}]_o[\mathrm{L}]_o}}{2}\right] \qquad \textbf{Eqn. 4}$$

$$K = \left(\frac{K_A K_B}{K_C}\right) \qquad \textbf{Eqn. 5}$$

$$\frac{v_o}{[\mathrm{tPA}]_o} = \frac{k_{\mathrm{ucat}}}{K_m}[\mathrm{Pg}]_o \qquad \textbf{Eqn. 6},$$

where $[Pg]_o$ is the total [Lys]Pg concentration, $[L]_o$ is the total SkzL concentration, k_{cat} is the rate of catalytic turnover for the SkzL-catalyzed reaction, K_A is the dissociation constant determined for the SkzL-tPA interaction (fixed at 14 μM), K_C is the dissociation constant determined for the SkzL-[Lys]Pg interaction (fixed at 82 nM), Pg_{free} is the concentration of free Pg given by the quadratic equation (Equation 4), K is the complex constant (Equation 5), and k_{ucat}/K_m is the bimolecular rate constant for the uncatalyzed reaction (Equation 6) (34). Parameters obtained from global analysis by least-squares fitting of the model, combining Equations 3 - 6, are listed in Table 3.

Alternatively, data were analyzed by mechanism-independent nonlinear least-squares fitting of the sum of the solution to the quadratic equation (analogous to Equation 1), with $(\Delta v_{max\ 1}/v_o)$ as the maximal change in rate for the high affinity interaction, and a hyperbola for the weak interaction,

$$\frac{\Delta v_{obs}}{v_o} = \frac{\Delta v_1}{v_o} + \left(\frac{\left(\Delta v_{max\,2}/v_o\right)\ [\mathrm{L}]_\mathrm{o}}{K_{D2} + [\mathrm{L}]_\mathrm{o}} \right) \qquad \textbf{Eqn. 7}$$

where K_{D1} and K_{D2} are the dissociation constants for the high and low affinity interactions, $\Delta v_{max\ 1}/v_o$ (obtained from the quadratic equation) and $\Delta v_{max\ 2}/v_o$ are the corresponding maximum changes in rate, and $[\mathrm{L}]_\mathrm{o}$ is the total ligand concentration. Experimental error in the fitted parameters represents ± 2 S.D.

The data were also analyzed using a model with an additional quaternary complex step, in which a second SkzL molecule binds to the proposed SkzL•Pg•tPA ternary complex (Equation 8).

$$\frac{v_{obs}}{[\mathrm{tPA}]_\mathrm{o}} = \frac{\left[\mathrm{Pg \cdot SkzL \cdot tPA}\right] k_{\mathrm{cat\ 1}} + \left[\mathrm{Pg \cdot SkzL \cdot tPA \cdot SkzL}\right] k_{\mathrm{cat\ 2}} + \frac{k_{\mathrm{ucat}}}{K_m}[\mathrm{Pg}]_\mathrm{o}}{[\mathrm{tPA}]_\mathrm{o}} \qquad \textbf{Eqn. 8}$$

where $[\mathrm{Pg}]_\mathrm{o}$ is the total [Lys]Pg concentration, $[\mathrm{tPA}]_\mathrm{o}$ is the total tPA concentration, [Pg•SkzL•tPA] and [Pg•SkzL•tPA•SkzL] represent the concentrations of the intermediate complexes, $k_{\mathrm{cat\ 1}}$ is the rate of catalytic turnover for the ternary complex, $k_{\mathrm{cat\ 2}}$ is the rate of catalytic turnover for the quaternary complex, and k_{ucat}/K_m is the bimolecular rate

constant for the uncatalyzed reaction. The data were analyzed by simultaneous solution of the expressions for the equilibrium constants and conservation of mass to obtain $[Pg]_{free}$, $[SkzL]_{free}$, and $[tPA]_{free}$ and the concentrations of the intermediate complexes. K_A represents SkzL-tPA binding, K_C represents SkzL-Pg binding**,** K_B represents binding of Pg to the SkzL•tPA complex, K_D represents tPA binding to the SkzL•Pg complex, and K_E represents formation of the Pg•SkzL•tPA•SkzL quaternary complex. Experimental error in the fitted parameters represents ± 2 S.D.

Results

Effect of SkzL on Plasminogen Activation by nctPA and tctPA

Chromogenic substrate kinetic assays of Pm generation were performed to determine the effect of SkzL on activation of [Lys]Pg and [Glu]Pg by nctPA and tctPA (Fig. 1). The rate of Pm generation from [Lys]Pg activation by nctPA and tctPA was enhanced by SkzL ~48-fold and ~7-fold, respectively (Table 1). The rate of Pm generation from [Glu]Pg activation by nctPA and tctPA was enhanced by SkzL ~490-fold and ~400-fold, respectively (Table 1). No SkzL-mediated enhancement of Pg activation by nctPA or tctPA was seen in the presence of 10 mM 6-AHA (data not shown), consistent with studies reported for sctPA in Chapter 2, indicating an entirely LBS-dependent mechanism of SkzL-enhanced Pg activation.

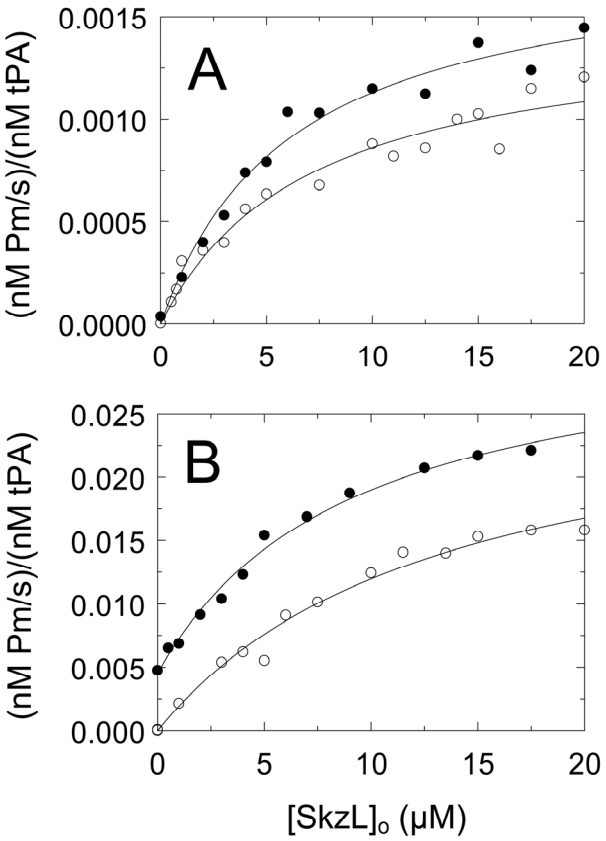

Figure 1. Effect of SkzL on Pg activation by nctPA and tctPA. Initial rates of Pm generation (*(nM Pm/s)/(nM tPA)*) for activation of 100 nM [Lys]Pg (●) and [Glu]Pg (○) by 3 nM nctPA (*A*) and 0.5 nM tctPA (*B*) as a function of total SkzL concentration ($[SkzL]_o$). *Solid lines* represent the least-squares fits by the quadratic rate equation with parameters listed in Table 1. Experiments were performed and data analyzed as described in "Experimental Procedures".

Fitting of the SkzL-dependences for [Lys]Pg activation by nctPA and tctPA gave apparent K_D's of 6 ± 2 μM and 9 ± 3 μM, respectively (Table 1). Fitting of the SkzL dependences for [Glu]Pg activation by nctPA and tctPA gave K_D's of 7 ± 3 μM and 13 ± 3 μM, respectively, indistinguishable from those for [Lys]Pg (Table 1). Consistent with parameters reported in Chapter 2 for Pg activation by sctPA, the apparent affinities of SkzL for [Glu]Pg agreed with K_D's of 3-16 μM obtained in SkzL-[Glu]Pg binding studies. However, the K_D's for [Lys]Pg of 6-9 μM were ~75-110-fold weaker than the

values of 80 nM determined for SkzL-[Lys]Pg in competitive binding studies (Table 1). In contrast to the studies reported in Chapter 2 for the effect of SkzL on Pg activation by uPA, in which the SkzL-induced α/β- to γ-conformational change resulted in enhanced [Glu]Pg activation but decreased [Lys]Pg activation, the results for tPA revealed a SkzL-mediated enhancement of both [Glu]Pg and [Lys]Pg activation, suggesting a more complex mechanism for nctPA and tctPA, than uPA.

Table 1. Parameters for the effect of SkzL on Pg activation by tPA. Dissociation constants (K_D), maximal rates of Pm generation ($\Delta v_{max}/v_o$), and fold *Rate Enhancement* listed from analysis of direct titrations of wtSkzL and SkzLΔK415 with the indicated enzyme-substrate pairs. *Rate Enhancement* represents the fold increase in Pm generation from the rate observed in the absence of ligand to the calculated v_{max} rate. Experimental error in parameters represents ± 2 S.D. Experiments were performed and the data analyzed as described under "Experimental Procedures".

Enzyme	Substrate	Ligand	K_D	$\Delta v_{max}/v_o$	Rate Enhancement
			(*μM*)	(*(nM Pm/s)/(nM tPA)*)	*(fold*)
nctPA	[Lys]Pg	wtSkzL	6 ± 2	0.0018 ± 0.0001	48
nctPA	[Lys]Pg	SkzLΔK415	7 ± 6	0.0005 ± 0.0002	13
nctPA	[Glu]Pg	wtSkzL	7 ± 3	0.0015 ± 0.0001	490
tctPA	[Lys]Pg	wtSkzL	9 ± 3	0.029 ± 0.004	7
tctPA	[Lys]Pg	SkzLΔK415	7 ± 5	0.005 ± 0.001	3
tctPA	[Glu]Pg	wtSkzL	13 ± 6	0.028 ± 0.006	400

Binding of SkzL to an Active Site-labeled Fluorescent sctPA Analog

Fluorescence equilibrium binding studies were performed to quantitate binding of wtSkzL and SkzLΔK415 to an active site tetramethylrhodamine-labeled analog of sctPA ([TMR]FFR-sctPA), in the absence and presence of 6-AHA to determine LBS-

dependence (Fig. 2). Analysis of titrations of [TMR]FFR-sctPA with wtSkzL and SkzLΔK415 revealed equivalent dissociation constants of 14 ± 4 μM and 15 ± 5 μM, respectively, and maximal fluorescence changes ($\Delta F_{max}/F_o$) of -54 ± 80% and -55 ± 100%, respectively. Both interactions were greatly decreased by 10 mM 6-AHA, indicating LBS-dependent interactions between sctPA-kringle 2 and wtSkzL/SkzLΔK415. Deletion of Lys^{415} failed to alter SkzL binding to [TMR]FFR-sctPA compared to wtSkzL, indicating that Lys^{415} does not mediate binding of SkzL to sctPA.

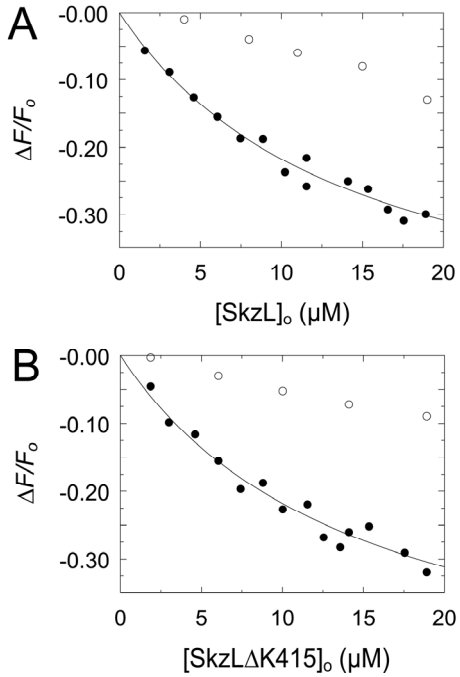

Figure 2. Fluorescence titrations of [TMR]FFR-sctPA with wtSkzL and SkzLΔK415. *A*. Titrations of the fractional change in fluorescence ($\Delta F/F_o$) of 100 nM [TMR]FFR-sctPA as a function of total wtSkzL concentration ($[SkzL]_o$) in the absence (●) and presence (○) of 10 mM 6-AHA. *B*. Titrations of the fractional change in fluorescence ($\Delta F/F_o$) of 100 nM [TMR]FFR-sctPA as a function of total SkzLΔK415 concentration ($[SkzL\Delta K415]_o$) in the absence (●) and presence (○) of 10 mM 6-AHA. *Solid lines* represent the least-squares fits of the data by the quadratic binding equation with the parameters given in "Results". Experiments were performed and the data analyzed as described in "Experimental Procedures".

Effect of SkzL Lys^{415} on [Lys]Pg Activation by nctPA and tctPA

Chromogenic substrate kinetic assays were performed to determine the effect of SkzL Lys^{415} on SkzL enhancement of [Lys]Pg activation by nctPA and tctPA (Fig. 3). The rate of Pm generation determined for [Lys]Pg activation by nctPA and tctPA was enhanced 48-fold and 7-fold, respectively, by wtSkzL (Table 1). The rate of Pm generation determined for [Lys]Pg activation by nctPA and tctPA was only enhanced 13-fold and 3-fold, respectively, by SkzLΔK415 representing a ~2.5-4-fold decrease in $\Delta v_{max}/v_o$ from that seen for wtSkzL (Table 1). Fitting of the SkzL dependences for SkzLΔK415 on [Lys]Pg activation by nctPA and tctPA gave identical K_D's of 7 μM for SkzLΔK415, indistinguishable from the K_D's of 6-9 μM obtained for wtSkzL (Table 1). Both wtSkzL and SkzLΔK415 enhancement effects were eliminated in the presence of 6-AHA (data not shown), indicating an entirely LBS-dependent mechanism for SkzL enhancement of Pg activation by tPA.

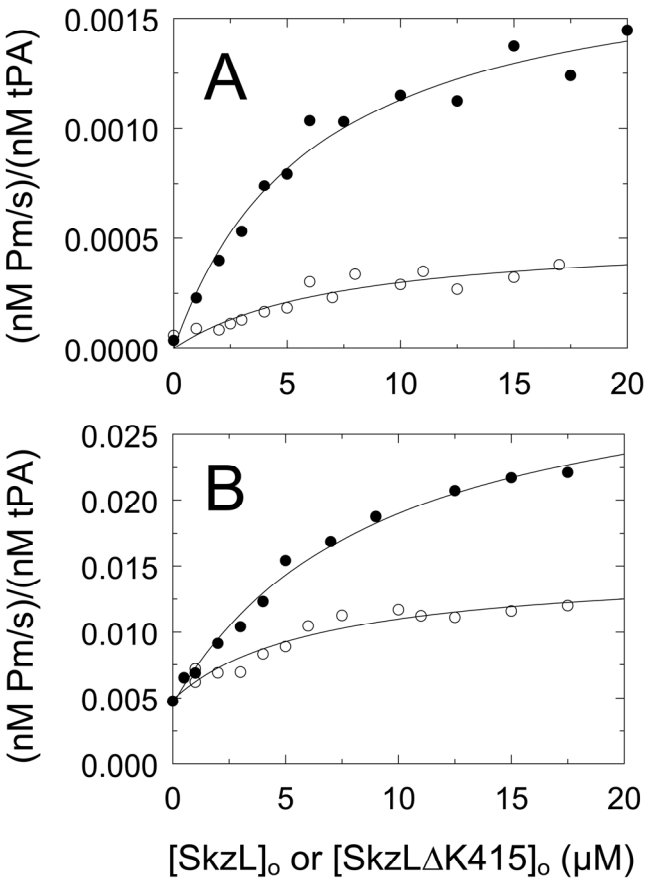

Figure 3. Effect of SkzL Lys^{415} on Pg activation by nctPA and tctPA. Initial rates of Pm generation (*(nM Pm/s)/(nM tPA)*) for activation of 100 nM [Lys]Pg by 3 nM nctPA (*A*) or 0.5 nM tctPA (*B*) as a function of total wtSkzL (●) or SkzLΔK415 (○) concentration (*[SkzL]$_o$ or [SkzLΔK415]$_o$*). *Solid lines* represent the least-squares fits by the quadratic rate equation with parameters listed in Table 1. Experiments were performed and data analyzed as described in "Experimental Procedures".

Effect of Chloride-regulated Pg Conformation on SkzL Enhancement of Pg Activation by tPA

Results of experiments reported in Chapter 2 indicated that wtSkzL binding to a small population of [Glu]Pg in the β-conformation initiated the [Glu]Pg β- to γ-conformational change. This was illustrated through SkzL-mediated enhancement of [Glu]Pg activation by uPA to levels indistinguishable from those of [Glu]Pg in the presence of 6-AHA or [Lys]Pg in the presence of saturating concentrations of wtSkzL

(15-20 μM) or 6-AHA (10 mM). In an effort to elucidate the role of chloride-regulated [Glu]Pg conformation in the mechanism of SkzL-mediated enhancement of Pg activation by tPA, chromogenic substrate assays were performed to determine the rates of Pm generation for [Lys]Pg and [Glu]Pg activation by nctPA and tctPA in the presence (100 mM) and absence (≤ 0.1 μM) of chloride ion as a function of wtSkzL concentration (Fig. 4). In contrast to studies reported in Chapter 2, in which 10 mM 6-AHA was used as a tool to confirm transition of Pg to the γ-conformation, the LBS-dependent SkzL-mediated enhancement of Pg activation by tPA was eliminated by 10 mM 6-AHA and therefore 6-AHA could not be used in the same capacity in these studies.

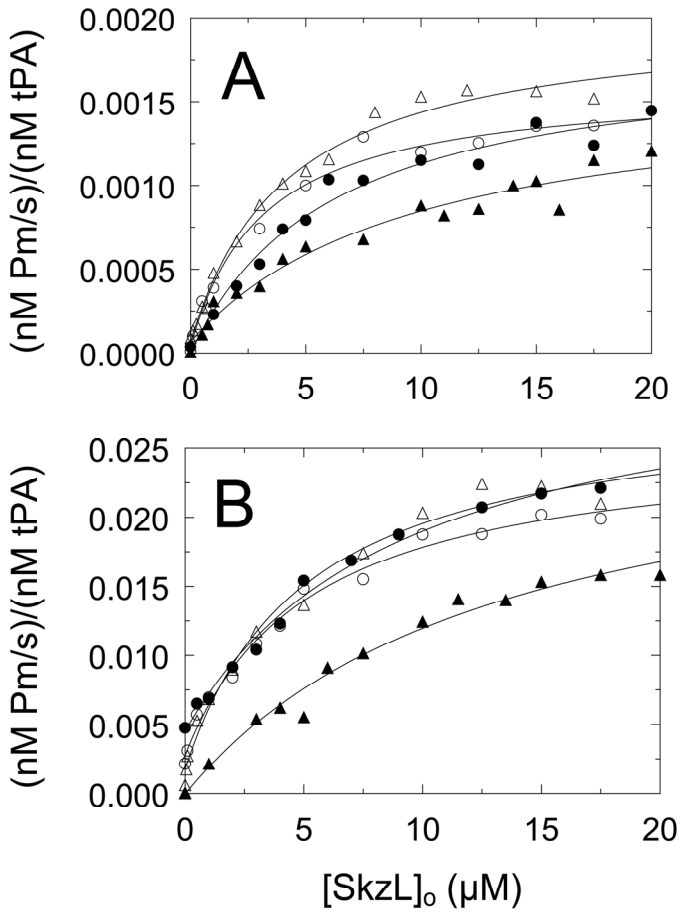

Figure 4. Role of Pg conformation in SkzL-mediated enhancement of Pg activation by nctPA and tctPA. Initial rates of Pm generation (*(nM Pm/s)/(nM tPA)*) for activation of 100 nM [Lys]Pg (●) and [Glu]Pg (▲) by 3 nM nctPA (*A*) and 0.5 nM tctPA (*B*) in buffer containing 100 mM chloride ion as a function of total wtSkzL concentration ($[SkzL]_o$). Rates of activation of 100 nM [Lys]Pg (○) and [Glu]Pg (Δ) by nctPA (*A*) and tctPA (*B*) in buffer containing ≤ 0.1 μM chloride ion as a function of total wtSkzL concentration ($[SkzL]_o$). *Solid lines* represent the least-squares fits of the data by the quadratic binding equation with the parameters listed in Table 2. Experiments were performed and the data analyzed as described in "Experimental Procedures".

Fitting of the SkzL dependence for enhancement of [Lys]Pg activation by nctPA and tctPA in the presence and absence of chloride ion gave indistinguishable apparent affinities of ~4-5 μM (nctPA) and ~5-7 μM (tctPA) (Table 2). Indistinguishable apparent maximal rates of Pm generation ($\Delta v_{max}/v_o$) were observed for SkzL enhanced [Lys]Pg

activation by nctPA and tctPA in the absence and presence of chloride ion (Table 2), confirming that [Lys]Pg conformation and activation by tPA were chloride-independent.

While the qualitative trend of the SkzL enhancement of [Glu]Pg activation by nctPA and tctPA appeared to indicate a chloride-dependence with respect to the effect of wtSkzL, no such effect was observed in the parameters obtained from fitting of the SkzL dependence (Fig. 4, Table 2). As expected, the SkzL dependence of enhanced [Glu]Pg activation by nctPA and tctPA in the absence of chloride ion overlays the enhancement of [Lys]Pg activation by nctPA and tctPA in the presence and absence of chloride ion. Analysis of the SkzL enhancement of [Glu]Pg activation by nctPA in the presence and absence of chloride ion revealed near-equal apparent affinities of 8 ± 3 μM and 4 ± 1 μM, respectively (Table 2). A slight increase in the apparent maximum rate of Pm generation ($\Delta v_{max}/v_o$) was seen for [Glu]Pg activation by nctPA, from 0.0015 ± 0.0001 (nM Pm/s)/(nM tPA) in the presence of chloride ion to 0.0020 ± 0.0002 (nM Pm/s)/(nM tPA) in the absence of chloride (Table 2). This apparent decrease may be a result of the limited saturation achieved at the highest wtSkzL concentration attainable in the assay, and it is thought that higher, fully saturating wtSkzL concentrations would cause the data sets to converge at the same apparent $\Delta v_{max}/v_o$ value.

The parameters obtained from analysis of the SkzL enhancement of [Glu]Pg activation by tctPA in the presence and absence of chloride ion revealed similar apparent affinities of 11 ± 6 μM and 7 ± 2 μM, respectively, equivalent within the experimental error (Table 2). The slight decrease seen in $\Delta v_{max}/v_o$ for [Glu]Pg activation by nctPA in the presence of chloride ion was not seen for [Glu]Pg activation by tctPA, with rates of 0.028 ± 0.006 (nM Pm/s)/(nM tPA) in the presence of chloride and 0.028 ± 0.003 (nM

Pm/s)/(nM tPA) in the absence of chloride (Table 2). This confirms the hypothesis that higher, fully saturating wtSkzL concentrations would cause the two data sets for [Glu]Pg activation by nctPA (± chloride ion) to converge at the same $\Delta v_{max,\ app}/v_o$ value, eliminating the apparent effect of chloride-regulated Pg conformation in the mechanism of SkzL enhancement of Pg activation by nctPA.

Table 2. Parameters for the role of Pg conformation on the effect of wtSkzL on Pg activation by nctPA and tctPA. Apparent dissociation constants (K_D) and apparent maximal rates of Pm generation ($\Delta v_{max,\ app}/v_o$) are listed from analysis of direct titrations of wtSkzL with the indicated enzyme-substrate pairs. Experiments were performed in the presence of low and high total chloride ion concentration ($[chloride\ ion]_o$). Experimental error in parameters represents ± 2 S.D. Experiments were performed and the data analyzed as described under "Experimental Procedures".

Enzyme	Substrate	$[\text{Chloride ion}]_o$	K_D	$\Delta v_{max,\ app}/v_o$
			(μM)	(*(nM Pm/s)/(nM tPA)*)
nctPA	[Lys]Pg	100 mM	5 ± 2	0.0018 ± 0.0001
nctPA	[Lys]Pg	≤ 0.1 μM	4 ± 1	0.0017 ± 0.0002
nctPA	[Glu]Pg	100 mM	8 ± 3	0.0015 ± 0.0001
nctPA	[Glu]Pg	≤ 0.1 μM	4 ± 1	0.0020 ± 0.0002
tctPA	[Lys]Pg	100 mM	7 ± 3	0.030 ± 0.004
tctPA	[Lys]Pg	≤ 0.1 μM	5 ± 2	0.026 ± 0.002
tctPA	[Glu]Pg	100 mM	11 ± 6	0.028 ± 0.006
tctPA	[Glu]Pg	≤ 0.1 μM	7 ± 2	0.028 ± 0.003

Effect of wtSkzL on [Lys]Pg Activation by tPA as a Function of Pg and SkzL Concentrations

To determine the mechanism of SkzL enhancement of Pg activation by tPA, chromogenic substrate kinetic assays were performed of [Lys]Pg activation by nctPA and tctPA as a function of both [Lys]Pg and wtSkzL concentration. The rates of Pm generated from [Lys]Pg activation by nctPA were determined in the presence of 0, 4, 10, and 15 μM wtSkzL as a function of [Lys]Pg concentration (Fig. 5*A* and *C*). Identical titrations were performed with tctPA (Fig. 5*B* and *D*). For both nctPA and tctPA, the uncatalyzed rate of Pg activation in the absence of wtSkzL was linear and slow through the highest achievable [Lys]Pg concentration of 2.6 μM. This suggested a K_m of ≥ 2.6 μM for the tPA-[Lys]Pg uncatalyzed reaction and that the uncatalyzed reaction was bimolecular under the conditions used. For Pg activation by both nctPA and tctPA, the rates of Pm generation in the presence of 10 and 15 μM wtSkzL were indistinguishable, indicating that SkzL saturation had been achieved (Fig. 5).

Paralleling the linear rates of Pm generation observed for the uncatalyzed reaction as a function of Pg concentration, linear rates with comparable slopes were observed for the SkzL-catalyzed reaction. Taking into consideration the dissociation constant of 80 nM determined for SkzL-[Lys]Pg binding, in titrations containing 4-15 μM SkzL, the vast majority (~ 95%) of [Lys]Pg in the reaction should be SkzL-bound. As a result, for titrations containing 4-15 μM SkzL, the increased rate of Pm generation as a function of [Lys]Pg concentration should be minimal and non-linear, representing activation of SkzL-bound Pg, and not free Pg (Fig. 5).

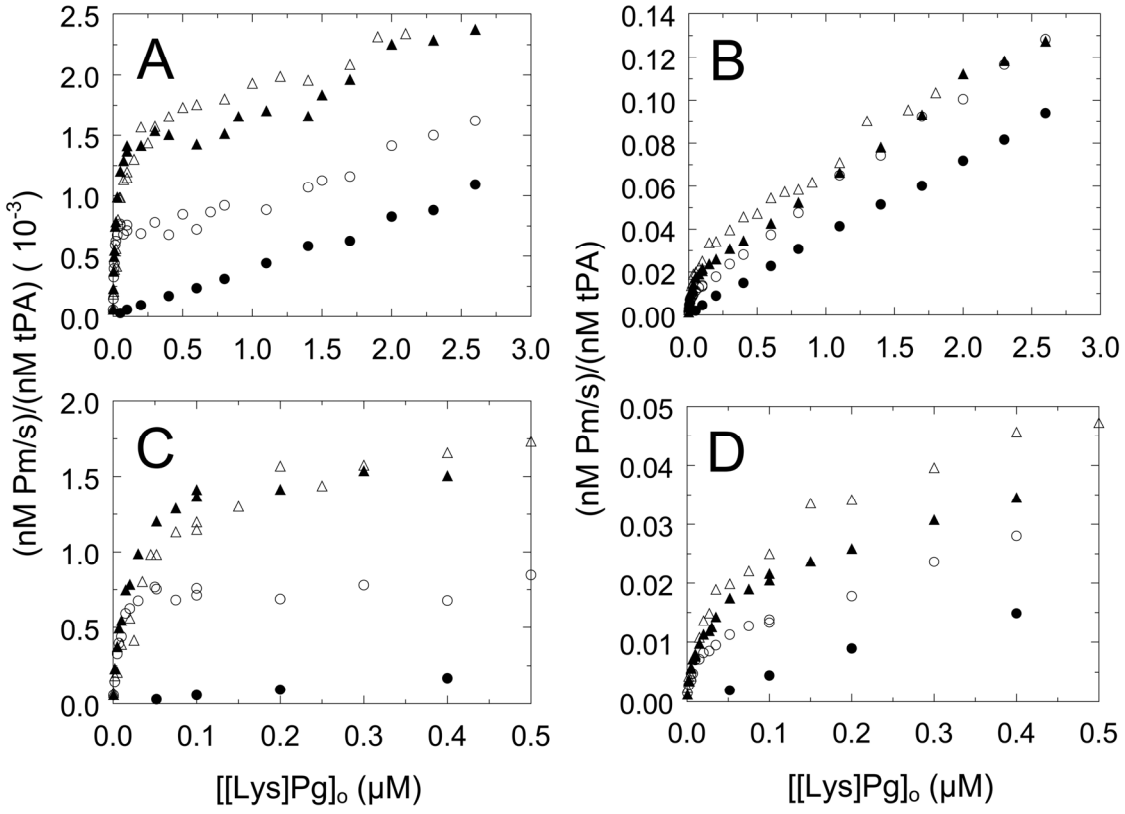

Figure 5. Pg and wtSkzL concentration-dependences on [Lys]Pg activation by nctPA and tctPA. *A and C*. Initial rates of Pm generation (*(nM Pm/s)/(nM tPA) (10^{-3})*) for [Lys]Pg activation by nctPA in the presence of 0 (●), 4 (○), 10 (▲), and 15 μM (Δ) wtSkzL as a function of [Lys]Pg concentration (*[[Lys]Pg]$_o$*), with *C* highlighting the low [Lys]Pg concentration range. *B and D*. Initial rates of Pm generation (*(nM Pm/s)/(nM tPA)*) for [Lys]Pg activation by tctPA in the presence of 0 (●), 4 (○), 10 (▲), and 15 μM (Δ) wtSkzL as a function of [Lys]Pg concentration (*[[Lys]Pg]$_o$*), with *D* highlighting the low [Lys]Pg concentration range. Experiments were performed and data analyzed as described in "Experimental Procedures".

Analysis of the Pg-dependence data was attempted using numerous variations of models of ternary complex formation without success. A model of rapid equilibrium ternary complex formation derived from the model for the effect of fibrin on Pg activation by tPA (34) offered a good fit to the data (Fig. 6*A* and *B*).

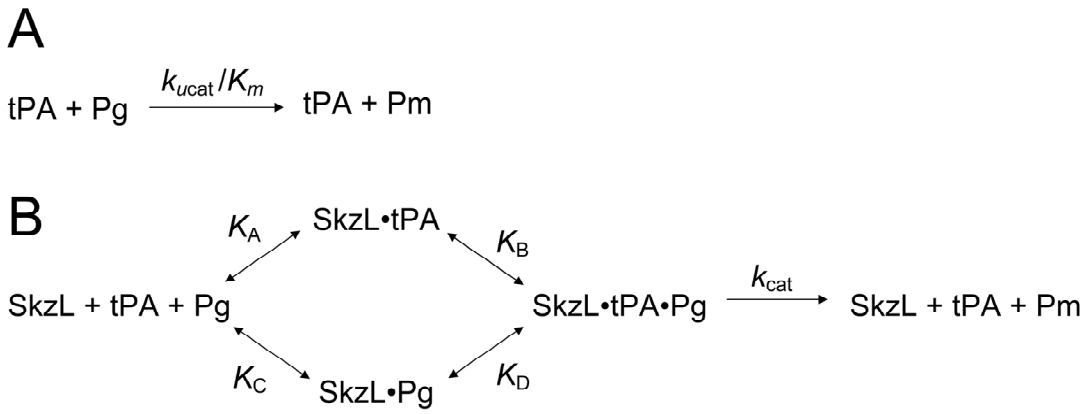

Figure 6. Mechanism of Pg activation by tPA in the absence and presence of SkzL. *A*. Activation of [Lys]Pg by tPA in the absence of SkzL with k_{ucat}/K_m representing the bimolecular rate constant of the uncatalyzed reaction. *B*. Proposed mechanism for SkzL enhanced Pg activation by tPA, where the dissociation constant for SkzL-tPA binding (K_A), the dissociation constant for SkzL-[Lys]Pg binding (K_C), the Michaelis constant or affinity for the SkzL•tPA complex binding [Lys]Pg (K_B), the complex constant (K), which by detailed balance is equal to $(K_A K_B)/K_C$, and the catalytic turnover of the SkzL enhanced reaction (k_{cat}).

Analysis of the data (Fig. 5) for the effect of SkzL on the Pg-dependence for Pg activation by tPA according to the mechanism illustrated in Fig. 6, including both the catalyzed and uncatalyzed reactions, gave kinetic parameters for each step in the reaction. The parameters for K_A and K_C were fixed at the known dissociation constants of 14 μM and 82 nM, determined for SkzL-tPA and SkzL-[Lys]Pg binding, respectively. The rate of catalytic turnover determined for the catalyzed (k_{cat}) and uncatalyzed (k_{ucat}/K_m) reactions of [Lys]Pg activation by nctPA were $2.6 \pm 0.4 \times 10^{-6}$ and $3.9 \pm 0.4 \times 10^{-7}$ $nM^{-1}s^{-1}$, respectively (Table 3). The rates determined for k_{cat} and k_{ucat}/K_m for [Lys]Pg activation by tctPA were $5.2 \pm 1.3 \times 10^{-5}$ and $4.0 \pm 0.2 \times 10^{-5}$ $nM^{-1}s^{-1}$, respectively (Table 3). The Michaelis constants or affinities of the nctPA- or tctPA-SkzL complex binding [Lys]Pg (K_B) were 0.11 ± 0.03 nM and 0.20 ± 0.09 nM, respectively (Table 3). The uncatalyzed activation of Pg by both nctPA and tctPA was represented by the bimolecular rate

constant (k_{ucat}/K_m). The fitted complex constant (K), however, for the SkzL•Pg complex binding of nctPA or tctPA was 11 ± 3 and 12 ± 6 μM, respectively. Under the assumption of rapid equilibrium kinetics, K is equivalent to K_D in the proposed mechanism (Fig. 6). Detailed balance, in which $K_D = (K_A K_B)/K_C$, yielded calculated apparent affinities of 18 nM and 33 nM for nctPA and tctPA binding to the SkzL•[Lys]Pg complex, respectively. The discrepancy between the K and K_D parameters represents a difference of nearly 3 orders of magnitude, and indicates a faulty global analysis using the model of ternary complex formation. Other models of ternary complex formation failed to appropriately represent the data.

Table 3. Parameters for the effect of [Lys]Pg and wtSkzL concentration-dependences on [Lys]Pg activation by nctPA and tctPA. The Michaelis constant for the SkzL-catalyzed reaction (K_B), complex constant (K), and catalytic turnover for the catalyzed and uncatalyzed reaction (k_{cat}, k_{ucat}/K_m) are listed from global analysis of [Lys]Pg concentration-dependence on [Lys]Pg activation by tPA in the presence of SkzL concentrations 4, 10, or 15 μM. Dissociation constants for interactions of SkzL with tPA (K_A) and [Lys]Pg (K_C) were fixed at the values determined by equilibrium binding. The value for K_D was calculated from detailed balance (Fig. 6), where $K_D = (K_A K_B)/K_C$. Experimental error in parameters represents ± 2 SD. Experiments were performed and the data analyzed as described in "Experimental Procedures".

Enzyme	K_A	K_B	K_C	K_D	K	k_{cat}	k_{ucat}/K_m
	(μM)	(nM)	(nM)	(nM)	(μM)	(s^{-1})	($nM^{-1}s^{-1}$)
nctPA	14	0.11 ± 0.03	82	18	11 ± 3	$2.6 \pm 0.4 \times 10^{-6}$	$3.9 \pm 0.4 \times 10^{-7}$
tctPA	14	0.20 ± 0.09	82	33	12 ± 6	$5.2 \pm 1.3 \times 10^{-5}$	$4.0 \pm 0.2 \times 10^{-5}$

To gain further insight into the mechanism, a mechanism-independent analysis of the bimodal data was performed for each data set at single SkzL concentrations separately (Figure 5). With the dissociation constant for the weak affinity interaction fixed at 5 μM, the dissociation constant for the high affinity interaction as a function of [Lys]Pg concentration varied with SkzL concentration for both nctPA and tctPA. For nctPA, K_D values of 4.5 ± 2, 13 ± 4, and 42 ± 10 nM were determined for the [Lys]Pg concentration dependences in the presence of 4, 10, and 15 μM SkzL, respectively (Table 4). Similarly, for tctPA, K_D values of 7.5 ± 6, 14 ± 8, and 34 ± 18 nM were obtained for the [Lys]Pg concentration-dependences in the presence of 4, 10, and 15 μM SkzL, respectively. The high affinity interaction represents the affinity of tPA for the substrate, SkzL-bound [Lys]Pg (K_D). This shows a ~60-570-fold increase in affinity for binding of

tPA to [Lys]Pg, when [Lys]Pg is in complex with SkzL, compared with ≥ 2.6 μM in the absence of SkzL.

Table 4. Parameters obtained from bimodal data analysis for the effect of wtSkzL concentration on the [Lys]Pg concentration-dependence of [Lys]Pg activation by nctPA and tctPA. The dissociation constant (K_D) is listed from bimodal analysis of [Lys]Pg concentration-dependences at single SkzL concentrations ($[SkzL]_o$) for nctPA and tctPA (*Enzyme*). Dissociation constants for the weak interaction were fixed at 5 μM, consistent with previously established parameters. Data were analyzed as described in "Experimental Procedures".

Enzyme	$[SkzL]_o$	K_D
	(μM)	(nM)
nctPA	4	4.5 ± 2
nctPA	10	13 ± 4
nctPA	15	42 ± 10
tctPA	4	7.5 ± 6
tctpA	10	14 ± 8
tctPA	15	34 ± 18

A second global analysis was performed for the Pg dependence data (Fig. 5), including data for activation of 100 nM [Lys]Pg as a function of SkzL concentration. To account for the apparent increase in k_{cat} with increasing fixed SkzL concentration, this analysis used a modified version of the ternary complex model (Fig. 6), in which a second SkzL molecule binds the SkzL•tPA•Pg ternary complex, with resulting Pm generation represented by $k_{cat\,2}$ (Fig. 7).

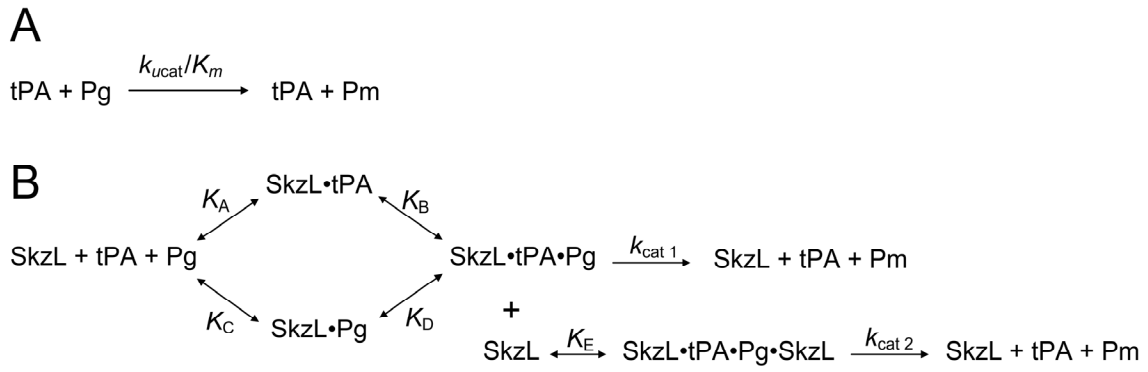

Figure 7. Mechanism of Pg activation by tPA in the absence and presence of SkzL, including quaternary complex formation. *A*. Activation of [Lys]Pg by tPA in the absence of SkzL with k_{ucat}/K_m for the uncatalyzed reaction. *B*. Proposed mechanism for SkzL enhanced Pg activation by tPA, where the dissociation constant for SkzL-tPA binding (K_A), the dissociation constant for SkzL-[Lys]Pg binding (K_C), the Michaelis constant or affinity of [Lys]Pg for the SkzL•tPA complex (K_B), K_D is the Michaelis constant for SkzL•Pg activation by tPA, which by detailed balance is equal to $(K_A K_B)/K_C$, catalytic turnover by the SkzL•tPA•Pg ternary complex, ($k_{cat\ 1}$). K_E represents binding of a second SkzL molecule to the SkzL•tPA•Pg ternary complex, and $k_{cat\ 2}$ is the catalytic turnover driven by the quaternary SkzL•tPA•Pg•SkzL complex.

Analysis of the data with the model of quaternary complex formation gave a good fit to the data and determined parameters for both the catalyzed and uncatalyzed reactions (Fig. 8). K_A and K_C were fixed at the known dissociation constants of 14,000 nM and 82 nM for SkzL-tPA and SkzL-[Lys]Pg binding, respectively (Table 5). The parameters of K_B for binding of Pg to SkzL-bound tPA were fit by 23 ± 8 nM and 530 ± 470 nM for nctPA and tctPA, respectively. The value determined for $k_{cat\ 1}$ rapidly approached zero and was therefore fixed at zero. Values of 6600 ± 1800 nM and 760 ± 660 nM were determined for the K_E parameter for nctPA and tctPA, respectively, corresponding to binding of SkzL to the SkzL•tPA•Pg ternary complex. The rates of catalytic turnover for the nctPA and tctPA reactions enhanced by formation of the SkzL•tPA•Pg•SkzL quaternary complex ($k_{cat\ 2}$) were 2.1± 0.2 x 10^{-3} s^{-1} and 32 ± 3.2 x 10^{-3} s^{-1}. The

bimolecular rate constants of the uncatalyzed reaction (k_{ucat}/K_m) determined for nctPA and tctPA were 1.3 ± 0.1 x 10^{-6} $nM^{-1}s^{-1}$ and 7.7 ± 0.3 x 10^{-6} $nM^{-1}s^{-1}$, respectively.

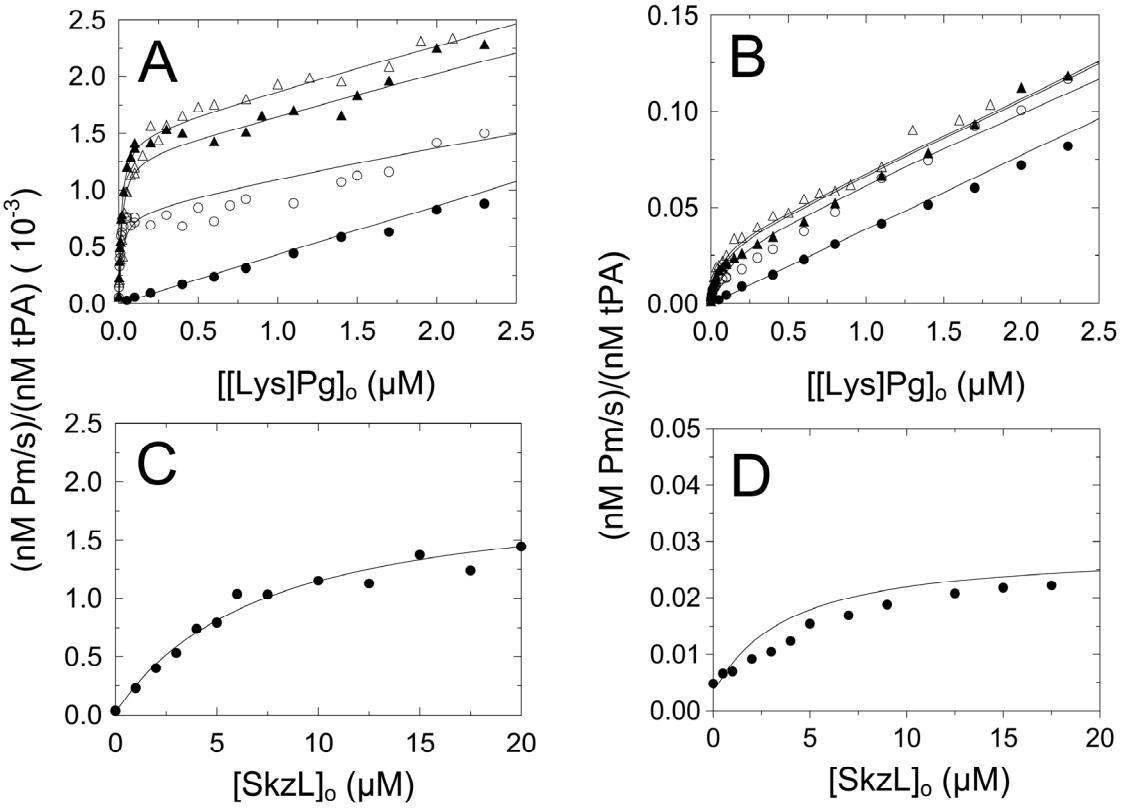

Figure 8. Evidence for productive quaternary complex formation in SkzL enhancement of [Lys]Pg activation by tPA. A and C. Initial rates of Pm generation (*(nM Pm/s)/(nM tPA*) (10-3)) for [Lys]Pg activation by nctPA in the presence of 0 (●), 4 (○), 10 (▲), and 15 μM (Δ) wtSkzL as a function of [Lys]Pg concentration (*[[Lys]Pg]$_o$*), with C showing 100 nM [Lys]Pg activation by nctPA as a function of SkzL concentration (*[SkzL]$_o$*). B and D. Initial rates of Pm generation ((*nM Pm/s)/(nM tPA*)) for [Lys]Pg activation by tctPA in the presence of 0 (●), 4 (○), 10 (▲), and 15 μM (Δ) wtSkzL as a function of [Lys]Pg concentration (*[[Lys]Pg]$_o$*), with D showing 100 nM [Lys]Pg activation by tctPA as a function of SkzL concentration (*[SkzL]$_o$*). *Solid lines* represent non-linear least squares fitting with the parameters listed in Table 5. Experiments were performed and data analyzed as described in "Experimental Procedures".

Table 5. Parameters for the effect of quaternary complex formation on [Lys]Pg activation by nctPA and tctPA. The Michaelis constant for the SkzL-catalyzed reaction (K_B), and bimolecular rate constant for the uncatalyzed reaction (k_{ucat}/K_m) are listed from global analysis of [Lys]Pg concentration-dependence on [Lys]Pg activation by tPA in the presence of SkzL concentrations 4, 10, or 15 μM using the model of quaternary complex formation. Dissociation constants for interactions of SkzL with tPA (K_A) and [Lys]Pg (K_C) were fixed at the values determined by equilibrium binding. K_D was calculated from detailed balance. The value for K_E represents binding of the second SkzL molecule to the ternary complex, with $k_{cat\ 2}$ representing catalytic turnover for the quaternary complex. Experimental error in parameters represents ± 2 SD. Experiments were performed and the data analyzed as described in "Experimental Procedures".

Enzyme	K_A	K_B	K_C	K_D	K_E	$k_{cat\ 2}$	k_{ucat}/K_m
	(μM)	(nM)	(nM)	(μM)	(nM)	(s^{-1})	($nM^{-1}s^{-1}$)
nctPA	14	23 ± 8	82	3.9	6580 ± 1800	$2.1 \pm 0.2 \times 10^{-3}$	$1.3 \pm 0.1 \times 10^{-6}$
tctPA	14	530 ± 470	82	90.4	760 ± 660	$32 \pm 3.2 \times 10^{-3}$	$7.7 \pm 0.3 \times 10^{-6}$

Discussion

Results presented in Chapter 2 support the proposed mechanism for SkzL binding to Pg/Pm; mediated by Lys^{415}, SkzL binds a small population of β-conformation [Glu]Pg through interaction with kringle 4, causing a transition to the γ-conformation. The interaction of SkzL with [Lys]Pg and Pm proved more complex, with binding studies revealing the presence of distinct high and low affinity interactions between wtSkzL and [Lys]Pg/Pm. The LBS-dependent high affinity interaction of SkzL with [Lys]Pg/Pm, mediated by SkzL Lys^{415}, was proposed to occur through interaction with Pg/Pm kringle 4, triggering the β- to γ-conformational transition (19,22,23). The LBS-dependent low affinity interaction between wtSkzL and [Lys]Pg/Pm was proposed to occur through interaction of a putative SkzL internal motif with [Lys]Pg/Pm kringle 5 (24,25). Kinetic

studies in Chapter 2 revealed a SkzL enhancement of [Glu]Pg and [Lys]Pg activation by sctPA, however the mechanism of action remained unclear.

Kinetic experiments in the present studies confirmed the SkzL-mediated enhancement of [Glu]Pg and [Lys]Pg activation seen for sctPA with cleavage-resistant nctPA and the more enzymatically active, tctPA. The SkzL enhancement of [Glu]Pg and [Lys]Pg activation by both nctPA and tctPA was eliminated by 10 mM 6-AHA. Mirroring SkzL-Pg binding, this result indicated that the mechanism of SkzL enhancement of Pg activation by tPA is entirely LBS-dependent. The apparent dissociation constant determined for SkzL enhancement of [Glu]Pg activation by nctPA and tctPA was near-identical to the dissociation constant determined for SkzL-[Glu]Pg binding interactions. However, the apparent dissociation constant determined for SkzL enhancement of [Lys]Pg activation was ~75-110-fold weaker than the dissociation constant of 80 nM determined for SkzL-[Lys]Pg binding. As a result, the mechanism for SkzL enhancement of [Lys]Pg, and possibly [Glu]Pg, activation by tPA could not be explained by SkzL-[Lys]Pg binding interactions alone.

Equilibrium binding studies showed that LBS-dependent, weak binding of SkzL to active site-labeled [TMR]FFR-sctPA was not affected by deletion of Lys^{415}. This result indicated that the LBS-mediated interaction between SkzL and sctPA-kringle 2 occurred through a site distinct from Lys^{415}, most likely through the putative SkzL internal motif proposed to mediate the low affinity interaction with Pg kringle 5.

Kinetic studies were performed to determine the effect of SkzL Lys^{415} deletion on SkzL enhancement of [Lys]Pg activation by nctPA and tctPA. The apparent affinities observed for the wtSkzL- and SkzLΔK415-dependences were indistinguishable for

[Lys]Pg activation by both nctPA and tctPA. This result suggested that the observed affinity did not represent SkzL-[Lys]Pg binding, which is decreased ~30-fold by Lys^{415} deletion (Chapter 2). Combined with the results of the SkzL-sctPA binding studies, which reported a Lys^{415}-independent interaction, the Lys^{415}-independent apparent affinity may reflect SkzL-tPA binding. The ~2-fold decrease in apparent affinity (K_D ~7 μM) obtained in the kinetic analysis compared with the dissociation constant determined by fluorescence equilibrium binding studies of [TMR]FFR-sctPA with SkzL (K_D ~14 μM), may reflect a small effect of the active site incorporated inhibitor and/or probe on the conformation of sctPA.

In kinetic studies of [Lys]Pg activation by nctPA and tctPA, deletion of Lys^{415} resulted in a ~2.5-4-fold decrease in $\Delta v_{max}/v_o$ for SkzLΔK415 from that seen for wtSkzL. As SkzL-sctPA binding was shown to be Lys^{415}-independent and SkzL-[Lys]Pg binding is largely mediated by Lys^{415}, the reduction in $\Delta v_{max}/v_o$ upon deletion of Lys^{415} suggested that the increase in $\Delta v_{max}/v_o$ observed in [Lys]Pg activation by tPA as a function of SkzL concentration was regulated by interaction of SkzL Lys^{415} with [Lys]Pg.

Kinetics experiments were performed in the presence and absence of chloride ion to determine the role of chloride-regulated [Glu]Pg conformation in the mechanism of SkzL enhancement of Pg activation by tPA. A slight ~25 % decrease in the calculated $\Delta v_{max,\ app}/v_o$ value was observed for [Glu]Pg activation by nctPA in the presence of chloride ion compared with [Glu]Pg activation by nctPA in the absence of chloride. This decrease in $\Delta v_{max,\ app}/v_o$ was not observed for [Glu]Pg activation by tctPA. Because Lys^{415}-mediated Pg binding has been shown to induce the [Glu]Pg β- to γ-conformational change, it was hypothesized that the maximum rate of Pm generation for the SkzL

dependence would be identical and chloride-independent. It is thought that at fully saturating SkzL concentrations, greater than those achievable in these studies, the SkzL-saturated data sets would converge to the same $\Delta v_{max,\ app}/v_o$ value, eliminating the apparent effect of chloride. These results suggest that in the presence of SkzL, the rates of tPA-catalyzed [Glu]Pg and [Lys]Pg activation are independent of Pg conformational changes.

To derive the mechanism of SkzL enhancement of Pg activation by tPA, kinetic studies of [Lys]Pg activation by nctPA and tctPA as a function of both [Lys]Pg and wtSkzL concentration were performed. A previous study of the stimulatory effect of fibrin on Pg activation by tPA generated a template model to describe the ternary complex mechanism of fibrin-mediated enhancement of Pg activation (34). In the present studies, this model, including both the uncatalyzed and SkzL-catalyzed reactions, offered a good fit to the data but was occasionally inconsistent with respect to fit reproducibility. However, the model of ternary complex formation offered only moderately reasonable kinetic parameters and large deviations of the complex constant (K).

Linear rates of Pm generation were observed for the uncatalyzed reaction as a function of Pg concentration. Similarly, linear rates with comparable slope were observed for the reaction in the presence of SkzL. However, the high affinity of the SkzL-Pg interaction would ensure that in reactions containing ≥ 4 μM SkzL, at least 95% of Pg would be SkzL-bound. Activation of SkzL-bound Pg would result in increased rates of Pm generation that were non-linear as a function of Pg concentration. The unpredicted and unexplained linear increase in Pm generation observed at saturating SkzL

concentrations may be a result of the complex high and low affinity binding interactions of SkzL-[Lys]Pg.

The major flaw in the global analysis is in the complex constant parameter (K); for SkzL-catalyzed activation of Pg by nctPA and tctPA K was 11 ± 3 and 12 ± 6 μM, respectively. Under the assumption of rapid equilibrium kinetics, K should be equivalent to K_D. Detailed balance of the mechanism, in which $K_D = (K_A K_B)/K_C$, offered apparent affinities of 18 nM and 33 nM for nctPA and tctPA binding to the SkzL•[Lys]Pg complex, respectively. This discrepancy between K and K_D represents a difference of nearly 3 orders of magnitude, and indicates a significant flaw in the global analysis using the ternary complex formation model.

Data analysis with the model of ternary complex formation, illustrated in Figs. 6 and 7, offered a good fit to the data but the flawed kinetic parameters obtained suggested that the model employed does not fully represent the proposed mechanism for SkzL enhancement of [Lys]Pg activation by tPA. As a result, a mechanism-independent analysis of the SkzL-containing [Lys]Pg dependence curves, separated by SkzL concentration, was performed. For [Lys]Pg activation by nctPA and tctPA, K_D values of 4.5-7.5, 13-14, and 34-42 nM were determined for the [Lys]Pg concentration dependences in the presence of 4, 10, and 15 μM SkzL, respectively. This increase in K_D indicates a decrease in apparent affinity with increasing SkzL concentration in the [Lys]Pg concentration dependence. The K_D values of 4.5 ± 2 (nctPA) and 7.5 ± 6 nM (tctPA) observed for the [Lys]Pg concentration dependence likely represent the high affinity interaction of tPA and SkzL-bound [Lys]Pg. Compared with the estimated K_m

value of ≥ 2.6 μM for the uncatalyzed reaction, these K_D values represent a ~350-570-fold increased affinity of tPA for SkzL-bound [Lys]Pg compared with unbound [Lys]Pg.

Data analysis with the model of quaternary complex formation, illustrated in Figs. 7 and 8, is very preliminary but offers a good fit to the data with acceptable kinetic parameters. There is inconsistency in the kinetic parameters determined, comparing nctPA and tctPA, suggesting an imperfect analysis. This analysis offers evidence for formation of a quaternary SkzL•tPA•[Lys]Pg•SkzL complex that enhances Pm generation in [Lys]Pg activation by both nctPA and tctPA.

Limited conclusions can be drawn from this analysis due to the lack of kinetic parameters determined for the uncatalyzed reaction. With limited attainable [Lys]Pg concentrations, we were unable to estimate a value for K_m in the uncatalyzed reaction. As a result, catalytic turnover rate for the uncatalyzed reaction, k_{ucat}/K_m, must be expressed as a bimolecular rate constant in units of $nM^{-1}s^{-1}$. This leaves us unable to draw comparisons with the rate of catalytic turnover determined for the reaction enhanced by quaternary complex formation. However, this analysis does suggest that Pm generation is enhanced only by the quaternary complex, not the ternary complex (Figure 9).

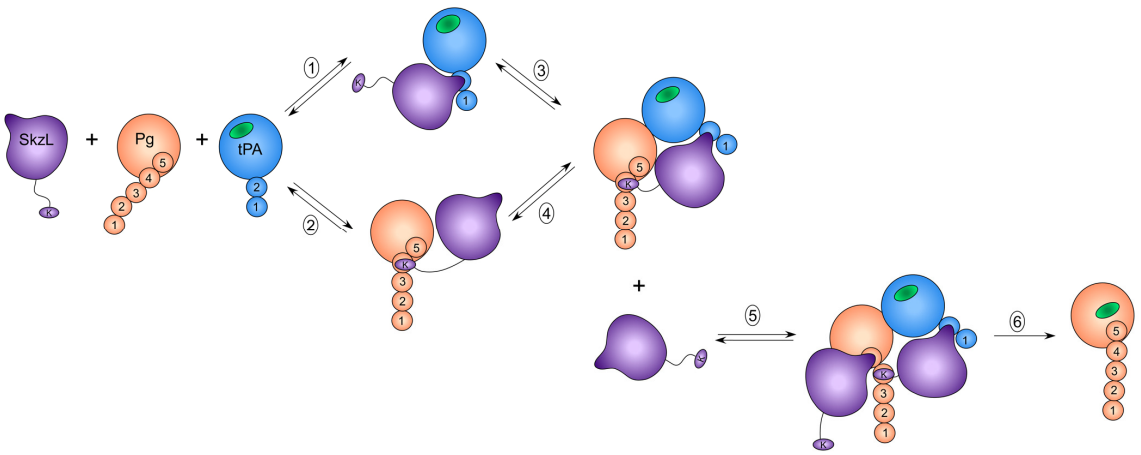

Figure 9. Proposed mechanism for SkzL-catalyzed enhanced Pg activation by tPA. SkzL is shown in *purple* with Lys^{415} (*K*) on a flexible segment, the proposed SkzL internal motif is represented by the "*nose*", [Lys]Pg in *light orange* is shown with five numbered kringle domains and the COOH-terminal catalytic domain, and tPA in *blue* is shown with two kringle domains and the COOH-terminal catalytic domain, with the active site in *green*. Low affinity (K_D ~ 14 μM) SkzL•tPA complex formation through the putative SkzL internal motif (*nose*)-tPA-kringle 2 interaction (Reaction 1) and SkzL•Pg complex formation through the proposed SkzL Lys^{415}-[Lys]Pg kringle 4 interaction (K_D 80 nM) (Reaction 2) . Reactions 3 and 4 result in formation of a non-productive ternary complex. With increasing SkzL concentrations (~5-20 μM), a second SkzL molecule binds the ternary complex (Reaction 5), mediated by the putative SkzL internal motif-kringle 5 interaction. Reaction 6 represents enhanced Pm generation (active site in *green*), compared with the uncatalyzed reaction not shown.

We therefore can infer that Lys^{415}-independent binding of SkzL to [Lys]Pg contributes strongly to enhanced [Lys]Pg activation through formation of the quaternary complex. This would suggest that the weak affinities observed for activation of [Lys]Pg by tPA as a function of SkzL concentration in Figure 1 can not be solely contributed to SkzL-tPA binding, but also to the weak SkzL-[Lys]Pg interaction resulting in quaternary complex formation. These analyses are preliminary and further study is needed to clarify this mechanism of higher order complex formation in SkzL enhanced [Lys]Pg activation by tPA.

The present studies identify SkzL as a novel cofactor of Pg activation by tPA. In addition to SkzL increasing the rate of [Glu]Pg activation by tPA, SkzL enhances clot lysis by tPA in plasma (Chapter 2). Together, these results provide strong support for a role of SkzL as a *Streptococcus agalactiae* secreted Pg-binding protein with established enhancement of the human fibrinolytic system. This interaction may lead to identification of SkzL as a virulence factor in *Streptococcus agalactiae* pathogenesis, a pathogen with increasing morbidity and mortality, particularly in the neonatal population.

References

1. Robbins, K. C., Boreisha, I. G., Arzadon, L., and Summaria, L. (1975) *J. Biol. Chem.* **250**, 4044-4047

2. Brockway, W. J., and Castellino, F. J. (1972) *Arch Biochem Biophys* **151**, 194-199

3. Markus, G., DePasquale, J. L., and Wissler, F. C. (1978) *J. Biol. Chem.* **253**, 727-732

4. Sjoholm, I. (1973) *Eur. J. Biochem.* **39**, 471-479

5. Violand, B. N., Byrne, R., and Castellino, F. J. (1978) *J. Biol. Chem.* **253**, 5395-5401

6. Castellino, F. J., and Powell, J. R. (1981) *Methods Enzymol.* **80 Pt C**, 365-378

7. Henkin, J., Marcotte, P., and Yang, H. C. (1991) *Prog. Cardiovasc. Dis.* **34**, 135-164

8. Castellino, F. J., Brockway, W. J., Thomas, J. K., Liano, H. T., and Rawitch, A. B. (1973) *Biochemistry* **12**, 2787-2791

9. Urano, T., Chibber, B. A., and Castellino, F. J. (1987) *Proc. Natl. Acad. Sci. U S A* **84**, 4031-4034

10. Hochschwender, S. M., and Laursen, R. A. (1981) *J. Biol. Chem.* **256**, 11172-11176

11. Plow, E. F., and Collen, D. (1981) *J. Biol. Chem.* **256**, 10864-10869

12. Vali, Z., and Patthy, L. (1982) *J. Biol. Chem.* **257**, 2104-2110

13. Markus, G. (1996) *Fibrinolysis* **10**, 75-85

14. Markus, G., Priore, R. L., and Wissler, F. C. (1979) *J. Biol. Chem.* **254**, 1211-1216

15. Weisel J. W., N. C., Korsholm B., Petersen L. C., Suenson E. (1984) *J. Mol. Biol.* **235**, 1117-1135

16. Marshall, J. M., Brown, A. J., and Ponting, C. P. (1994) *Biochemistry* **33**, 3599-3606

17. McCance, S. G., and Castellino, F. J. (1995) *Biochemistry* **34**, 9581-9586

18. Urano, T., Sator de Serrano, V., Chibber, B. A., and Castellino, F. J. (1987) *J. Biol. Chem.* **262**, 15959-15964

19. Ponting, C. P., Marshall, J. M., and Cederholm-Williams, S. A. (1992) *Blood Coagul Fibrinolysis* **3**, 605-614

20. Cummings, H. S., and Castellino, F. J. (1985) *Arch Biochem Biophys* **236**, 612-618

21. Ploplis, V. A., Cummings, H. S., and Castellino, F. J. (1982) *Biochemistry* **21**, 5891-5897

22. Lerch, P. G., Rickli, E. E., Lergier, W., and Gillessen, D. (1980) *Eur. J. Biochem.* **107**, 7-13

23. Petros, A. M., Ramesh, V., and Llinas, M. (1989) *Biochemistry* **28**, 1368-1376

24. Tharp, A. C., Laha, M., Panizzi, P., Thompson, M. W., Fuentes-Prior, P., and Bock, P. E. (2009) *J. Biol. Chem.*

25. Novokhatny, V. V., Matsuka Yu, V., and Kudinov, S. A. (1989) *Thromb Res* **53**, 243-252

26. Novokhatny, V., Medved, L., Lijnen, H. R., and Ingham, K. (1995) *J. Biol. Chem.* **270**, 8680-8685

27. de Munk, G. A., Caspers, M. P., Chang, G. T., Pouwels, P. H., Enger-Valk, B. E., and Verheijen, J. H. (1989) *Biochemistry* **28**, 7318-7325

28. Hoylaerts, M., Rijken, D. C., Lijnen, H. R., and Collen, D. (1982) *J. Biol. Chem.* **257**, 2912-2919

29. Medved, L., and Nieuwenhuizen, W. (2003) *Thromb. Haemost.* **89**, 409-419

30. Zamarron, C., Lijnen, H. R., and Collen, D. (1984) *J. Biol. Chem.* **259**, 2080-2083

31. Ranby, M. (1982) *Biochim Biophys Acta* **704**, 461-469

32. Silverstein, R. L., Nachman, R. L., Leung, L. L., and Harpel, P. C. (1985) *J. Biol. Chem.* **260**, 10346-10352

33. Fleury, V., Loyau, S., Lijnen, H. R., Nieuwenhuizen, W., and Angles-Cano, E. (1993) *Eur. J. Biochem.* **216**, 549-556

34. Horrevoets, A. J., Pannekoek, H., and Nesheim, M. E. (1997) *J. Biol. Chem.* **272**, 2183-2191

35. Rijken, D. C., Hoylaerts, M., and Collen, D. (1982) *J. Biol. Chem.* **257**, 2920-2925

36. Tate, K. M., Higgins, D. L., Holmes, W. E., Winkler, M. E., Heyneker, H. L., and Vehar, G. A. (1987) *Biochemistry* **26**, 338-343

37. Deutsch, D. G., and Mertz, E. T. (1970) *Science* **170**, 1095-1096

38. Boxrud, P. D., Fay, W. P., and Bock, P. E. (2000) *J. Biol. Chem.* **275**, 14579-14589

39. Violand, B. N., and Castellino, F. J. (1976) *J. Biol. Chem.* **251**, 3906-3912

40. Bean, R. R., Verhamme, I. M., and Bock, P. E. (2005) *J. Biol. Chem.* **280**, 7504-7510

41. Bock, P. E., Day, D. E., Verhamme, I. M., Bernardo, M. M., Olson, S. T., and Shore, J. D. (1996) *J. Biol. Chem.* **271**, 1072-1080

42. Boxrud, P. D., and Bock, P. E. (2000) *Biochemistry* **39**, 13974-13981

43. Bock, P. E. (1992) *J. Biol. Chem.* **267**, 14963-14973

CHAPTER IV

SIGNIFICANCE AND FUTURE DIRECTIONS

Identification of Skizzle as a Plasminogen and Plasmin Binding Protein

The work in this thesis identifies skizzle (SkzL) as a novel protein secreted by *Streptococcus agalactiae*, the only known species of streptococci that does not express the secreted bacterial plasminogen (Pg) activator streptokinase (SK). The studies show that SkzL binds Pg and Pm and enhances Pg activation and plasma clot lysis by the two endogenous Pg activators, uPA and tPA. *Streptococcus agalactiae* expresses two membrane-bound proteins, glyceraldehyde-3-phosphate dehydrogenase and enolase, with established Pg binding interactions. The current studies identify SkzL as the first *Streptococcus agalactiae*-secreted protein that targets the human fibrinolytic system.

SkzL binds [Glu]Pg with weak affinity through LBS-dependent putative interaction with Pg kringle 4. The SkzL Lys^{415}-dependent binding is hypothesized to occur preferentially through interaction with the low concentration of [Glu]Pg in the partially extended β-conformation in unfavorable equilibrium with activation resistant, α-conformation [Glu]Pg. Proposed occupation of kringle 4 results in a conformational transition to [Glu]Pg-γ, observed via enhanced activation of SkzL-bound [Glu]Pg by uPA. Binding of SkzL to [Lys]Pg-β and [Lys]Pm-β occurs through two LBS-dependent interactions; high affinity interaction of Lys^{415} with kringle 4, and low affinity interaction of a putative SkzL internal motif with kringle 5. Proposed occupation of kringle 4, in parallel with [Glu]Pg, results in conformational transition to [Lys]Pg-γ. Specific kringle

interactions remain hypothetical and will require further investigation with Pg variants to confirm. While we hypothesize the putative SkzL internal motif to be analogous to the 250-loop of SK, responsible for interaction with Pg kringle 5, further mutagenesis studies will be necessary to determine the residues responsible for the low affinity interaction of SkzL with Pg/Pm (1).

Significance of SkzL Enhancement of Pg Activation

These studies provide evidence of two mechanisms by which SkzL enhances Pm formation, specific for uPA and tPA. SkzL enhances activation of both [Glu]Pg and [Lys]Pg by LBS-containing tPA, in contrast with [Glu]Pg-specific enhancement of Pg activation by uPA. The kringle domain of uPA, unlike tPA, contains no LBS, leaving uPA incapable of binding SkzL (2). Enhanced Pg activation by uPA is therefore specific for [Glu]Pg through a mechanism in which SkzL-[Glu]Pg binding induces a transition to [Glu]Pg in the γ-conformation, which like [Lys]Pg is more readily activated by uPA.

SkzL binds tPA with relatively weak affinity through LBS-dependent interaction of the putative SkzL internal motif and tPA kringle 2. Together with the high affinity interaction of SkzL Lys^{415} and Pg kringle 4, we hypothesize that SkzL forms a non-productive SkzL•tPA•Pg ternary complex. At higher SkzL concentrations, low affinity Lys^{415}-independent binding of a second SkzL molecule to the SkzL•tPA•Pg ternary complex occurs.

The mechanism of fibrin-mediated enhancement of Pg activation by tPA involves ternary complex formation. Formation of this fibrin•tPA•Pg ternary complex affects the Michaelis-Menten kinetic parameters observed for Pg activation by tPA. Compared with

the uncatalyzed reaction, fibrin•tPA•Pg ternary complex formation results in a decrease in K_m and a slight increase in k_{cat}, although there is variation in the amplitude of increase or decrease in the published parameters (Table 1).

Of particular interest to the current studies are the published parameters for activation of [Lys]Pg by tctPA, which reveal K_m values of 19 μM without fibrin (effector) and 0.02 μM with fibrin (effector), representing a 950-fold decrease in K_m. The K_m value of 19 μM observed in the absence of effector is consistent with the value of ≥ 2.6 μM estimated in the current studies. The presence of fibrin (effector) decreased the K_m value to 20 nM, compared with 4.5-7.5 nM in the present studies, yielding an overall fold decrease in K_m observed for fibrin (950-fold) compared with SkzL (~350-750-fold), estimated by mechanism-independent analysis.

Table 1. Michaelis-Menten kinetic parameters for effect of fibrin on [Glu]Pg and [Lys]Pg activation by tPA. Illustration of the distribution in the published parameters for the effect of fibrin on K_m and k_{cat} determined for activation of [Glu]Pg and [Lys]Pg by tPA obtained from various sources (*mtPA* represents melanoma-derived tPA).

tPA	Pg	K_m	K_m + effector	$(K_m + effector)/K_m$	k_{cat}	k_{cat} + effector	$(k_{cat}$ + effector$)/k_{cat}$	Ref.
		(μM)	(μM)	(*fold*)	(s^{-1})	(s^{-1})	(*fold*)	
sctPA	[Glu]Pg	4.9	0.46	11	0.0013	0.084	65	(3)
tctPA	[Glu]Pg	7.6	0.18	42	0.008	0.12	15	(3)
mtPA	[Glu]Pg	3.0	0.1	30	0.0005	0.008	16	(4)
mtPA	[Glu]Pg	83	0.18	460	0.07	0.28	4	(5)
tctPA	[Glu]Pg	65	0.16	410	0.06	0.1	2	(6)
tctPA	[Lys]Pg	19	0.02	950	0.2	0.2	1	(6)

Additional preliminary analysis of the data suggests that a second SkzL molecule binds the SkzL•tPA•Pg ternary complex and that the quaternary, not ternary complex

results in enhanced [Lys]Pg activation by tPA. This indicates a mechanism of action distinct from the ternary complex model employed by fibrin. Both the weak second SkzL-[Lys]Pg interaction and weak SkzL-tPA interaction are Lys^{415}-independent. As a result, further study including mutagenesis to elucidate the residues involved in binding is required to clarify further this mechanism.

Proposed Skizzle ternary complex formation

Streptococcus agalactiae is the only known streptococcal species that does not express the potent conformational Pg activator, SK. Comparison of sequence alignment and secondary structure prediction illustrated in Chapter 2; Fig. 1 suggests both sequence and structural similarity between SkzL and SK resulting in predicted functional similarity. One major difference between SK and SkzL is the presence of three Cys residues within SkzL, which may have an impact on protein folding and function. Partially LBS-dependent SK-Pg binding occurs through both LBS-dependent kringle-Lys^{414} interaction and LBS-independent interaction of the SK three-domain structure with the Pg catalytic domain, as shown by the crystal structure (7). In constrast, binding of SkzL to Pg is entirely LBS-dependent, supporting a hypothesis of altered protein folding possibly due to presence of SkzL Cys residues, specifically internally located residue Cys^{120}. Altered SkzL folding and subsequently altered Pg binding may be the reason for the failure of SkzL to directly activate Pg. We hypothesize that SkzL•tPA•Pg ternary complex formation occurs in a manner similar to SK-Pg binding in the mechanism of Pg activation by SK, which also involves ternary complex formation (Fig. 1). In both complexes, LBS-dependent interactions occur between the COOH-terminal Lys residue

of the ligand (SkzL or SK) and Pg, followed by LBS-dependent interaction of the internal motif (250-loop for SK) with the respective second substrate protein through the kringle domain closest to the catalytic domain (Pg or tPA). Mutagenesis studies are needed to determine the residues of SkzL responsible for LBS-dependent interaction of the proposed internal motif with both Pg and tPA.

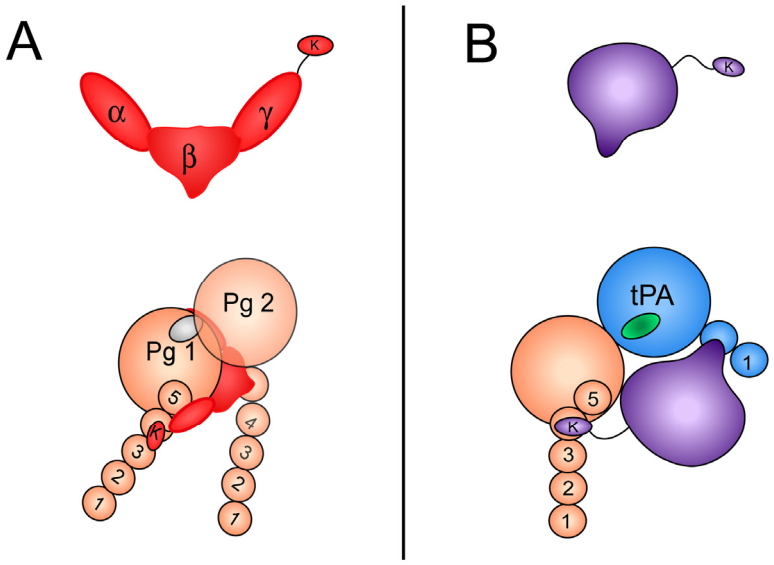

Figure 1. Comparison of SK- and SkzL-enhanced Pg activation. *A*. Representation of the three domain structure of SK with Lys^{414} (*K*) on a flexible linker and the 250-loop in the β-domain responsible for Pg binding in the substrate mode represented by the "*nose*". Conformational Pg activation by SK involves binding of SK to Pg (*Pg 1*), partially mediated by LBS-dependent Lys^{414} binding and partially through wrapping of SK around the Pg catalytic domain. The resulting conformationally activated SK•Pg 1 complex binds a second Pg molecule (*Pg 2*) in the substrate mode through interaction of the 250-loop in the SK β-domain with the LBS of Pg kringle 5, which undergoes proteolysis to Pm (not shown). *B*. While the tertiary structure of SkzL is unknown, proposed SkzL•tPA•Pg ternary complex formation occurs through LBS-dependent interaction of SkzL Lys^{415} (*K*) with Pg kringle 4 and LBS-dependent interaction of the putative SkzL internal motif (*nose*) with tPA kringle 2.

Hijacking the Fibrinolytic System to Evade Fibrinolytic Regulation

Inhibition of the fibrinolytic system is critical to maintaining the balance between wound healing and vascular repair and aberrant thrombus formation. The balance of this system is regulated, in part, through inhibition of Pm and tPA by the serine proteinase inhibitors (serpins) α_2-antiplasmin (α_2-AP) and plasminogen activator inhibitor-1 (PAI-1), respectively (2,8-11). Both SK-bound and fibrin-bound Pm are protected from inactivation by α_2-AP, allowing for efficient, localized fibrin proteolysis (8,9). Similarly, fibrin-bound tPA is protected from inactivation by PAI-1 (8-10). As a result, fibrin-mediated resistance to inhibition by α_2-AP and PAI-1 ensures that fibrin•tPA•Pg ternary complex formation and resulting fibrin-mediated amplification of Pm generation are locally restricted to the fibrin-stabilized thrombus.

Based on the structural similarity to SK, and the established SkzL LBS-dependent kringle interactions with both Pg and tPA, it is hypothesized that SkzL binding may render Pm and tPA resistant to inhibition by α_2-AP and PAI-1, respectively. Putative resistance of SkzL-bound tPA to PAI-1 inhibition would allow for fluid phase activation of Pg by tPA, not restricted to the thrombus, as in the case of fibrin. Putative resistance of SkzL-bound Pm to α_2-AP inhibition could result in circulating active Pm poised for rapid degradation of cross-linked fibrin. While tPA functions predominantly in the vasculature for fibrinolysis, uPA facilitates extracellular proteolysis (12). Activation of native [Glu]Pg by uPA occurs at very low level in the absence of fibrin or other LBS-ligands, therefore the dramatic enhancement of SkzL-bound [Glu]Pg activation by uPA may indicate a major role of SkzL in invasive *S. agalactiae* infection. If generated by uPA in the extracellular milieu, α_2-AP-resistent SkzL-bound Pm could facilitate proteolysis of

fibronectin and other extracellular matrix proteins allowing for higher permeability between cell layers, increasing the propensity for invasive infection (2). Animal studies are needed to determine if SkzL is a virulence factor in *S. agalactiae* infection and its related disease processes.

While purely speculative, the proposed resistance of SkzL-bound Pg and tPA to inhibition by their respective inhibitors may result in unregulated amplification of Pm generation and unregulated Pm proteolytic function in circulating plasma within the vascular system. This unregulated activity would disrupt the delicate balance of the fibrinolytic system between ensuring proper vascular repair and prevention of aberrant thrombus formation. Unregulated fibrinolysis could result in hemorrhage following improper wound healing. This imbalance could also leave the closed vasculature system open to assault from infectious agents resulting in bacteremia and septicemia, major disease processes in *S. agalactia*e infection (13,14).

Role of Skizzle in Streptococcus agalactiae Pathogenesis

Streptococcus agalactiae, specifically, serotype V, is emerging as an invasive pathogen with particular morbidity and mortality in neonates (13-17). The mechanisms of pathogenesis involved in the virulence of this pathogen within this patient population are poorly understood. Similar to immune-compromised patients, neonates possess inherently underdeveloped or weakened immune systems. It is unclear whether the enhanced virulence in both neonates and pregnant women is purely opportunistic with respect to decreased innate host defense, or if a more complex mechanism of pathogenesis involving host fibrinolysis is involved.

One possible rationalization for increased invasive *S. agalactiae* infection in neonates, may lie in the inherent differences in the maturity and function of the fibrinolytic system compared with the normal adult population. While all components of the fibrinolytic system are present before birth, the structural composition and relative abundances of many key factors are different from adults (18,19). The neonate possesses slightly altered forms of some fibrinolytic proteins. For example, both fibrinogen and Pg in the neonate, known as fetal fibrinogen and fetal Pg, contain increased phosphorus and sialic acid content and increased carbohydrate modification, respectively (18-20). Whether fetal fibrinogen is structurally or functionally different from the adult form remains unclear (19). Although early studies suggested decreased activation of fetal Pg by uPA and tPA due to the increase in carbohydrate modification, recent detailed examinations concluded that activation of fetal Pg in the absence or presence of fibrin by uPA and tPA is comparable to activation of adult Pg (20-22).

The major difference in the fibrinolytic system of the neonate compared with adults is the relative abundance of key fibrinolytic proteins. Compared with levels determined 6 months after birth (*6 months*) and for adults (levels not shown), neonates (*day 1*) have decreased levels of Pg (day 1, 1.95 U/mL; 6 months, 3.01 U/mL) and α_2-AP (day 1, 0.85 U/mL; 6 months, 1.1 U/mL) and increased tPA levels (day 1, 9.6 ng/mL; 6 months, 2.8 ng/mL) (19,23). Many of the clotting factors occur at low levels in neonates (*day 1*) compared with levels determined 6 months after birth (*6 months*) and for adults (levels not shown), specifically but not limited to factor II (day 1, 0.48 U/mL; 6 months, 0.88 U/mL), factor V (day 1, 0.72 U/mL; 6 months, 0.91 U/mL), factor IX (day 1, 0.53 U/mL; 6 months, 0.86 U/mL), and factor X (day 1, 0.4 U/mL; 6 months, 0.78 U/mL).

This results in delayed and decreased thrombin formation (19). While there is no evidence for increased bleeding risk in healthy neonates, should the already decreased levels of key clotting factors decrease due to illness, sick neonates are at increased risk for fibrinolysis and hemorrhage (19). Together with the decrease in plasma Pg concentration and increase in plasma tPA concentration, this would likely suggest a system poised for enhanced fibrinolytic activity. Enhancement of Pg activation by *S. agalactiae*-secreted SkzL, particularly the proposed inhibitor-resistant enhancement, could shift this already delicate balance to an overly fibrinolytic state. Animal studies are needed to determine if SkzL is a virulence factor in *S. agalactiae* infection, particularly in neonates.

Subversion of the host fibrinolytic system is a mechanism of pathogenesis employed by most streptococci, in part through expression of cell-surface Pg binding proteins. In this mechanism, the streptococci hijack the fibrinolytic system causing enhanced Pm generation, which can degrade fibrin, laminin, fibronectin and other extracellular matrix proteins to disseminate spread of the bacteria through soft tissue (2,12). Activation of Pg localized on the bacterial surface through Pg binding proteins such as Pg-binding Group A Streptococcal M-like protein (PAM, Group A, C, G streptococci), glyceraldehyde-3-phosphate dehydrogenase (GAPDH, Group A, B, C streptococci), and α-enolase (Group A, B streptococci) can result in coating of the cell surface with readily activated Pg or active Pm (12,24-29). Active Pm can degrade extracellular matrix proteins as discussed above, allowing streptococci to transmigrate through cell layers (30). Transmigration may occur via extracellular matrix degradation or via bacterial internalization into host cells (30). *Streptococcus agalactiae* has been

shown to transmigrate through both endothelial and epithelial barriers as well as through the microvascular endothelium of the blood brain barrier, critical for meningitis caused by *S. agalactiae* in neonates (30).

Streptococcus agalactiae is known to interact with the host fibrinolytic system through bacterial surface expression of α-enolase and GAPDH (24,27,28,31). A recent study indicated that Pg activation on the surface of *S. agalactiae* occurs through GAPDH-bound Pg. GAPDH-mediated Pg binding enhanced *S. agalactiae* virulence and promoted systemic bacterial invasion in a murine model (26). While SkzL was identified in the secreted protein profile of *S. agalactiae* in the present studies, it is unclear if post-secretion SkzL also exists bound to the bacterial surface through unknown binding interactions. SkzL possesses affinity for Pg and has been shown to induce a conformational change in the native zymogen [Glu]Pg to the extended, more readily activated, γ-conformation, in parallel with the function of known streptococcal surface Pg binding proteins, such as PAM. This would suggest that SkzL is a Pg cofactor secreted by *S. agalactiae* that may or may not bind to the bacterial surface post-secretion.

Nevertheless, these studies indicate that secreted SkzL acts as a novel fluid phase cofactor for enhanced Pg activation by both uPA and tPA (Figure 2). Based on the predominant functions of tPA and uPA in vascular fibrinolysis and extracellular proteolysis, respectively, the conformational change induced upon SkzL-Pg binding and enhanced [Glu]Pg activation by both enzymes provides strong evidence for a bifunctional role of SkzL in *S. agalactiae* pathogenesis. Enhancement of tPA-mediated Pg activation in the vessel could result in degradation of thrombi critical for vessel repair, rendering the damaged vessel permeable to bacterial transmigration (Fig. 2*A*). In contrast, enhancement

of uPA-mediated Pg activation, functioning in extracellular proteolysis, could result in increased extracellular matrix (ECM) degradation and bacterial transmigration through soft tissue (Fig. 2*B*). As a result of the enhanced tPA- and uPA-mediated Pg activation by SkzL, we hypothesize that SkzL is a secreted virulence factor in *S. agalactiae* pathogenesis.

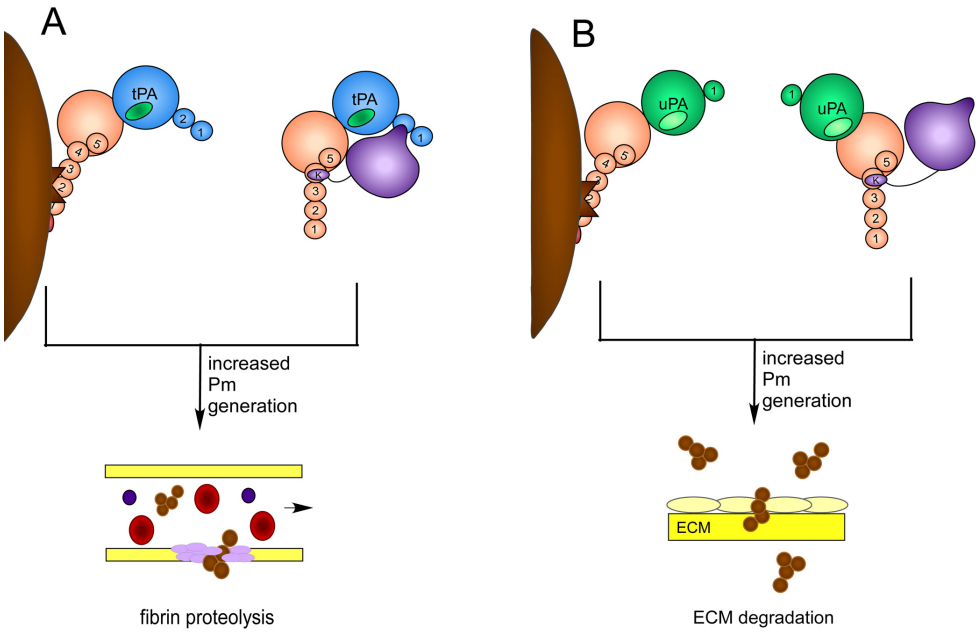

Figure 2. Comparison of surface-bound Pg receptor-mediated and secreted SkzL-mediated enhanced Pg activation. Bacterial surface receptors, such as α-enolase and GAPDH (*brown*), bind Pg through LBS-dependent kringle interactions. Surface-bound Pg is readily activated by both uPA and tPA. *A*. Pg (*light orange*) activation by tPA (*blue*), predominantly occurring in the vascular system, is enhanced by the conformational change induced upon surface-bound receptor Pg binding and by SkzL•tPA•Pg ternary/quaternary complex formation. Increased Pm generation results in enhanced fibrin proteolysis and degradation of thrombi involved in vessel wall repair, leaving the vessel vulnerable to bacterial transmigration. *B*. Pg activation by uPA (*green*), predominantly functioning in extracellular proteolysis, is enhanced by the conformational change induced upon both surface-bound receptor Pg binding and SkzL binding. Increased Pm generation results in enhanced extracellular matrix (*ECM*) proteolysis, bacterial transmigration, and bacterial dissemination into soft tissue.

The known interaction of *S. agalactiae* surface proteins, α-enolase and GAPDH, with Pg in fibrinolysis provided a solid rationale for the investigation of SkzL and its potential interaction with the human fibrinolytic system. The interaction of SkzL with Pg, resulting in enhanced Pg activation by both uPA and tPA, provides an additional novel interaction of *S. agalactiae* with the human fibrinolytic system and a new branch in the potential mechanism for *S. agalactiae* pathogenesis.

References

1. Tharp, A. C., Laha, M., Panizzi, P., Thompson, M. W., Fuentes-Prior, P., and Bock, P. E. (2009) *J. Biol. Chem.*
2. Henkin, J., Marcotte, P., and Yang, H. C. (1991) *Prog. Cardiovasc. Dis.* **34**, 135-164
3. Ranby, M. (1982) *Biochim Biophys Acta* **704**, 461-469
4. Silverstein, R. L., Nachman, R. L., Leung, L. L., and Harpel, P. C. (1985) *J. Biol. Chem.* **260**, 10346-10352
5. Zamarron, C., Lijnen, H. R., and Collen, D. (1984) *J. Biol. Chem.* **259**, 2080-2083
6. Hoylaerts, M., Rijken, D. C., Lijnen, H. R., and Collen, D. (1982) *J. Biol. Chem.* **257**, 2912-2919
7. Wang, X., Lin, X., Loy, J. A., Tang, J., and Zhang, X. C. (1998) *Science* **281**, 1662-1665
8. Kvassman, J. O., Verhamme, I., and Shore, J. D. (1998) *Biochemistry* **37**, 15491-15502
9. Rau, J. C., Beaulieu, L. M., Huntington, J. A., and Church, F. C. (2007) *J Thromb Haemost* **5 Suppl 1**, 102-115
10. Fay, W. P., Garg, N., and Sunkar, M. (2007) *Arterioscler Thromb Vasc Biol* **27**, 1231-1237
11. Medved, L., and Nieuwenhuizen, W. (2003) *Thromb. Haemost.* **89**, 409-419
12. Boyle, M. D., and Lottenberg, R. (1997) *Thromb. Haemost.* **77**, 1-10

13. Pietrocola, G., Schubert, A., Visai, L., Torti, M., Fitzgerald, J. R., Foster, T. J., Reinscheid, D. J., and Speziale, P. (2005) *Blood* **105**, 1052-1059

14. Schuchat, A. (1999) *Lancet* **353**, 51-56

15. Blumberg, H. M., Stephens, D. S., Modansky, M., Erwin, M., Elliot, J., Facklam, R. R., Schuchat, A., Baughman, W., and Farley, M. M. (1996) *J. Infect. Dis.* **173**, 365-373

16. Brochet, M., Couve, E., Zouine, M., Vallaeys, T., Rusniok, C., Lamy, M. C., Buchrieser, C., Trieu-Cuot, P., Kunst, F., Poyart, C., and Glaser, P. (2006) *Microbes Infect.*

17. Fluegge, K., Schweier, O., Schiltz, E., Batsford, S., and Berner, R. (2004) *Eur. J. Clin. Microbiol. Infect. Dis.* **23**, 818-824

18. Albisetti, M. (2003) *Semin Thromb Hemost* **29**, 339-348

19. Andrew, M., Paes, B., and Johnston, M. (1990) *Am J Pediatr Hematol Oncol* **12**, 95-104

20. Summaria, L. (1989) *Haemostasis* **19**, 266-273

21. Ries, M., Easton, R. L., Longstaff, C., Zenker, M., Corran, P. H., Morris, H. R., Dell, A., and Gaffney, P. J. (2001) *Thromb Res* **103**, 173-184

22. Ries, M., Zenker, M., and Gaffney, P. J. (2000) *Thromb Res* **100**, 341-351

23. Richardson, M. W., Allen, G. A., and Monahan, P. E. (2002) *Thromb. Haemost.* **88**, 900-911

24. Bergmann, S., Wild, D., Diekmann, O., Frank, R., Bracht, D., Chhatwal, G. S., and Hammerschmidt, S. (2003) *Mol. Microbiol.* **49**, 411-423

25. Lahteenmaki, K., Kuusela, P., and Korhonen, T. K. (2001) *FEMS Microbiol. Rev.* **25**, 531-552

26. Magalhaes, V., Veiga-Malta, I., Almeida, M. R., Baptista, M., Ribeiro, A., Trieu-Cuot, P., and Ferreira, P. (2007) *Microbes Infect.* **9**, 1276-1284

27. Whiting, G. C., Evans, J. T., Patel, S., and Gillespie, S. H. (2002) *J. Med. Microbiol.* **51**, 837-843

28. Bergmann, S., and Hammerschmidt, S. (2007) *Thromb. Haemost.* **98**, 512-520

29. Cork, A. J., Jergic, S., Hammerschmidt, S., Kobe, B., Pancholi, V., Benesch, J. L., Robinson, C. V., Dixon, N. E., Aquilina, J. A., and Walker, M. J. (2009) *J. Biol. Chem.* **284**, 17129-17137

30. Nitsche-Schmitz, D. P., Rohde, M., and Chhatwal, G. S. (2007) *Thromb. Haemost.* **98**, 488-496

31. Hughes, M. J., Moore, J. C., Lane, J. D., Wilson, R., Pribul, P. K., Younes, Z. N., Dobson, R. J., Everest, P., Reason, A. J., Redfern, J. M., Greer, F. M., Paxton, T., Panico, M., Morris, H. R., Feldman, R. G., and Santangelo, J. D. (2002) *Infect. Immun.* **70**, 1254-1259